CHARLES UNIVERSITY IN PRAGUE
Faculty of Science

Department of Cell Biology

Bc. Jitka Šimandlová

Characterization of Antirecombinase Activity of Human FBH1 Helicase

Charakterizace antirekombinázové aktivity lidské FBH1 helikázy

Master Thesis

Supervisor: Pavel Janščák, Ph.D.

Prague, 2012

This Master Thesis was worked out under leadership of Pavel Janščák, Ph.D. and Igor Chevelev, Ph.D. in the Laboratory of Chromosomal Stability at the Institute of Molecular Genetics ASCR in Prague.

Declaration

With this, I declare that I have compiled this work on my own, cited all used references properly, and used no other than listed resources. The material used in this work has not previously been accepted in whole, or in part, to gain any other academic title.

Prague, 9th May 2012 .....

Acknowledgement

First of all I would like to thank to Pavel Janščák and Igor Chevelev who gave me a chance to work in their laboratory and thus enabled me to open new horizons.

I would also like to thank to all members of the Laboratory of Chromosomal Stability at the Institute of Molecular Genetics ASCR for creating a nice working environment and helping me with my experiments.

I would like to thank to Vašek Urban for the plenty of critical advices he gave me, chocolate supply, table football and dart lectures.

I want to express my gratitude and appreciation to Kamila Burdová. She taught me to culture insect cells, to purify proteins, to measure ATPase activity, to study protein interactions, and much much more. She followed all my steps and was always open for any discussions. I am grateful to her for proofreading of my thesis and endless patience with my questions.

Moc ráda bych poděkovala své rodině a přátelům, kteří vždy stáli na mé straně a všemi možnými způsoby a prostředky mě podporovali.

Abstract

Homologous recombination (HR) is an essential mechanism for accurate repair of DNA double-strand breaks (DSBs). However, HR must be tightly controlled because excessive or unwanted HR events can lead to genome instability, which is a prerequisite for premature aging and cancer development. A critical step of HR is the loading of RAD51 molecules onto single-stranded DNA regions generated in the vicinity of the DSB, leading to the formation of a nucleoprotein filament. Several DNA helicases have been involved in the regulation of the HR process. One of these is human FBH1 (F-box DNA helicase 1) that is a member of SF1 superfamily of helicases. As a unique DNA helicase, FBH1 additionally possesses a conserved F-box motif that allows it to assemble into an SCF complex, an E3 ubiquitin ligase that targets proteins for degradation. FBH1 has been implicated in the restriction of nucleoprotein filament stability. However, the exact mechanism of how FBH1 controls the RAD51 action is still not certain. In this work, we revealed that FBH1 actively disassembles RAD51 nucleoprotein filament. We also show that FBH1 interacts with RAD51 and RPA physically *in vitro*. Based on these data, we propose a potential mechanism of FBH1 antirecombinase function.

Key words: homologous recombination, FBH1, RAD51, nucleoprotein filament, antirecombinase, RPA

Abstrakt

Homologní rekombinace (HR) je mechanismus nezbytný pro bezchybnou opravu dvouvláknových zlomů v DNA. Tento proces musí být přísně regulován, protože nadměrné množství nežádoucích HR může v buňce vést k nestabilitě genomu, od které je už jen krůček k symptomu předčasnému stárnutí či vývoji zhoubných onkologických onemocnění. Rozhodujícím krokem v procesu HR je tvorba tzv. presynaptického filamentu. Ten vzniká po navázání molekul RAD51 na úsek jednořetězcové DNA, který se vytvoří v okolí dvouvláknových zlomů. Proces HR je kontrolován mj. DNA helikázami. Mezi nimi je i lidská FBH1 (F-box DNA helicase 1) ze SF1 rodiny helikáz. Jedinečným znakem FBH1 helikázy je přítomnost konzervovaného F-box motivu. Díky němu se FBH1 váže v SCF komplexu fungujícího jako E3 ubiquitin ligáza, která určuje proteiny pro degradaci. V procesu HR plní FBH1 úlohu v regulaci stability presynaptického filamentu. Ovšem přesný mechanismus jak FBH1 kontroluje činnost RAD51 ještě nebyl zcela popsán. V této diplomové práci jsme ukázali, že FBH1 helikáza aktivně rozrušuje RAD51 presynaptický filament. Dále jsme *in vitro* odhalili přímou interakci FBH1 s RAD51 a RPA. Na základě našich výsledků jsme navrhli možný model mechanismu antirekombinázové funkce FBH1 helikázy.

Klíčová slova: homologní rekombinace, FBH1, RAD51, presynaptický filament, antirekombináza, RPA

Abbreviations

aa	amino acid
ATM kinase	ataxia telangiectasia mutated kinase
ATP	adenosine triphosphate
ATR kinase	ataxia telangiectasia and Rad3-related kinase
BCA	bicinchoninic acid
BER	base-excision repair
BLM	Bloom helicase
BSA	bovine serum albumine
CBD	chitin binding domain
co-IP	complex protein-immunoprecipitation
CTP	cytidine triphosphate
dHJ	double Holliday junction
D-loop	displacement loop
dATP	deoxyadenosine triphosphate
dCTP	deoxycytidine triphosphate
dGTP	deoxyguanosine triphosphate
DMEM	Dulbecco's modified Eagle medium
DNA-PK	DNA-dependent protein kinase
dNTP	deoxyribonucleotide triphosphate
dsDNA	double-stranded DNA
DSB	double-strand break
DSBR	double-strand break repair
DTT	dithiotreitol
dTTP	deoxythymidine triphosphate
ECL	enhanced chemiluminescence
EDTA	ethylenediaminetetraacetic acid
Fbh1	*Schizosaccharomyces pombe* F-box DNA helicase 1
FBH1	human F-box DNA helicase 1
$FBH1^{D698N}$	ATPase-dead variant of FBH1
FBS	fetal bovine serum
GSH	glutathione
GST	glutathione S-transferase
GTP	guanosine triphosphate
His6x	histidine tag
HJ	Holliday junction
HR	homologous recombination
HRP	horseradish peroxidase
Ig	immunoglobulin
IPTG	isopropyl-beta-D-thiogalactopyranoside
LB	Luria Broth
MMR	mismatch repair
MRN complex	MRE11/RAD50/NBS1 complex
NER	nucleotide-excision repair

NHEJ	non-homologous end joining
NHS	N-hydroxysuccinimide
NTP	ribonucleotide triphosphate
OD_{600}	optical density at 600 nm
PBS	phosphate buffer saline
PCR	polymerase chain reaction
PEG	polyethylenglycol
P_i	inorganic phosphate
PMSF	phenylmethylsulfonyl fluoride
PVDF	polyvinylidine fluoride
$RAD51^{K133R}$	ATPase-dead variant of RAD51
RE	restriction enzyme
RNAi	RNA interference
RPA	replication protein A
RT	room temperature
SCE	sister chromatid exchange
SCF complex	Skp1-Cullin-F-box complex
SCF^{FBH1}	FBH1 in SCF complex
SDS	sodium dodecyl sulfate
SDS-PAGE	sodium dodecyl sulfate polyacrylamide gel electrophoresis
SDSA	synthesis dependent strand annealing
SF	superfamily
siRNA	small interfering RNA
SSB	single-stranded binding protein
ssDNA	single-stranded DNA
TEMED	tetramethylethylenediamine
UTP	uridine triphosphate
v/v	volume/volume percentage
w/v	weight/volume percentage
WCE	whole cell extract

Table of contents

1 Introduction

An indisputable goal of each living organism is to produce offspring and hand over its genetic material to the next generation. From the perspective of evolution, the fundamental process that drives biological diversity, certain degree of genomic alteration is an advantage. However, at the level of the individual, intact genetic information is required to guard against diseases, and thus crucial for survival of all organisms.

Genome integrity is constantly challenged by genotoxic stress. DNA damage can arise spontaneously during normal DNA metabolism or be induced by various endogenous and exogenous factors. Their potential deleterious effect to the DNA integrity is unpredictable. While some DNA lesions are considered to be relatively benign, other lesions can be quite toxic. Then even a single base change in an important gene may have ongoing and catastrophic effect on the health and viability of an organism. Moreover, DNA lesion is not a rare event. For example, it has been estimated that a single day in the sun can induce up to 10^5 DNA lesions per cell per day (Hoeijmakers, 2009).

Because DNA is the repository of genetic information in each cell, maintenance of its integrity and stability are essential. Cells have therefore evolved a number of strategies to sense and repair various types of damage that can occur to DNA.

Homologous recombination (HR) is, beside its essential role in meiosis and antibody variation, one of the key mechanisms that promotes repair of DNA double-strand breaks (DSB), the most harmful DNA lesion. If left unrepaired, DSBs can trigger mutagenic accidents such as chromosome loss, duplication or translocation, events that can lead to carcinogenesis and/or cell death. Although, HR is undoubtedly a beneficial for genome maintenance, excessive and unscheduled HR events can be harmful as well. Hence, tight control of HR events to balance between these two consequences is essential for viability of an organism.

Many proteins have been found to be involved in the HR process. Among them, several DNA helicases play crucial roles in regulation of HR. So called “prorecombinases” function to mediate the repair progression, on the other hand, “antirecombinases” are believed to suppress the recombination events.

DNA helicases are motor proteins that utilize energy from NTP hydrolyses to translocate on DNA. They pose an important enzymatic tool involved in almost all biological processes where complementary nucleic acid strands have to be separated. The majority of helicases are able to disconnect strands in double-stranded DNA (dsDNA), selected few are additionally endowed with the ability to remove proteins from either single-stranded DNA (ssDNA) or dsDNA. Defects in certain DNA repair helicases lead to various inherited human

diseases sharing common features such as genome instability, premature aging and cancer predispositions (Hoeijmakers, 2001).

One of the novel putative player in the repair pathway by HR is F-box DNA helicase 1 (FBH1) (Kim et al., 2002). FBH1 accumulates at sites of DNA damage where it acts as regulator of HR repair in *Schizosaccharomyces pombe* and human cells. When depleted, the cells display an increased sensitivity to DNA-damaging agents (Morishita et al., 2005, Osman et al., 2005). FBH1 is suggested to have antirecombinase function by preventing assembly of nucleoprotein filament, a key structure in HR. However, the mechanism how FBH1 operates in the process of HR remains to be established.

Besides the helicase domain, FBH1 possesses an additional F-box motif which allows it to act within a SCF (Skp1-Cullin-F-box) complex as a ubiquitin ligase and target proteins for degradation.

In this Master thesis, I first provide an overview of current knowledge regarding the DSB repair, HR and FBH1 protein. In the experimental part, we provide further characterization of FBH1 as an antirecombinase.

2 Current state of knowledge

2.1 DNA damage and DNA damage repair

Our genomic material is constantly threatened by various harmful factors, both exogenous and endogenous. Ultraviolet light and ionizing radiation coming from the cosmos, x-rays, numerous genotoxic chemicals including alkylating agents and polycyclic aromatic hydrocarbons present in cigarette smoke, can have dangerous consequences to the DNA structure (Hoeijmakers, 2001). For example, mitomycin C, a chemotherapy agent, induces covalent links between DNA bases on the same or on the opposite DNA strands causing DNA lesions termed intrastrand and interstrand cross-links, respectively (Noll et al., 2006). Beside the environmental sources of DNA damage, also products of normal cellular metabolism, such as free radicals and reactive oxygen species, can have harmful effect on the cellular DNA, for instance, by generating DNA breaks (Hoeijmakers, 2009). In addition, DNA replication is a common source of DNA insults, e.g. misincorporated bases (Kunkel, 2004) or stalled replication fork can result in DNA breakage. Furthermore, DNA molecules are susceptible to spontaneous chemical reactions, mostly hydrolysis.

It is therefore not surprising that multiple efficient detection and repair reactions specific for many of lesions have evolved (Figure 1). For instance, mispaired DNA bases are corrected by mismatch repair (MMR), small chemical alteration of DNA bases or single-strand breaks are repaired by base-excision repair (BER) through excision of the damaged base (Jiricny, 2006). More complex lesions, such as pyrimidine dimers, bulky adduct and intrastrand cross-links, are corrected by nucleotide-excision repair (NER), through the removal of an oligonucleotide containing the damaged bases (Hoeijmakers, 2009, Moldovan and D'Andrea, 2009). DSBs and interstrand cross-links are repaired either by non-homologous end joining (NHEJ) or by HR (Hiom, 2010).

As the topic of this thesis deals with the regulatory role of FBH1 helicase in HR, this repair pathway is described in detail in following chapter.

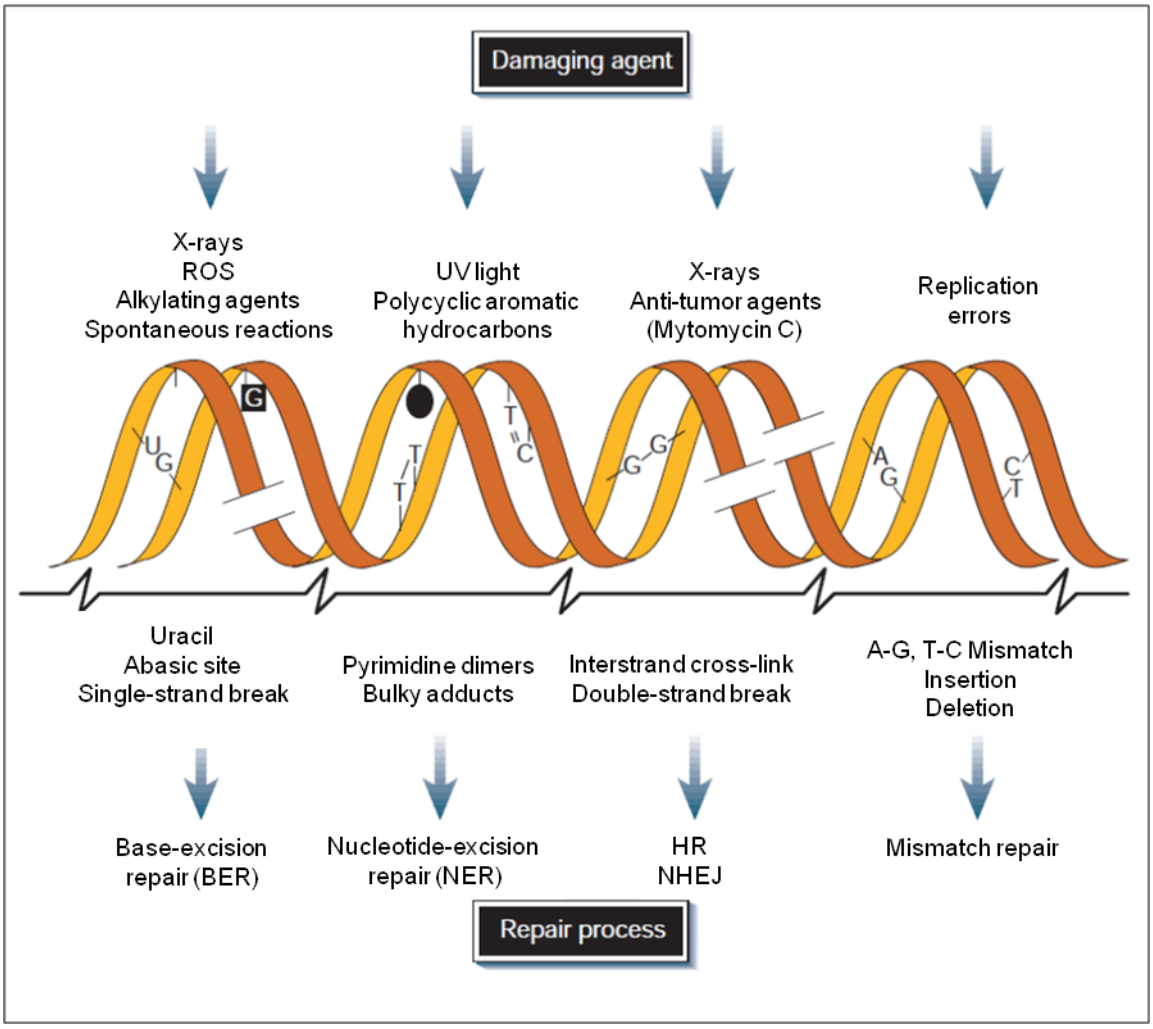

Figure 1 Illustration of DNA damage and repair mechanisms.
Common DNA damaging factors (top); examples of DNA lesions caused by these factors (middle); and repair mechanism responsible for removal of the lesions (bottom). ROS, reactive oxygen species; HR, homologous recombination; NHEJ, non-homologous end joining (Hoeijmakers, 2001).

2.2 Repair of DNA double-strand breaks by homologous recombination

DSB is the most toxic form of DNA lesion in the cell. Inappropriate repair of broken DNA strands may result in generation of harmful genomic rearrangements, such as DNA translocations that are common in many tumors. Although DSBs are often considered by the cell as DNA damage that needs to be repaired, there are several specialized cellular processes that generate DSB as part of normal programmed genomic rearrangement. Examples of this are V(D)J recombination, which is important for production of a diverse antibody repertoire in the immune system (Soulas-Sprauel et al., 2007), class-switch recombination, which is responsible

for the creation of antibody isotypes (Bransteitter et al., 2006) or recombination between homologous chromosomes in meioses (Neale and Keeney, 2006). Unscheduled DSBs pose a serious threat for the cell. They must be repaired quickly and with sufficient accuracy to restore the integrity and functionality of the genome.

As mentioned above, cell has two main pathways to correct DSBs: NHEJ and HR. The most straightforward way to repair a DSB is simply to rejoin the broken ends regardless of the genetic sequence at the break. This process is called NHEJ. The ends of the broken DNA are recognized and targeted for NHEJ through the high affinity binding of the heterodimeric Ku70/80 complex (Mimori and Hardin, 1986) and processed to join directly (Pfeiffer and Vielmetter, 1988, Thode et al., 1990). In mammalian cells, NHEJ is the prominent pathway for DSBs repair and during the cell cycle it functions predominantly in G1 phase (Delacôte and Lopez, 2008). However, because of frequent lost of nucleotides at the break site, this pathway is considered to be error-prone and does not guarantee the preservation of genetic stability (Guirouilh-Barbat et al., 2004).

HR is, in contrast to NHEJ, an accurate and error-free repair mechanism of DSBs. HR relies on the presence of an intact homologous duplex, generally sister chromatid, to template the repair of the broken chromosome (Pâques and Haber, 1999). Mechanism of HR will be discussed in more detail in the following chapter. This repair pathway requires the presence of homologous DNA and functions therefore preferentially during the S and G2 phase of the cell cycle where the sister chromatid is available (Takata et al., 1998). Products of HR are gene conversion associated either with or without crossing-over, a reciprocal exchange of adjacent sequences. Gene conversion (asymmetric transfer of genetic information) between two heteroalleles can result in loss of heterozygosity, or can transfer an inactivating mutation from one pseudo-gene to one related active gene. Excessive HR events can thus generate mutagenic alterations. Evidently, HR must be carefully regulated to match specific cellular needs.

The cellular mechanism that regulates the decision between NHEJ and HR is not yet elucidated. Recent studies in mammalian cells suggest that tumor suppressor protein CtIP, which is a central regulator of DNA resection (Sartori et al., 2007), shifts the balance of DSB repair from NHEJ to HR according to the cell cycle phase (Yun and Hiom, 2009, You and Bailis, 2010).

2.2.1 Mechanism of homologous recombination

The classical model of DSB repair by HR predicts several distinct outcomes through two main subpathways (Figure 2), termed "double-strand break-repair" (DSBR) and "synthesis dependent strand annealing" (SDSA) that have identical initial steps.

To initiate HR, the ends of the broken DNA are resected by 5´to 3´ nucleolytic degradation to create an extended region of 3´ ssDNA that serves as substrate for the HR machinery. This step is mediated by the MRE11/RAD50/NBS1 (MRN) complex (Lamarche et al., 2010), which is the primary damage sensor in the cellular response to DSBs. It binds to DSBs to promote DNA end processing and takes part in activation of ATM , the DNA damage checkpoint kinase (Assenmacher and Hopfner, 2004). MRN complex also activates the CtIP protein, which is responsible for DNA end resection (Yun and Hiom, 2009).

In the second step, the resulting ssDNA tail is rapidly coated by replication protein A (RPA), an essential eukaryotic ssDNA-binding protein. RPA is a heterotrimeric complex that stabilizes ssDNA regions. Next, RAD51 recombinase assembles onto the ssDNA to form a nucleoprotein filament (also known as nucleofilament or presynaptic filament), the catalytic core of HR. The resulting RAD51 nucleoprotein filament then searches for a homologous sequence within dsDNA and promotes the invasion of the ssDNA into the homologous dsDNA target to create a three-stranded DNA intermediate called displacement loop (D-loop). Both, RPA and RAD51 will be further described in the following chapters 2.2.2 and 2.2.3, respectively.

Nucleoprotein filament assembly as well as D-loop formation are dependent on several recombination mediators and accessory proteins (San Filippo et al., 2008). Firstly, the nucleation of the RAD51 recombinase onto ssDNA is a slow process, because the RPA proteins compete with RAD51 for sites on the ssDNA and pose a challenge to successful nucleoprotein filament assembly. To overcome the inhibitory effect of bound RPA, mediator proteins such as BRCA1, BRCA2, the RAD51 paralogs (RAD51B, RAD51C, RAD51D, XRCC2 a XRCC3) and RAD52 serve to promote filament assembly. Secondly, dsDNA translocases such as RAD54 and RAD54B assist RAD51 in search for DNA homology and stimulate D-loop reaction (Heyer et al., 2006, Sugiyama and Kowalczykowski, 2002).

In the following stage of HR, the invaded DNA strand is extended from the 3´-end by DNA synthesis catalyzed by DNA polymerase eta utilizing the intact DNA template (McIlwraith et al., 2005).

The DSBR model predicts that the second end of the break is captured by the displaced strand from the D-loop and is used to prime a second round of leading strand DNA synthesis. The resulting DNA heteroduplex contains a double Holliday junction (dHJ) structure, the

intermediate needed to be resolved to allow the repaired DNA molecules to separate. This step is carried out by specialized endonucleases, so-called resolvases, that can bind to an HJ and introduce two symmetrically related cuts in the DNA strands at the junction. Depending on which pairs of DNA strand are nicked, dHJ resolution can give rise to crossover or non-crossover products (Sung and Klein, 2006).

During the SDSA, the invading strand that has been extended by DNA synthesis is displaced and anneals to the second resected DSB end. The remaining gaps can be filled by DNA synthesis and the nicks ligated. This subpathway forms only non-crossover products (San Filippo et al., 2008).

Generation of crossovers by dHJ resolution can have stabilizing, but also destabilizing effects on the genome. In meiosis, crossovers are highly regulated such that at least one crossover occurs between each pair of homologous chromosomes, yet excess crossovers are suppressed (Champion and Hawley, 2002). In mitosis, crossovers pose serious risk of large-scale genome alterations. The SDSA repair mechanism reduces the potential for genomic rearrangements and is therefore the predominant pathway of HR-mediated repair of DSBs (Sung and Klein, 2006).

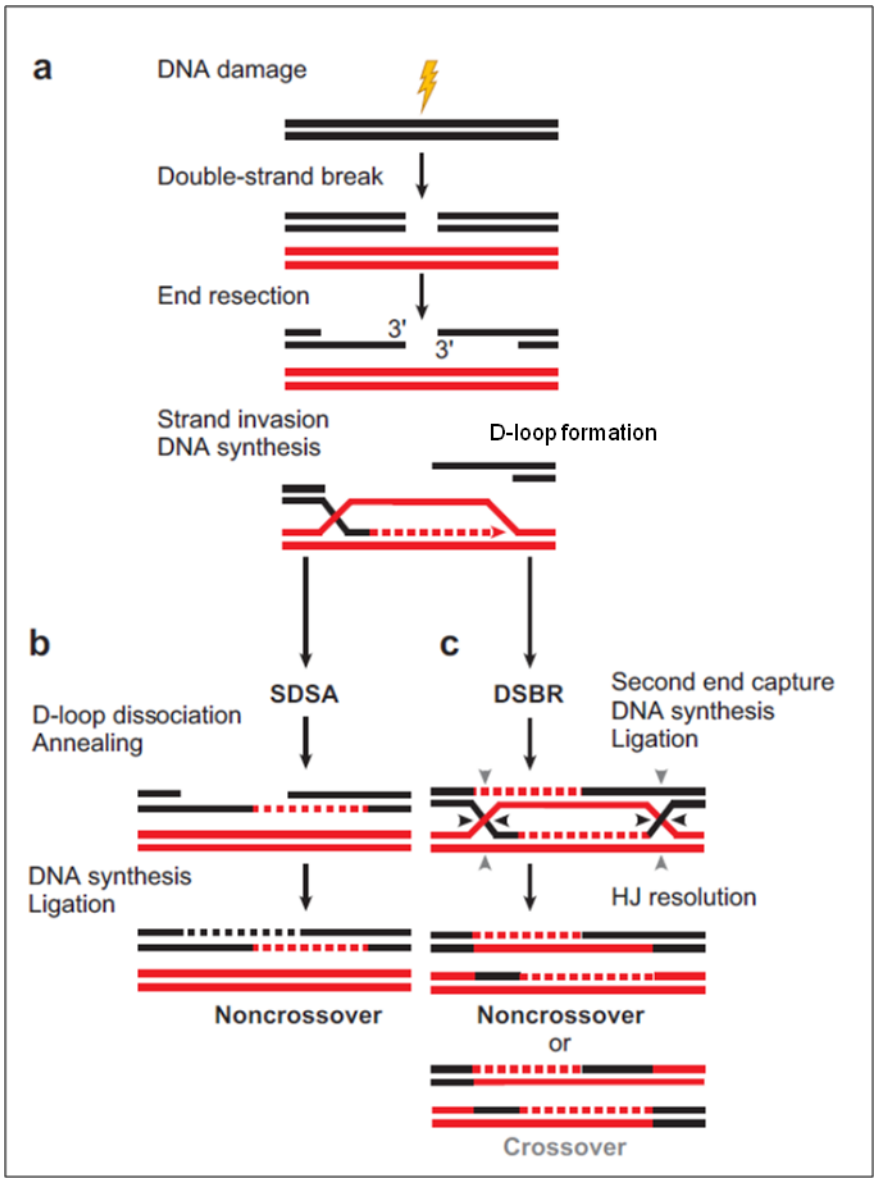

Figure 2 Schematic model of repair of DNA double-strand breaks by homologous recombination. Double-strand breaks (DSBs) can be repaired by two principal homologous recombination (HR)-mediated subpathways, including synthesis-dependent strand annealing (SDSA) and classical double-strand break repair (DSBR). (a) In both pathways, repair is initiated by DSB resection to provide 3´ single-stranded DNA (ssDNA) overhangs, which become a substrate of the HR protein machinery to catalyze a search for homologous sequence in a partner chromosome. Strand invasion and D-loop formation are followed by DNA synthesis. (b) In the SDSA subpathway, the D-loop is displaced and the extended ssDNA anneals to ssDNA overhang on the other break end. The gaps are filled by DNA synthesis and the reaction is completed by ligation. The repair products of SDSA are always non-crossovers. (c) Alternatively, the second DSB end can be captured to form an intermediate with two Holliday junctions (HJs). After gap-filling DNA synthesis and ligation, the structure is resolved at the HJs to give rise to non-crossover (black triangles) or crossover (gray triangles) products (San Filippo et al., 2008).

2.2.2 The Replication protein A

The single-stranded DNA binding proteins (SSBs) are ubiquitous molecules present in all organisms. They bind and thus stabilize ssDNA regions. Among them, RPA is the major eukaryotic SSB protein. It consist of three subunits including RPA70, RPA32 and RPA14 (Figure 3), where the numbers indicate approximate molecular weight in kDa (Wold, 1997). As a heterotrimer, RPA binds tightly to ssDNA via oligonucleotide binding (OB)-folds (Bochkareva et al., 2002). The DNA binding activity has been localized predominantly to the 70-kDa subunit. dsDNA and RNA can also serve as binding substrate for RPA, however the affinity is at least three times lower than its affinity to ssDNA (Wold and Kelly, 1988).

In the cell, RPA plays essential roles in many aspects of DNA metabolism, including DNA replication, DNA repair, DNA recombination, telomere maintenance and DNA damage signaling. In response to DNA damage, RPA becomes phosphorylated (Brush et al., 1994) by checkpoint kinases including ATM, ATR and DNA-PK. This modification may change the functions of RPA, and thus the activities of individual pathways in which it is involved (Zou et al., 2006).

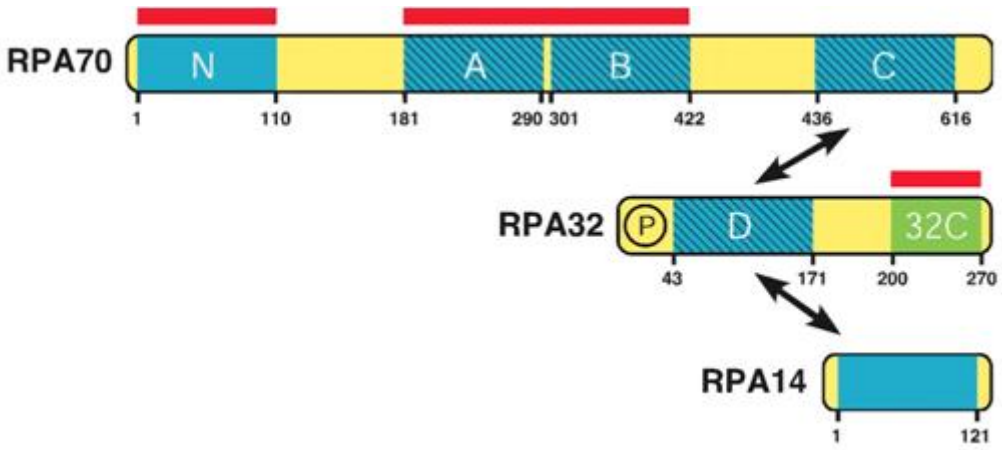

Figure 3 Schematic diagram of domain structure of RPA.
Replication protein A (RPA) is heterotrimeric complex, which consists of RPA70, RPA32 and RPA14 subunits. Domains are presented as boxes: oligonucleotide binding (OB)-folds in blue; single-strand DNA binding domains A-D by hatching; winged helix domain in green; protein-protein binding domains in red bars; site of phosphorylation by a circled P; regions of subunit interaction are indicated by arrows; numbers under each subunit denote the domain edge in amino acids (Fanning et al., 2006).

RPA has been found to interact specifically with various proteins. During HR, RPA has been shown to interact with RAD51, RAD52, BRCA1, BRCA2, p53 to modulate their activities (Zou et al., 2006). Although many different proteins interact with RPA, the RPA70 seems to be the main subunit responsible for protein interactions. There is evidence that RPA32 also participates in protein-protein interactions via C-terminal winged helix domain (Wold, 1997). RPA32 becomes phosphorylated at its N-terminus in a cell-cycle dependent manner and in response to DNA damage (Liu and Weaver, 1993, Treuner et al., 1999). RPA70 alone cannot fulfill its proper function, demonstrating that the 32-kDa and 14-kDa subunits of RPA are essential.

Depending on the circumstances, RPA can exert a stimulatory or an inhibitory effect on the nucleoprotein filament formation. RPA may facilitate filament assembly via removal of possible secondary structure present on the ssDNA (Eggler et al., 2002). On the other hand, RPA poses a hurdle for an efficient RAD51 polymerization on the ssDNA (Fanning et al., 2006).

2.2.3 The RAD51 recombinase

The catalytic core of the HR machinery is composed of proteins belonging to the RecA/Rad51 family of recombinases that assemble into nucleoprotein filament on ssDNA to promote pairing of homologous DNA molecules and strand exchange. In most eukaryotes, two orthologs of *Escherichia coli* (*E. coli*) recombinase RecA are present: RAD51 and DMC1 (Figure 4). Both have the unique ability to search for homologous sequence and to catalyze the exchange of DNA strands. Whereas RAD51 is ubiquitously expressed, DMC1 expression is restricted only to meiosis. In higher eukaryotes, RAD51 is essential, as indicated by the embryonic lethality associated with RAD51 deletion from the mouse genome (Lim and Hasty, 1996, Tsuzuki et al., 1996).

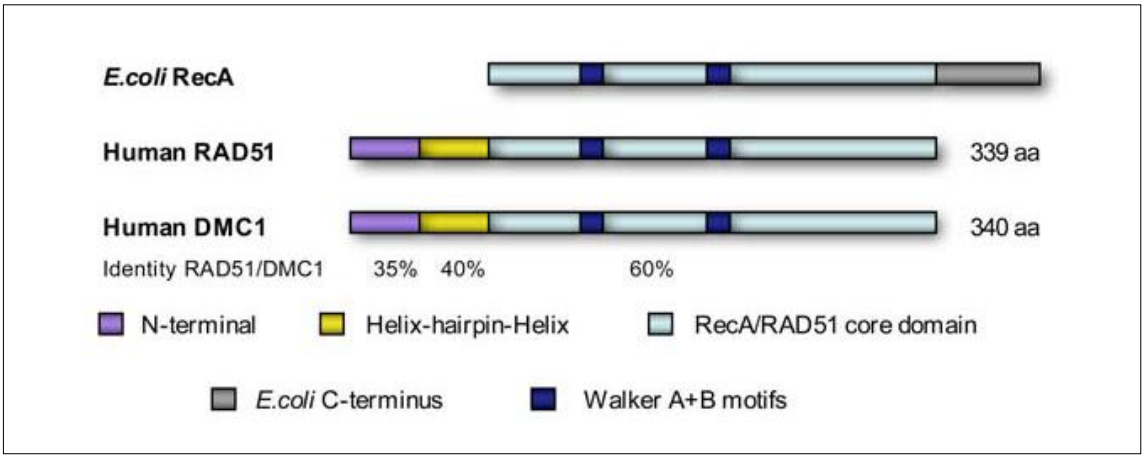

Figure 4 The RecA/RAD51 family of recombinases.
Schematic illustration of *Escherichia coli (E. coli)* RecA, human RAD51 and human DMC1 proteins. Domains and regions are represented as boxes of different colors according to the key at the bottom of the figure (Thorslund and West, 2007).

The human RAD51 recombinase is relatively small protein of about 37 kDa and shares with other members of family a large core domain containing the Walker A and B motifs responsible for binding and hydrolysis of ATP. RAD51 exists as homo-oligomer and, in solution, forms heptameric ring structure (Figure 5) (Shin et al., 2003). RAD51 binds to both, dsDNA and ssDNA, but its preferred substrate is dsDNA with ssDNA overhangs (Mazin et al., 2000). On ssDNA, RAD51 polymerases to create a highly ordered, right-handed helical nucleoprotein filament, the catalytically active form (Ogawa et al., 1993). The nucleoprotein filament is capable to hold three DNA strands, a ssDNA and a homologous double helix, to allow them to test the complementarities and exchange strands if a match is found (Sinha and Peterson, 2008).

Binding of ATP to the Walker motif A is an important prerequisite for catalytically competent RAD51 filament activity. ATP hydrolysis is linked to dynamic disassembly of the filament (Ristic et al., 2005). The fast turnover of the RAD51 filament is thought to generate an intracellular pool of free RAD51 proteins available for HR and DNA repair reactions (Chi et al., 2006).

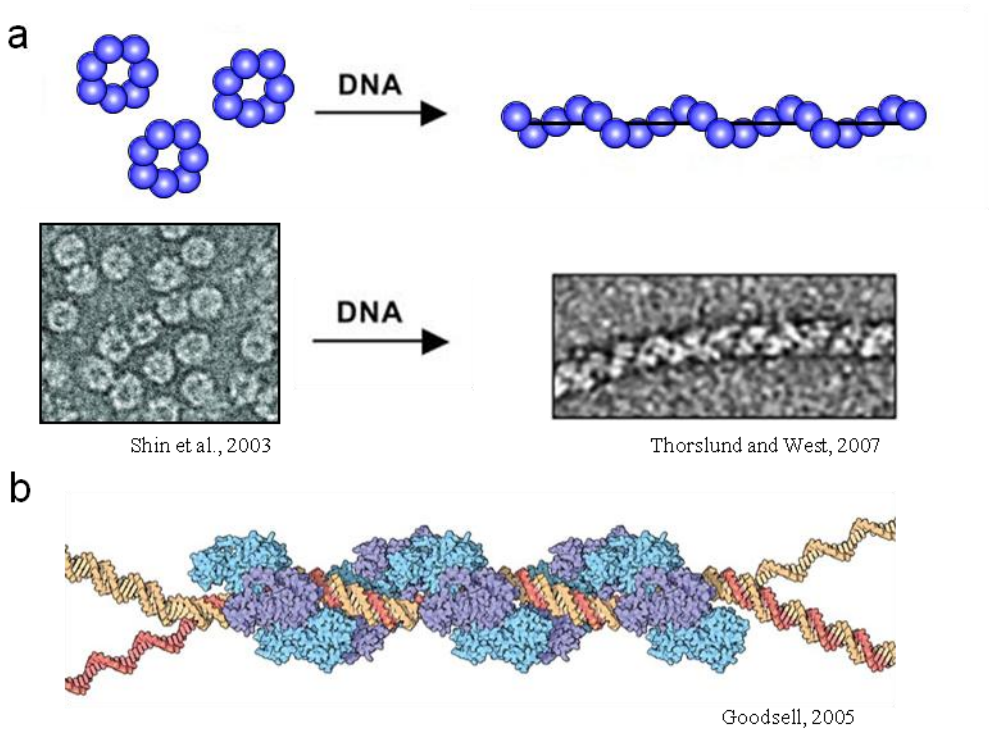

Figure 5 Illustration of RAD51 structure and nucleoprotein filament.
a) In solution, RAD51 forms heptameric ring structures (left), whereas in the presence of single-strand DNA (ssDNA), RAD51 monomers assemble into a highly ordered right-handed nucleoprotein filament (right), as indicated schematically and by electron microscope visualization (Shin et al., 2003, Thorslund and West, 2007). **b)** The nucleoprotein filament on triplex DNA. RAD51 in shown in blue and violet, ssDNA in pink, and homologous duplex DNA in yellow, (Goodsell, 2005).

2.2.4 Regulation of homologous recombination

Recombinational DNA repair is not constitutive but is tightly controlled by positive and predominantly negative regulatory mechanisms (Heyer et al., 2010). There are many stages where HR can be regulated. The most salient regulatory stages represent: 3´ ssDNA resection, nucleoprotein filament assembly, D-loop structure formation and dHJ resolution. A class of enzymes known as recombinases and large spectrum of other specialized proteins have been involved in the proper modulation of certain steps in HR (Holthausen et al., 2010). In the following part, I will focus only on the regulation of nucleoprotein filament assembly in more details.

2.2.5 Regulation of nucleoprotein filament assembly

The nucleoprotein filament poses an ingenious checkpoint for HR regulation. The efficiency of HR is enhanced by mediator proteins, such as Rad52 in yeast (Sugiyama and Kowalczykowski,

2002), that promote the loading of Rad51 onto ssDNA. On the other hand, specialized DNA helicases (DNA helicases are described in following chapter) have the ability to translocate along the ssDNA and remove RAD51 from the nucleoprotein filament. Specifically, Srs2 helicase (described in chapter 2.3.3) in yeast and RECQ5 helicase (described in chapter 2.3.5) in mammals have been shown to harbour this competency (Colavito et al., 2010). Through this action, these helicases efficiently prevent undesirable HR events.

2.3 DNA helicases

Helicases are ubiquitous enzymes with nucleic acid-dependent NTPase activity to move along the DNA and catalyze breaking of hydrogen bonds that hold the DNA strands together. Although DNA helicases were discovered on the bases of the ability to catalyze separation of the complementary strands of dsDNA during replication, recombination and DNA repair, it is now evident that this class of enzymes also functions in a range of other biological processes, including displacement of proteins from DNA, remodeling of chromatin, movement of HJs, and the catalysis of various of nucleic acid conformational changes (Tuteja and Tuteja, 2004). Recently, it has become clear that several putative helicases use NTP to translocate with biased directionality along ss- or dsDNA, they are so-called translocases. Selected few helicases/translocases endowed with the ability of displacement of proteins from either ss- or dsDNA (Lohman et al., 2008, Singleton et al., 2007). Therefore, it is not surprising that most organisms encode multiple helicases, for example, *E. coli* has at least 12 and humans even 24 different helicases (Tuteja and Tuteja, 2004).

Studies over the last decades have identified a variety of helicases that differ in both structure and mechanism of reaction. Helicases have been classified into six superfamilies (SF), SF1-SF6, based on the presence and organization of short conserved amino acid (aa) sequences (Q, I, Ia, Ib, II, III, IV, V and VI), called helicase motifs (Singleton et al., 2007). DNA helicases move along the DNA with a processivity and directionality, i.e. 3´ to 5´ or 5´ to 3´, specific to each particular enzyme. Some of them are active as monomers, some of them as oligomers (Singleton et al., 2007).

The well known ring-shaped hexameric helicases, which encircle the nucleic acid and move usually in the 5´ to 3´ direction, function mainly, but not exclusively, as the primary helicases in DNA replication. However the majority of helicases/translocases is non-hexameric and belongs to SF1 and SF2. The two largest SFs, SF1 (Figure 6) and SF2, contain at least seven conserved helicase motifs (I, Ia, II-VI) in their primary structure. Motifs I and II are equivalent to the classical Walker A (phosphate-binding loop) and Walker B (Mg^{2+}-binding

site) motifs found in ATPases, respectively (Walker et al., 1982). Well-characterized members of SF1 are the bacterial helicases Rep, PcrA, UvrD and the *Saccharomyces cerevisiae* (*S. cerevisiae*) Srs2. Intensively studied members belonging to SF2 are, for example RecQ family helicases.

The importance of DNA helicases is underscored by the numerous human diseases such as Werner syndrome, Bloom syndrome, Rothmund-Thomson syndrome or Xeroderma pigmentosum, that are associated with defective helicases/translocases (Wu and Hickson, 2006).

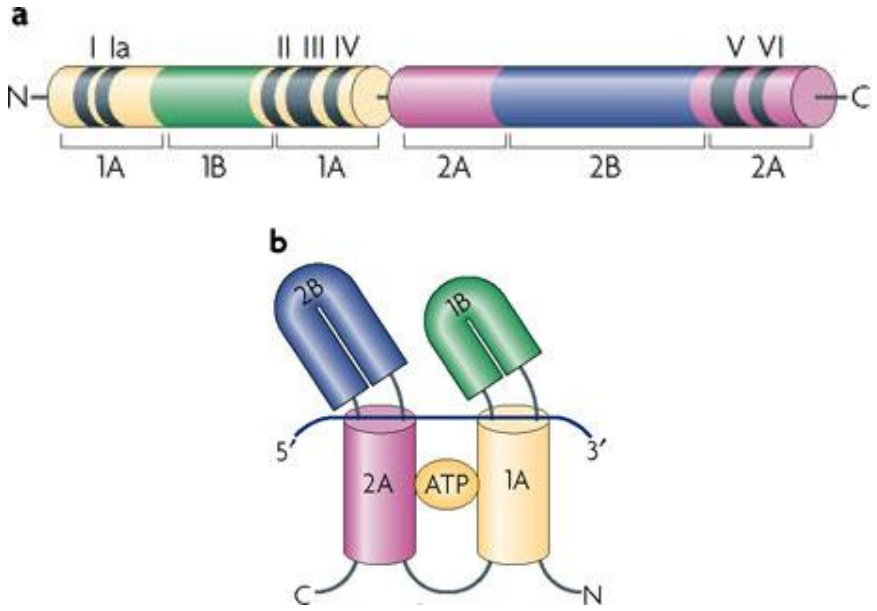

Figure 6 Domain structure of Superfamily 1 helicases/translocases.
a) Superfamily 1 (SF1) of helicases/translocases contains seven conserved helicase motifs (I, Ia, II-IV). The protein structure of these helicases is divided into two domains (1 and 2) that are further organized into two subdomains (1A and 1B; 2A and 2B). **b)** Modular model of folding of the helicase subdomains with regard to single-stranded DNA, shown as blue line, and ATP (Lohman et al., 2008).

2.3.1 Antirecombinases

DNA helicases control HR pathways at several stages and affect HR in both a positive and a negative manner. So-called prorecombinases are believed to positively modulate HR to promote the repair process. As antirecombinases are collectively termed DNA helicases/translocases, which negatively regulate HR pathway, thus, suppress crossovers production (Wu and Hickson, 2006). Helicases with antirecombinase function are conserved from bacteria to human.

In the following sections, I will emphasize several important enzymes, which were shown to exert antirecombinase activity, involving UvrD, Srs2, BLM, RECQ5, and RTEL1. FBH1, the subject of this thesis is described in more detail in chapter 2.4.

2.3.2 The bacterial UvrD helicase

Bacterial UvrD is the founding member of SF1 helicases. It translocases along ssDNA in the 3´ to 5´ direction (Matson and George, 1987). UvrD can act as monomers or dimers. Beside its critical role in replication, repair of mismatched base pairs, UvrD possesses antirecombinase activity by dismantling RecA (the bacterial RAD51 ortholog) nucleoprotein filament and inhibits RecA-mediated strand-exchange reaction *in vitro* (Veaute et al., 2005).

2.3.3 The yeast Srs2 helicase

Srs2 helicase, a central player in regulation of HR in *S. cerevisiae* and *S. pombe* (Wang et al., 2001), is the best understood eukaryotic antirecombinase. It belongs to the SF1 helicase family and is structurally and functionally related to the UvrD helicase (Colavito et al., 2009). Experimental data showed that Srs2 restricts inappropriate recombination events by Rad51 nucleoprotein filament disassembly (Krejci et al., 2003, Veaute et al., 2003). Mutations in the *SRS2* gene exert elevated level of crossover products after DNA damage (Chanet et al., 1996). Additionally, further experiments suggest that Srs2 promotes DSB repair by SDSA pathway to generate harmless non-crossover products (Dupaigne et al., 2008). Although Srs2 is conserved in budding and fission yeast, no direct Srs2 homolog have been found in higher eukaryotes.

2.3.4 The human BLM helicase

BLM belongs to a highly conserved RecQ family of helicases. This whole group of proteins is actively involved in genome surveillance. Beside BLM helicase, RecQ family includes five members (Figure 7), namely RECQ1, WRN, RECQ4 and RECQ5, in humans. What makes RecQ helicases subject of intense research is their implication in human diseases. Loss of function of three of the five RecQ family genes (*BLM*, *WRN* and *RECQ4*) has been shown to give rise to inheritable disorders Bloom´s, Werner´s and Rothmund-Thomson´s syndrome, respectively, associated with genomic instability, cancer predisposition, developmental abnormalities and premature aging (Hanada and Hickson, 2007).

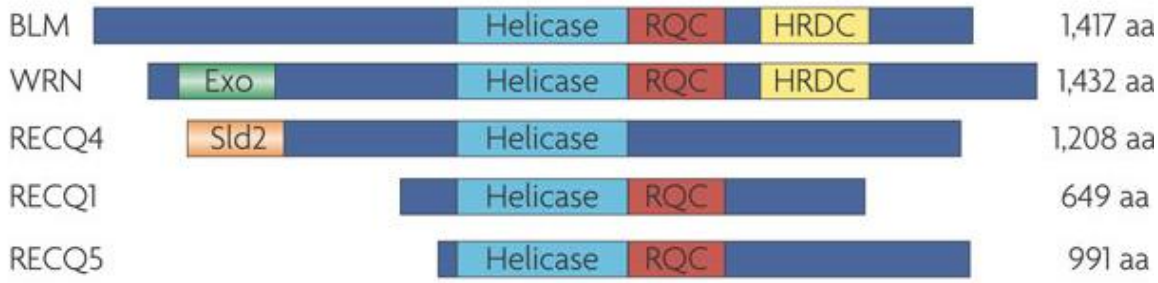

Figure 7 The human RecQ family of helicases.
Members of humans RecQ family, BLM, WRN, RECQ4, RECQ1 and RECQ5β are shown. Proteins are aligned by the conserved helicase domain, which is shown as a light blue box. The additional domains included are illustrated as follows: RecQ carboxy-terminal (RQC) by red box; Helicase and RNase D C-terminal (HRDC) by yellow box; exonuclease (Exo) domain in green box; and Sld2-like domain is depicted in orange. Here, only the largest isoform of RECQ5, RECQ5β, is shown. The size in amino acids (aa) of each protein is displayed on the right (Chu and Hickson, 2009).

Bloom helicase (BLM) is named after Bloom´s syndrome, a rare autosomal recessive disorder caused by mutation in its gene. Patients with this syndrome are predisposed to development of most types of cancer (Hickson, 2003). Among the human RECQ helicases, BLM has the unique property to display a broad spectrum of activities that exert both pro- and anti-recombinase character at different stages (Bugreev et al., 2007). In the early phase of HR, BLM can prevent premature initiation of recombination events by disrupting RAD51 nucleoprotein filament. On the other hand, it may also stimulate recombination by co-operation with exonuclease EXO1 to resect one strand of the broken DNA to generate 3´ ssDNA overhangs. Recent studies also showed that BLM is active at later stages of HR, where it may catalyze the D-loop dissociation to push the repair process to non-crossover SDSA pathway (Bugreev et al., 2007, van Brabant et al., 2000, Wu and Hickson, 2003).

2.3.5 The RecQ5 helicase

The human RECQ5 protein is another representative of RecQ family helicases. It exists in 3 different isoforms resulting from alternative splicing of the RECQ5 transcript. The variants are RECQ5α, RECQ5β (here referred to RECQ5) and RECQ5γ (Sekelsky et al., 1999, Shimamoto et al., 2000). Only the largest form RECQ5 possesses the zinc-finding motif (a region responsible for DNA binding), exhibits ATP-dependent 3´ to 5´ helicase activity and localizes in nucleus (Garcia et al., 2004). Recent data indicate that RECQ5 physically interacts with RAD51 and has the capability to disrupt nucleoprotein filament (Hu et al., 2007, Schwendener et al., 2010). At present, no genetic disease has been associated with RECQ5 dysfunction.

Nevertheless, RECQ5 deficiency in mice is associated with cancer susceptibility, suggesting that RECQ5 acts as a tumor suppressor (Hu et al., 2007).

2.3.6 The RTEL1 helicase

Recent studies have revealed that RTEL1, the regulator of telomere elongation helicase 1, is one of the putative Srs2 functional homolog. It plays an essential role in genome and telomere length maintenance. After DNA damage, RTEL1 is recruited to DSB, where it acts as antirecombinase by D-loop disassembly to promote harmless SDSA repair subpathway. Dysfunction of RTEL1 is linked to glioma predisposition (Ding et al., 2004, Barber et al., 2008, Uringa et al., 2011).

2.4 The F-box DNA helicase 1

F-box DNA helicase I (Fbh1; also known as FBXO18 according the Human Genome Organization Gene Nomenclature Committee) was first isolated by Park and colleagues from *S. pombe* as a DNA helicase I (Park et al., 1997). Its human homolog, FBH1, has been identified by the same group few years later (Kim et al., 2002). Further biochemical and bioinformatic screening revealed that FBH1 harbors 7 conserved helicase motifs at the C-terminus and belongs to UvrD class of SF1 family of helicases. Currently, there are 4 isoforms of FBH1 that vary in the N-terminal part (Internet source 1). The longest version of FBH1 with 1094 aa, isoform 1, isoform 2 that has 1043 aa, isoform 3 with 986 aa, and the shortest, isoform 4 spanning 969 aa (Figure 8). Homologs of the human FBH1 have been found in mammals, birds and *S. pombe*. However, FBH1 is absent in organisms such as fish, frog, fruit fly, plants and *S. cerevisiae* (Chiolo et al., 2007, Kim et al., 2002, Park et al., 1997, Osman et al., 2005). As a DNA helicase, FBH1 posses ATPase activity and translocates in the 3´ to 5´ direction preferentially on ssDNA (Kim et al., 2002).

Interestingly, beside the helicase domain FBH1 is endowed by presence of highly conserved F-box motif at the N-terminal part (Kim et al., 2002). This is a feature, which makes FBH1 unique among all DNA helicases.

Figure 8 A schematic outline of FBH1 isoforms.
Four FBH1 isoforms are shown. The F-box motif is shown as violet box and the helicase domain as red box. The numbers on the right denote length of each protein in amino acids (aa).

2.4.1 FBH1 as a member of SCF complex

The presence of the F-box motif allows FBH1 to act as an F-box protein, which is the interchangeable element of multisubunit enzyme, the SCF complex (named after the main components, Skp1, Cullin, and an F-box protein) (Figure 9). When established, the SCF complex functions as an E3 ubiquitin ligase, which specifically targets substrates for degradation in proteasome.

The SCF complex is a multiprotein enzyme composed of an invariant core containing three basic components:

- Skp1 is an adaptor protein, which is responsible for recognition and binding of F-box proteins *via* the F-box motif.
- Cullin functions as a scaffold element of the complex to link the Skp1 protein with Rbx1 protein.
- Rbx1 protein possesses a RING finger domain and mediates binding to the E2 (ubiquitin-conjugating) enzyme.

The substrate specificity of the SCF complex is dictated by the interchangeable F-box protein that recruits specific set of proteins for ubiquitination and proteosomal degradation. In general, phosphorylation of the target substrate is a common prerequisite for recognition by individual F-box protein. The ability of the Skp1 protein to bind to multiple F-box proteins with distinct substrate specificities substantially increases the target protein repertoire (Bai et al., 1996, Cardozo and Pagano, 2004).

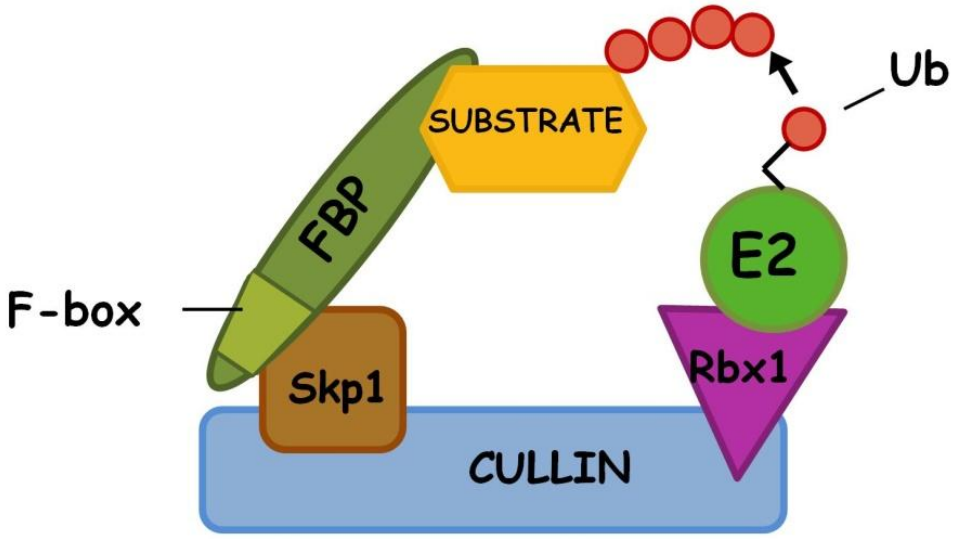

Figure 9 A schematic model of SCF complex.
The core of the SCF (Skp1-Cullin-F-box) complex constitutes of four major compounds: F-box protein (FBP) containing F-box motif, adaptor protein Skp1, scaffold protein Cullin and Rbx1. E2, ubiquitin-conjugating enzyme; Ub, ubiquitin.

2.4.2 FBH1 as an F-box protein

The F-box motif, approximately 50 aa long region (Figure 10), is a protein-protein interaction site, generally present at the N-terminal half of a protein. The name is derived from its

occurrence in cyclin F, the first protein in which this motif was identified (Bai et al., 1996). F-box proteins constitute a large family in eukaryotic kingdom. For instance, 69 representatives of the F-box protein family have been identified in human to date (Internet source 2), ~20 in yeast species (Skaar et al., 2009), ~30 in *Drosophila melanogaster* (Ou et al., 2003), ~520 in *Caenorhabditis elegans* (Thomas, 2006), and ~700 in *Arabidopsis thaliana* (Gagne et al., 2002).

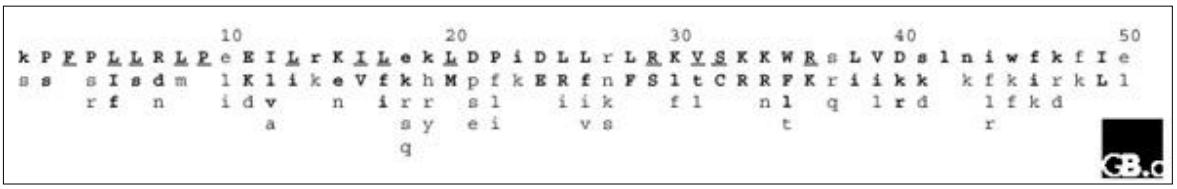

Figure 10 A consensus sequence of F-box motif.
The single-letter amino acid code is used. The most prevalent residues at each position within the alignment are shown as bold and underlined capital letters. Similar residues are represented as bold and non-underlined capital letters. Amino acids exhibiting less than 20% overall similarity are signified as bold lower case letters and the residues found in 10-14% of the F-box sequences are shown as non-bold lower case letters. The consensus was generated from alignment of 234 sequences. Digits above the residues sequence show the length in amino acids (Kipreos and Pagano, 2000).

F-box proteins are sorted out into three major groups based on the type of substrate interaction domain identified in addition to the F-box motif. The two most common of which are leucine-rich repeats, FBXL, and WD40 domain, FBXW group. In the third group of F-box proteins, FBXO, various other type of domain is present or absent at all (Jin et al., 2004). FBH1 protein falls into the last group of F-box proteins, FBXO (Figure 11), and moreover, FBH1 is the only example of the F-box protein family that retains intrinsic enzymatic activity.

Not only FBH1 alone, but also bound to the SCF complex (SCF^{FBH1}) retains ATPase activity and can act as DNA helicase to translocate along the ssDNA (Kim et al., 2004). The multiple activities present in the SCF^{FBH1} complex are independent of each other, so that the enzyme can possibly function as E3 ubiquitin ligase while translocating along the DNA.

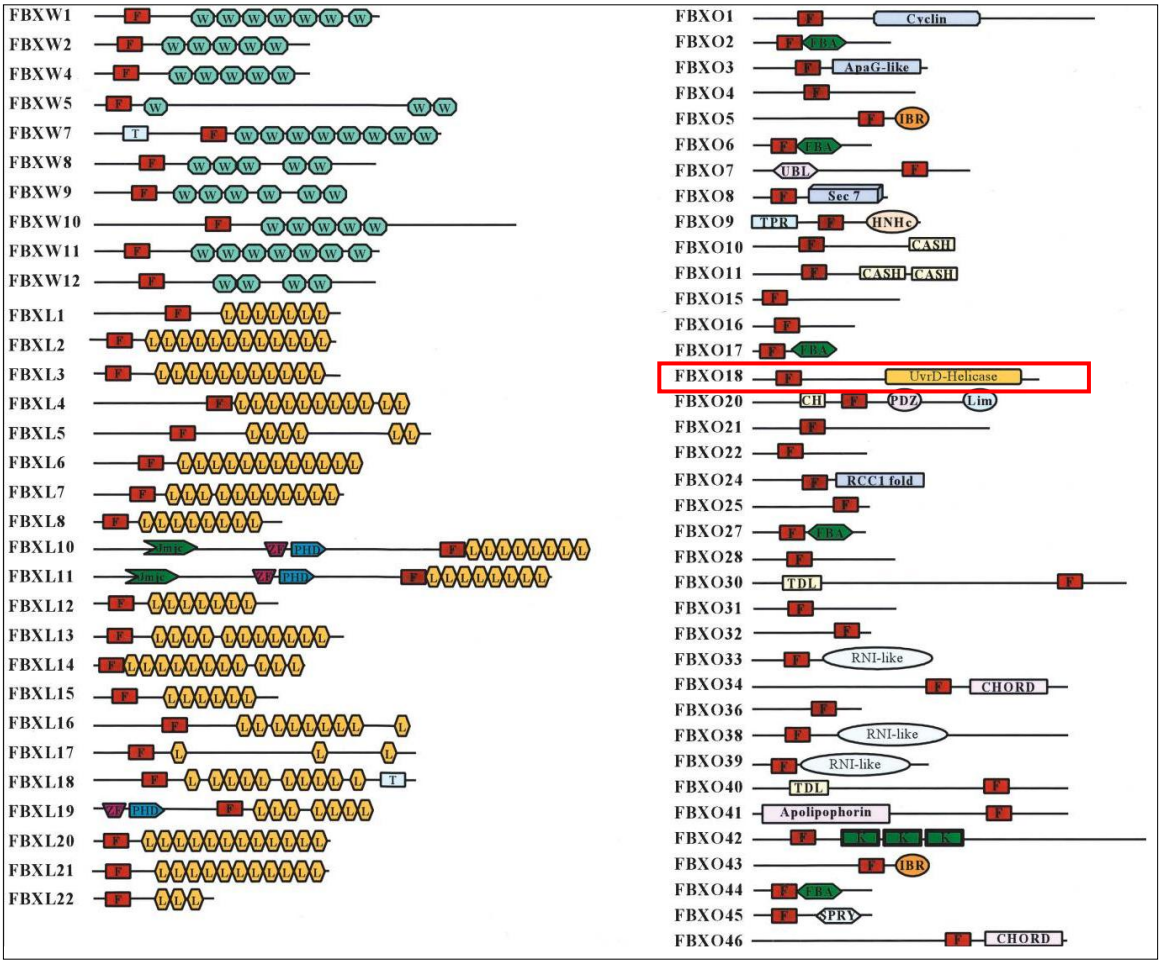

Figure 11 Domain organization of representative F-box proteins.
The family of mammalian F-box proteins is grouped into three classes, FBXW, FBXL and FBXO. FBXW includes proteins with an F-box (F) and WD40 (W) repeats; FBXL includes proteins with an F-box and leucine-rich repeats (L); and FBXO denotes proteins with an F-box and either another or no other motifs. The other less common protein motifs are: transmembrane domain (T); F-box associated domain (FBA); between-ring domain (IBR); domain in carbohydrate binding proteins and sugar hydrolases (CASH); kelch repaet (K); calponin homology domain (CH); domain found in cupin metalloenzyme family (Jmjc); domain present in PSD-95, Dlg, and ZO-1 (PDZ); zinc-binding domain found in Lin-11, Isl-1, and Mec-3 (Lim); HNH nuclease family (HNHc); novel eukaryotic zinc-binding domain (CHORD); tetratrico peptide repeat (TPR); ApaG-like domain (ApaG-like); ubiquitin-like fold (UBL); Traf-domain like (TDL); Apolipophorin; RNI-like; and RCC1. FBH1 (FBXO18), highlighted by the red box, is the only F-box protein containing enzymatic (UvrD helicase) activity (Jin et al., 2004).

Beside its role in the SCF complex, the F-box motif is further required for both the recruitment of FBH1 to nucleus and DNA damage-induced foci formation (Sakaguchi et al., 2008, Kim et al., 2004), showing that the F-box motif, the element responsible for binding of Skp1, is necessary for the proper catalytic function of FBH1.

At present, target substrate of SCF^{FBH1} complex has not been identified. Recent experiments in *S. pombe* revealed one potential ubiquitination target recognized by Fbh1, however without any known role during DNA repair. It is a transcription factor Atf1, which plays a vital role in stress-induced response in *S. pombe* (Lawrence et al., 2009, Lawrence et al., 2007). In absence of stress, Atf1 is basally phosphorylated, recognized by Fbh1 and targeted for degradation. Upon the stress exposure, Atf1 becomes hyper-phosphorylated and no recognition occurs (Lawrence et al., 2009). Since the most of F-box protein–substrate interactions are mediated positively by phosphorylation, this kind of recognition is very untypical among the F-box protein family.

2.4.3 Role of FBH1 as DNA helicase

In DNA metabolism, FBH1 is believed to be another member of the group of proteins that control recombination (Osman et al., 2005). The helicase domain of FBH1 is structurally very similar to those present in Srs2 and UvrD (Figure 12). In order to gain more insight into the FBH1 function in the cell, the FBH1 protein has been studied in yeast and human cells. Human FBH1 seems to be a functional homolog of Srs2 in *S. cerevisiae* (Chiolo et al., 2007). Similar to Srs2, FBH1 accumulates at sites of DNA damage and appears to play a role in controlling Rad51 activity (Morishita et al., 2005, Fugger et al., 2009). Evidence for this comes from observation in both *S. pombe* and humans showing that levels of DNA damage-induced RAD51 foci are reduced in cells over-expressing FBH1, whereas spontaneous RAD51 foci increase in FBH1 deficient cells (Morishita et al., 2005, Lorenz et al., 2009, Fugger et al., 2009). Another experiments revealed, that FBH1 is a competitor of Rad22, one of the mediator proteins responsible for Rad51 nucleation in *S. pombe* (Osman et al., 2005). The failure to restrict RAD51 nucleoprotein filament formation in *S. pombe* Fbh1 deficient cells results in elevated levels of sister chromatid exchange (SCE), which can lead to genomic instability (Kohzaki et al., 2007). The exact mechanism, how FBH1 controls RAD51 is currently not known, however it appears to be dependent on its DNA helicase/translocase activity (Sakaguchi et al., 2008, Lorenz et al., 2009). Fugger and colleagues moreover suggest FBH1 to retain prorecombinase activity at sites of replication block (Fugger et al., 2009).

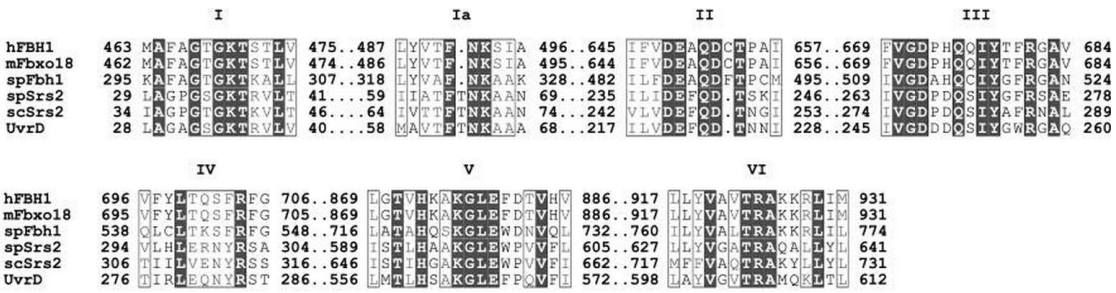

Figure 12 Amino acid sequence alignment of helicase domains present in UvrD-like helicases. Helicases are aligned by the seven helicase motifs (I, Ia, II-IV) found in: *Escherichia coli* (ec) UvrD; *Saccharomyces cerevisiae* (sc) Srs2; *Schizosaccharomyces pombe* (sp) Srs2; *Schizosaccharomyces pombe* Fbh1; mouse (m) Fbox18; and human FBH1. Identical and conserved amino acids are indicated by gray and white boxes, respectively. The numbers between individual helicase motifs represent the location in amino acids of each motif within its parent protein (Chiolo et al., 2007).

2.4.4 Role of FBH1 in meiosis and chromosome segregation

Interestingly, very recent studies have shown that FBH1 plays an additional role during meiosis. According to experiments in *S. pombe* and mouse embryonic stem cells, Fbh1 and FBH1 appear to be essential for proper chromosome segregation (Sun et al., 2011, Okamoto et al., 2012, Laulier et al., 2010). Exactly how a failure of Fbh1 function can cause abnormal chromosome segregation is uncertain.

3 Aims of the work

FBH1 DNA helicase is implicated in regulation of homologous recombination. It has been suggested to exert its antirecombinase function through disruption of RAD51 nucleoprotein filaments. However, this proposal has never been tested experimentally. To understand the mechanism of how FBH1 controls RAD51 action, we pursued the following experiments:

1. Preparation of chicken polyclonal antibody against N-terminal fragment of human FBH1.
2. Expression and purification of the wild type and ATPase-dead forms of the human FBH1 protein, and examination of their enzymatic activities.
3. Investigation of the interaction of human FBH1 with RPA and RAD51.
4. Test the ability of human FBH1 to disrupt RAD51 nucleoprotein filament.

4 Material and methods

4.1 Chemicals

Chemicals used:	Company:
25- and 35-oligonucleotide	Microsynth
53- and 93-oligonucleotide	IDT
Acetic adic	Penta
Acrylamide solution	Serva
Agarose	Serva
Ammonium persulphate	Serva
ATP	Fermentas
Bestatin	Biochemica
Boric acid	Penta
Bradford reagent	Biorad
Bromophenol blue	Lachema
BSA	Sigma-Aldrich
Calf intestine alkalic phosphatase	Fermentas
Cellfectin II	Invitrogen
Chitin beads	BioLabs
Coomassie Brilliant Blue R250	Sigma-Aldrich
Creatine phosphate	Sigma-Aldrich
Creatine phosphokinase	Sigma-Aldrich
Dithiotreitol	Sigma-Aldrich
DMEM medium	Sigma-Aldrich
dNTPs	Fermentas
ECL western blot substrate	Thermo Pierce
EDTA	Applichem
Ethanol	Penta
Ethanolamine	Sigma-Aldrich
Ethidium bromide	Biorad
Fetal bovine serum	Gibco
Formaldehyde	Penta
Glucose	Applichem
Glutathione agarose	Macherey-Nagel
Glutathione	Applichem
Glycerol	Lachner
Glycine	Applichem
Grace´s Insect Cell Culture Medium	Sigma-Aldrich
Heparin beads	GE Healthcare
HCl	Penta
IPTG	Fermentas
Isopropanol	Lachner
K_2HPO_4	Sigma-Aldrich
KCl	Lachema

Lactalbumin hydrolysate	Applichem
LB Miller Broth powder	Sigma-Aldrich
Leupeptin	Applichem
Ligation buffer	Fermentas
Lipofectamine RNAiMAX	Invitrogen
Malachite green	Sigma-Aldrich
Methanol	Penta
$MgCl_2$	Sigma-Aldrich
$MgSO_4$	Sigma-Aldrich
Na_2CO_3	Penta
NaCl	Lachner
NaF	Applichem
$NaHCO_3$	Serva
Natrium orthovanadate	Applichem
$(NH_4)_6Mo_7O_{24}$	Sigma-Aldrich
NHS-activated agarose column	GE Healthcare
Nonidet P-40	Applichem
NTP	Fermentas
Opti-MEM	Invitrogen
PEG 2000	Serva
PEG 6000	Fluka
Pepstatin A	Applichem
Pfu polymerase	Fermentas
Pluronic F68	Sigma-Aldrich
PMSF	Applichem
Ponceau S	Sigma-Aldrich
Protease inhibitor cocktail	Roche
Protein A/G PLUS-Agarose	Santa Cruz
Proteinase K	Roche
RNase A	Applichem
Silver nitrate	Safina Vestec
Sodium acetate	Sigma-Aldrich
Sodium citrate	Fluka
Sodium dodecyl sulphate	Applichem
Sodium pyrophosphate	Fluka
Sodium thiosulphate	Lachema
SuperSignal® West Dura	Thermo Pierce
SuperSignal® West Femto	Thermo SCIENTIFIC
T4 ligase	Fermentas
Tango buffer	Fermentas
TEMED	Applichem
Topoisomerase I	Invitrogen
Tris(hydroxymethyl)-aminomethane (Tris)	Applichem
Triton X-100	Applichem
Tween-20	Sigma-Aldrich
X-gal	Fermentas

Yeastolate	Applichem
β-mercaptoethanol	Applichem

Kits

DNA fragments were isolated using NucleoSpin® Extract II Kit (Macherey-Nagel) from agarose gel. Plasmids were purified using NucleoSpin® Plasmid purification Kit (Macherey-Nagel).

QuantiPro™ BCA Assay Kit (Sigma-Aldrich) and Quick Start™ Bradford Protein Assay (Bio-Rad Laboratories) were used for determination of protein concentration.

Protein markers

PageRuler™ Plus Prestained Protein Ladder (Thermo SCIENCE)

PageRuler™ Unstained Protein Ladder (Thermo SCIENCE)

HMW-SDS Marker Kit (GE Healthcare)

LMW-SDS Marker Kit (GE Healthcare)

4.2 Antibiotics

Used antibiotics:	Concentration:	Company:
Ampicillin	100 μg/ml	Applichem
Gentamicin	7 μg/ml	Lek Pharmaceutical
Kanamycin	50 μg/ml	FisherBiotech
Penicillin/Streptomycin solution	100 U/100 μg/ml	Sigma
Tetracycline	10 μg/ml	Sigma

4.3 Technical equipment

Technical equipment used:	Company:
Analytical balance BBI-32	BOECO
Balance	BEL engineering
Bioruptor TM Next gen	Diagenode
Centrifuge 5415R	Eppendorf
Centrifuge 5810R	Eppendorf
Centrifuge ROTANTA 460R	Hettrich
Centrifuge J2-21M	Beckman
Centrifuge NF 400	Nüve
Centrifuge Spectrafuge 24D	Labnet
CO_2 Incubator	Thermo SCIENTIFIC
X-ray film processor Optimax 2010	Protec
Electroblotter Hep-1	Thermo SCIENTIFIC

Electroblotter HorizBlot AE-6675L	ATTO
Flow box Bio-II-A	Teslar
Ice flaker	Brema
Incubator EN-120	Nüve
Light Microscope Eclipse TS100	Nicon
Magnetic stirrer CB161	Stuart
Magnetic stirrer MSH-300	Biosan
Memmert incubator INE 400	LAB system
PCR cycler Biometra TPersonal	LABRepCo
PCR cycler MJ Mini Gradient	Biorad
pH meter W3B	BEL engeneering
Power supply EDURO	Labnet
Power supply PS304	APELEX
Rocker 25	Labnet
Roller SRT6	Stuart
Rotator Bio RS-24	Biosan
Shaking incubator 311DS	Labnet
Shaking incubator S16R-HS	SHEL LAB
Sonicator soniprep 150	Schoeller
Spectrophotometer MULTISCAN* EX	Thermo SCIENTIFIC
Spectrophotometer ND-1000	NanoDrop
Spectrophotometer S-30	BOECO
Thermo shaker NB-205	N-Biotek
Thermoblock HB-102	Labolan
Thermoblock QBD2	Grant
Water bath JB Aqua 12	Grant

4.4 Cells

Escherichia coli:

For general cloning purposes, strain **Top10** [genotype: F- mcrA Δ(mrr-hsdRMS-mcrBC) φ80lacZΔM15 ΔlacX74 nupG recA1 araD139 Δ(ara-leu)7697 galE15 galK16 rpsL(Str^R) endA1 λ^-] was used. Strains **XA90** (genotype: [F' $LacI^{Q1}$ Z^+Y^+ $proAB^+$ *Δ*$(lac\text{-}pro)_{XIII}$ ara^- $nalA^-$ $argE^-$ am thi^- rif^R]) and **BL21**[genotype: *fhuA2 [lon] ompT gal (λ DE3) [dcm] ΔhsdS λ DE3 = λ sBamHIo ΔEcoRI-B int::(lacI::PlacUV5::T7 gene1) i21 Δnin5*] were used for protein expression. For bacmid production **DH10Bac** strain was used [genotype: F^- *endA1 recA1 galU galK deoR nupG rpsL ΔlacX74 Φ80lacZΔM15 araD139* Δ(*ara,leu*) *7697 mrcA* Δ(*mrr-hsdRMS-mrcBC*)].

Human:

HeLa cell line was derived from cervical cancer.

U2OS cell line was derived from an osteosarcoma.

HEK293 cell line was generated by transformation of human embryonic kidney cells.

Insect:

Sf9 cell line was derived from pupal ovarian tissue of *Spodoptera frugiperda.*

4.5 Plasmids

pAS2-1-FBH1(1-969 aa) was a kind gift from Giordano Liberi, Italy.

pTYB12-FBH1(1-484 aa) was prepared for antigen production in *E. coli*.

pEGFP-N2-FBH1(1-969 aa) and pFastBac-streptavidin-FBH1(1-969 aa)-His6x were prepared by Igor Chevelev, Ph.D.

pFastBac-GST-FBH1(1-969 aa)-His6x and pFastBac-GST-FBH1^{D698N}(1-969 aa)-His6x were prepared for FBH1 and FBH1^{D698N}, respectively, production in Sf9 cells.

pGEM-7Zf(+) was used for Topoisomerase I-linked DNA topology modification assay.

4.6 Primers

Primers used for antigen production:		RE:	Ann.temp:
F	5´- catg **gct agc** atg gcc aaa agc aat tct gtt g -3´	*Nhe I*	60°C
R	5´- gca **ctc gag** ttc ggc ctg ctt tgc gat -3´	*Xho I*	62°C

Highlighted sequences denote restriction sites of restriction enzymes (RE) listed in the middle. Annealing temperature of each primer is shown on the right. All used primers were synthesized by Microsynth. All used REs were produced by Fermentas.

4.7 siRNA

siFBH1 5'-GAUACAGAGUGAAGAAUGUdTdT-3' (Microsynth)

siLuciferase 5'-CGUACGCGGAAUACUUCGAdTdT-3' (Microsynth)

4.8 Recombinant proteins

FBH1 antigen (1-484 aa) used for immunization, RPA, GST, RAD51^{K133R} and *Taq* polymerase were produced and purified by Igor Chevelev, Ph.D. from bacteria.

RECQ5β was produced and purified by Ing. Václav Urban from bacteria.

FBH1 antigen (1-484 aa) used for anti-FBH1 antibody purification, GST-FBH1(1-969 aa)-His6× and GST-FBH1^{D698N}(1-969 aa)-His6× were produced and purified as a part of this project.

4.9 Antibodies

Used primary antibodies:

Chicken polyclonal anti-FBH1 (purification is described in this thesis)

Mouse monoclonal anti-FBH1 (Santa Cruz catalogue number SC-81563)

Rabbit polyclonal anti-RAD51 (produced and purified by Igor Chevelev, Ph.D.)

Rabbit control IgG (purified by Ing. Václav Urban)

Rabbit polyclonal anti-GST (produced and purified by Igor Chevelev, Ph.D.)

Used HRP conjugated secondary antibodies:

Rabbit anti-chicken IgY (Sigma-Aldrich)

Goat anti-rabbit IgG (Sigma-Aldrich)

Rabbit anti-mouse IgG (Sigma-Aldrich)

4.10 Agarose gel electrophoresis

Agarose gel electrophoresis is a method used to separate nucleic acids; DNA or RNA molecules by size and structure. This is achieved by moving negatively charged nucleic acid molecules through an agarose matrix in an electric field (electrophoresis). The negative charge of the molecules is due to the phosphate backbone they possess. The separated DNA fragments are stained with ethidium bromide for visualization by UV-light. The size of the DNA fragments can be determined by comparing them to DNA-ladders with fragments of known size.

In order to determine the quality of DNA, the samples such as PCR products, products of restriction digestion or plasmid purification, were separated by electrophoresis in 1% agarose gel. DNA samples were mixed with 1×DNA loading buffer containing 0.5 μg/ml of ethidium bromide. The gels were prepared in 1×TAE buffer containing 0.5 μg/ml of ethidium

bromide and the samples were mixed with 2×DNA loading buffer. The electrophoresis was performed in 1×TAE buffer at 80 V and gels were observed using a UV transilluminator.

DNA loading buffer (10×)	0.25% (w/v) Bromophenol Blue; 50 mM Tris-HCl, pH 7.6; 60% glycerol
TAE buffer (10×)	0.4 M Tris-HCl, pH 8.0; 0.25 M acetic acid; 10 mM EDTA

4.11 Cloning methods

4.11.1 Polymerase chain reaction

Polymerase chain reaction (PCR) is a method for enzymatic amplification of specific sequences of DNA. The PCR reaction goes through three different steps defined by the critical aspects of time and temperature; denaturation, annealing and elongation. These steps make up a cycle that is repeated 20-35 times to achieve a satisfying amount of amplified DNA. In the denaturation step, the PCR reaction is heated to a temperature of around 95 °C where the hydrogen bonds of the double helix are broken resulting in single-stranded molecules to be used as templates. In the annealing step, the reaction temperature is lowered to around 50-60°C so that the primers can anneal to the single-stranded DNA template forming short segments of double-stranded DNA where the polymerase attaches and begins DNA synthesis. During the extension/elongation step, the DNA polymerase synthesizes new DNA strands complementary to the DNA template strands.

The standard PCR mixture was prepared as follows:

Component	**Volume (µl)**
Pfu/Taq DNA polymerase (0.8 U)	1.0
Primers F+R	2.0
PCR buffer 10x	2.5
dNTPs (1.3 mM)	2.5
plasmid DNA	2.0
H_2O to final-volume	25.0

PCR reaction conditions:

Phase	Temperature	Time	
Initial	94°C	3 min	
Denaturation	94°C	30 s	20 cycles
Annealing		30 s	
Elongation	72°C	30 s	
	72°C	5 min	
Cooling	4°C	>10 h	

Annealing temperatures of individual primers are listed in chapter 4.1.6.

PCR buffer (10×) 200 mM Tris-HCl, pH 8.5; 100 mM $(NH_4)_2SO_4$; 100 mM KCl; 20 mM $MgSO_4$

4.11.2 Restriction digestion

To prepare fitting sites for ligation, plasmid vector and insert DNA were digested (in separate tubes) with appropriate pair of restriction enzymes (RE). DNA digest reactions were carried out by overnight incubation of the following mixture at RT.

Component	Quantity
Tango buffer 10x	3.6 µl
RE1	1.0 µl
RE2	1.0 µl
DNA	~2 µg
H_2O to final-volume	36.0 µl

Reaction mixture was then separated by agarose electrophoresis and digested fragments were purified using NucleoSpin® Extract II Kit.

4.11.3 DNA ligation

Ligation is the process in which an insert is ligated into a vector. The enzyme used to ligate DNA fragments is called T4 DNA ligase from bacteriophage T4.

Ligation reactions were performed by overnight incubation of following ligation mix at 16°C.

Component	Volume (µl)
Ligation buffer 10x	2
T4 ligase	1
Molar ratio of insert:vector	3:1
H_2O to final-volume	20

To do a self-ligation test, a control reaction containing all the reagents listed above except the DNA insert was set up.

To increase ligation efficiency by preventing of self-ligation of plasmid vectors in ligation reaction, the terminal 5'-phosphate groups may be removed using alkalic phosphatase. This dephosphorylation reaction will thus decrease the number of "empty" vectors. 1 µl of calf intestine alkalic phosphatase was incubated with the vector DNA for 30 min at RT. The alkalic phosphatase was subsequently inactivated by incubation at 85°C for 15 min. The products of ligation reaction were then used for transformation of competent bacteria.

4.11.4 Preparation of competent cells

Competent cell is a cell that is chemically treated to allow its membrane to be permeated by plasmids.

A single colony of the required *E. coli* strain was picked and grown overnight in 2 ml of LB medium at 37°C. 0.3 ml of the cell culture was subcultured into 15 ml of LB medium supplemented with 1% (w/v) glycine and the culture was grown ~3 h at 37°C to get OD_{600}=0.4-0.8. Cells were harvested by centrifugation (9 000×g; 5 min) and the pellet was ressuspended in 0.9 ml of fresh cold (4°C) LB medium supplemented with 1% (w/v) glycine. After, a brief incubation at 4°C, 0.1 ml of cold (4°C) Transformation buffer was added and mixed by inverting with the cell suspension. Competent cells were used for transformation directly or aliquoted (à 120 µl) and stored at -80°C until needed.

LB medium	20g/l LB Miller Broth powder
Transformation buffer	20% (w/v) PEG 2000; 0.96% (w/v) sodium citrate; 4.92% (w/v) $MgSO_4$, pH 5.5

4.11.5 Transformation of bacterial cells by heat shock

Transformation is the introduction of a plasmid into a competent cell. The plasmid will be replicated in the bacteria, which will copy the DNA of interest. Often the plasmid carries a

gene that makes the bacteria resistant to an antibiotic. Only the bacteria that carry the plasmid will grow on substrate containing appropriate antibiotic.

Aliquots of competent cells were thawed out on ice. After addition of 1 µl of plasmid DNA or 10 µl of ligation mixture, cells were very gently mixed and incubated at 4°C for 20 min. Cells were then exposed to heat shock at 42°C for 1 min, immediately supplemented by 800 µl LB medium with 20 mM glucose, prewarmed to 37°C, and incubated in shaker at 37°C for 1 hour. After brief spinning (9 000×g; 5 min) and removing of majority of supernatant, cells were resuspended in the residual medium, plated on LB agar plate containing appropriate antibiotics and incubated overnight at 37°C.

LB medium 20 g/l of LB Miller Broth powder

LB agar plates 15 g/l of agar in LB medium

4.11.6 Plasmid DNA purification from bacterial culture

Plasmid DNA can be isolated from bacterial cultures using differential alkaline denaturation. In this method cells are lysed in presence of sodium dodecyl sulphate (SDS) and NaOH. Both chromosomal and plasmid DNA and proteins are denatured in this process but after the neutralization of the solution with sodium acetate only the plasmid DNA can re-anneal and stay dissolved in the solution. Chromosomal DNA and proteins stay in the complex with SDS and NaOH and are removed by centrifugation. Plasmid DNA can be then concentrated by precipitation with ethanol (Birnboim and Doly, 1979).

Isolation of plasmid DNA was performed by either NucleoSpin® Plasmid purification KIT according to manual protocol or using "hand-made" purification according to following protocol. Colonies picked from agar plate were grown in 5 ml of LB medium with appropriate antibioticum overnight in shaker at 37°C. Next day, the cell pellet was resuspended in 250 µl of buffer S1. After incubation for 5 min at RT, 250 µl of buffer S2 was added, mixed by inverting and incubated for next 5 min at RT. 300 µl of buffer S3 was mixed with the cell suspension and incubated for 5 min at 4°C. Supernatant after centrifugation (16 000×g; 15 min; 4°C) was mixed with 600 µl of isopropanol and incubated for 10 min at 4°C. Pellet after centrifugation (16 000×g; 15 min; 4°C) was washed by cold 75% ethanol and dried for 20 min at RT. Finally, the DNA pellet was resuspended in 50 µl of TE buffer.

Buffer S1 50 mM Tris-HCl, pH 8.0; 10 mM EDTA; 20 mg/ml RNase A

Buffer S2 200 mM NaOH; 1% (w/v) SDS

Buffer S3 3 M sodium acetate, pH 4.8

TE buffer 10 mM Tris-HCl, pH 8.0; 0.1 mM EDTA

4.11.7 Determination of DNA concentration

Isolated DNA samples were qualitatively checked by agarose gel electrophoresis. The concentration was determined by measuring the absorbance at 260 nm using ND-1000 Spectrophotometer .

4.12 Baculovirus expression system

The baculovirus expression system is based on the insertion of a foreign gene into nonessential region in the bacmid DNA via site-specific transposition using transfer vector pFastBac containing target gene. Thus gene of our interest is placed under control of strong polyhedrin promoter of the fall armyworm *Autographa californica* nuclear polyhedrosis virus (virus). The *Spodoptera frugiperda* (Sf9), cells are highly susceptible to infection by the virus. Proper insertion of the expression cassette into bacmid disrupts the *lacZ* gene encoding β-galactosidase and can be monitored as white colonies in the presence of a chromogenic substrate (X-gal) and the inducer IPTG. Transfection of the recombinant bacmid into insect cells leads to generation of recombinant baculovirus particles that will be amplified and used for protein expression.

4.12.1 Preparation of bacmid DNA

Recombinant baculovirus was generated using the Bac-to-Bac® Baculovirus Expression System (Invitrogen) (Figure 13). *E. coli* DH10Bac strain was then transformed by produced recombinant pFastBac vector to transpose the foreign DNA into bacmid. Cells were then grown on Luria agar plates. White colonies were selected and streaked on to a fresh plate to verify the phenotype. Recombinant bacmid DNA was isolated from the bacteria by "hand-made" plasmid purification procedure (described in chapter 4.3.6) and used for transfection of Sf9 cells to produce recombinant baculovirus.

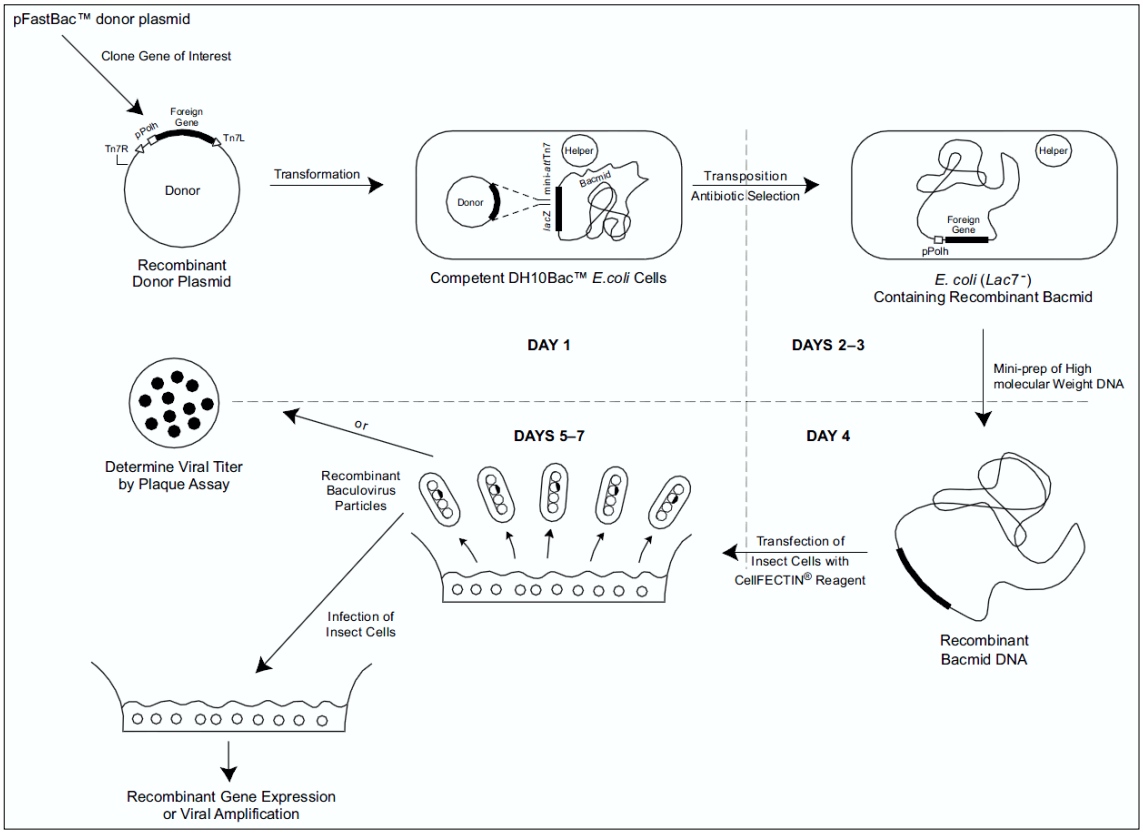

Figure 13 Bac-to-Bac baculovirus Expression System (adapted from Invitrogen Instruction Manual 2002).

4.12.2 Subculturing of Sf9 insect cells

Sf9 cells were ordinarily grown in suspension in Grace´s medium supplemented with yeastolate and lactalbumin hydrolysate containing 10% (v/v) fetal bovine serum (FBS) and 0.1% (v/v) pluronic F68 at 28°C in shaking incubator. Cells used for virus amplification were grown adherently in supplemented Grace´s medium containing 10% (v/v) FBS in incubator at 28°C. Condition of the adherently growing cells was observed under light microscope Eclipse TS100.

4.12.3 Transfection of Sf9 insect cells

Transfection of Sf9 cells by bacmid DNA was performed as following. 5 µl of bacmid DNA in 100 µl of supplemented Grace´s medium was added to 8 µl of Cellfectin II reagent in 100 µl of supplemented Grace´s medium and incubated 30 min at RT. This solution was afterwards dropwise added to adherently growing Sf9 cells (0.8×10^6) in 2 ml of supplemented Grace´s medium in 6-well plate and incubated for 3-5 hours. Then, cell medium was replaced by supplemented Grace´s medium containing 10% (v/v) FBS and incubated for 72 hours.

4.12.4 Virus amplification

To amplify the virus titer after transfection, 0.8 ml of medium from cells was used for infection of another adherently growing Sf9 cells (8×10^6) in 10 ml of fresh supplemented Grace´s medium containing 10% (v/v) FBS in 25cm^2-tissue culture flask. After incubation for 5-7 days, until the majority of cells lysed (Figure 14), the virus titer was amplified in larger volume in 75cm^2- or 150cm^2-tissue culture flask. This process of amplification was repeated 3-4 times with increasing amount of cells to obtain sufficient quantity of virus for pilot and large-scale protein expression. Amount of medium containing virus for infection of cells varied according to the virus concentration.

Supplemented Grace´s medium	3.3 g/l of yeastolate and 3.3 g/l of lactalbumin hydrolysate in Grace´s Insect Cell Culture Medium
Luria agar plates	1.2% (w/v) agarose; 50 µg/ml kanamycin; 7 µg/ml gentamicin; 10 µg/ml tetracycline; 100 µg/ml X-gal; 40 µg/ml IPTG, in LB medium

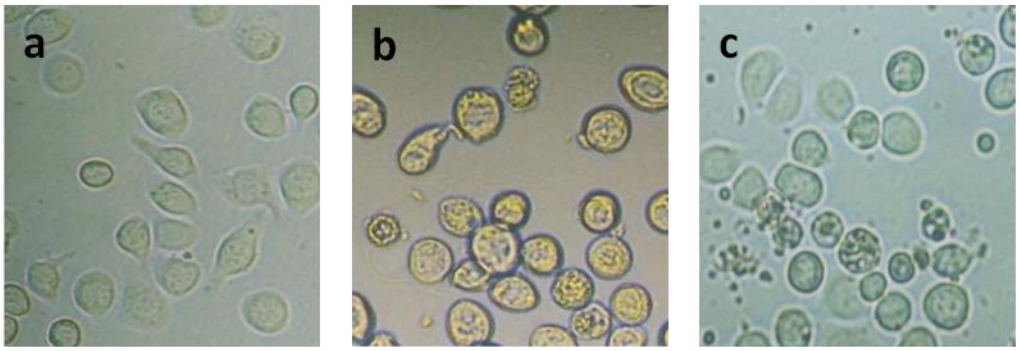

Figure 14 Sf9 insect cells.
(a) Normal non-transfected cells; **(b)** cells 72 h after transfection by recombinant baculovirus; **(c)** lysing cells 96 h after transfection. Original magnification ×200. Adopted from (Cui et al., 2007)

4.13 Transfection of human cells by siRNA

Small interfering RNA (siRNA) is a double-stranded RNA molecule involved in RNA interference (RNAi) pathway. RNAi is an evolutionary conserved process nowadays widely used in research as a tool for specific gene silencing.

To facilitate siRNA uptake by human HEK293 and U2OS cells, Lipofectamine RNAiMAX, a lipid-based transfection reagent was used. 9 µl of Lipofectamine RNAiMAX in

250 µl of Opti-MEM was added to 4 µl of 40 uM siRNA in 250 µl of Opti-MEM and incubated 15 min at RT. This solution was afterwards dropwise added to cells in 6-cm plates with 3.5 ml of DMEM medium (Dulbecco's Modified Eagle's Medium) supplemented with 10% (v/v) FBS and penicillin/streptomycin solution and incubated for 48 hours at 37°C, 5% CO_2.

Whole cell extract (WCE) was prepared as followed. Cells were washed by 0.5 ml PBS and scraped into 100 µl of 2×SDS buffer. Samples were sonicated (amplitude 3 µm, 2×15 s, RT) and the protein concentration measured using bicinchoninic acid (BCA) protein determination assay. WCE samples were mixed with 10×DB buffer, boiled 5 min at 95°C and analyzed by SDS-PAGE (7% gel) and western blot.

Complete DMEM medium	DMEM medium; 10% (v/v) FBS; penicillin/streptomycin solution
SDS buffer (4×)	250 mM Tris-HCl, pH 6.8; 8% (w/v) SDS; 40% glycerol
DB buffer (10×)	400 mM DTT; 0.01% Bromphenol Blue

4.14 Expression of recombinant proteins

Nowadays, there is a number of efficient proteins expression systems. The choice of right system depends on many factors. Each expression system has its pros and cons. *E. coli* is one of the most widely used expression hosts. Expression of recombinant protein in prokaryotic system has advantages including ease of culture, very rapid cell growth, simple induction of protein expression by IPTG, etc. Disadvantages are common expression of a protein in inclusion bodies and dysfunction of an expressed protein due to the lack of posttranslation modifications. These inconveniences can be overcame by expression of a protein in eukaryotic system, such as expression in yeast or in Sf9 insect cells. This system is more time-consuming in comparison to prokaryotic system and requires more expensive facility. Pilot or small-scale protein expressions are ordinarily used for optimization of the process using all kinds of expression hosts. To produce higher quantities of a protein for further analysis, a protein is expressed in large-scale.

4.14.1 Expression in bacterial cells

Small-scale expression

Single colony was picked out from LB agar plates and inoculated into 1-5 ml of LB medium containing appropriate antibiotic and incubated at 37°C for 2-3 hours until the optical density of the culture (OD_{600}) reached ~0.5. Then the expression of protein was induced by addition of

0.1-1 mM IPTG for 2-36 h at 14-37°C. Concentration of IPTG, time and temperature of following incubation are varying, the exact expression condition of each experiment are described in the text in chapter 5.1.1. Cells were harvested by centrifugation (9 000×g, 5 min). According to further purpose, cell pellet was either directly boiled in appropriate volume of Laemmli buffer at 95°C for 5 min, or resuspended in appropriate volume of chitin-lysis buffer, sonicated (amplitude 10 μm, 2×10 s, 4°C) and centrifuged (16 000×g, 15 min, 4°C) to obtain soluble protein extract, which was afterwards boiled in Laemmli buffer at 95°C for 5 min.

Chitin-lysis buffer 30 mM Tris-HCl, pH 8; 500 mM NaCl; 1 mM EDTA; 10% glycerol; 0.1% Triton X-100

Large-scale expression

80 ml of overnight culture gained by inoculation of single *E. coli* colony from LB agar plate was diluted into 5 l LB medium containing appropriate antibiotics and grown at 37°C for 2 hours. When the OD_{600} reached ~0.2, the cells were additionally incubated at 12°C for about 3 hours. Protein expression was induced by 0.2 mM IPTG at the moment when OD_{600} reached ~0.9 and then incubated at 12°C for 43 hours. Cells were harvested by centrifugation (300×g, 35 min, 4°C) and the pellet was frozen at -80°C.

4.14.2 Expression in Sf9 insect cells

Small-scale expression

25×10^6 insect cells grown in 25ml of supplemented Grace´s medium containing 10% (v/v) FBS and 0.1% (v/v) pluronic F68 in suspension were infected by 2.5 ml of medium containing virus. The cells were incubated for 2 or 3 days at 28°C on rotary shaker. Cells were collected by centrifugation (300×g; 5 min) and washed in PBS.

The cell pellet was resuspended in 1.2 ml of GST-lysis buffer supplemented with protease inhibitor cocktail, sonicated (amplitude 10 μm, 2×15 s, 4°C) and centrifuged (16 000×g, 45 min, 4°C). The obtained soluble protein extract was incubated with 0.2 ml of 50% glutathione (GSH)-agarose for 2 and 4 h at 4°C on rotary shaker. After binding, beads were collected by centrifugation (300×g, 3 min, 4°C) and washed four times by 1 ml of GST-washing buffer. Beads were boiled in 2×Laemmli buffer at 95°C for 5 min and 10 μl aliquots of the elution fraction from the GSH agarose were subjected to SDS-PADE and western blot analysis.

Large-scale expression

1.5×10^8 insect cells were infected by virus and incubated for 2 days at 28°C on rotary shaker. Cells were collected by centrifugation (300×g; 7 min) and washed in PBS. The cell pellet was frozen in liquid nitrogen and stored at -80°C until used.

GST-lysis buffer 50 mM Tris-HCl, pH 8.0; 300 mM NaCl; 1 mM EDTA; 10% glycerol; 2 mM DTT; 0.1% Triton X-100

GST-washing buffer 0.2% (v/v) Triton X-100 in GST-lysis buffer

4.15 Purification of recombinant proteins

4.15.1 Chitin affinity chromatography

Chitin affinity chromatography is based on the capture of chitin binding domain (CBD), the affinity tag, to beads coated by chitin (chitin beads). The great advantage of this purification system is that the target protein is released directly from the CBD-tag in presence of DTT, when the CBD undergoes specific self-cleavage resulting in elution of tag-freed protein.

Cell pellet was thawed out on ice and resuspended in 35 ml chitin-lysis buffer supplemented with protease inhibitors [100mM PMSF, bestatin 1 ug/ml, pepstatin A 1 ug/ml, leupeptin 5 ug/ml, 1 mM sodium orthovanadate]. Cells were lysed by sonication (amplitude 14 μm, 2×2 min, 4°C) and centrifuged (47 000 × g, 1 hour, 4°C) to gain soluble protein extract. 5 ml of 50% chitin beads was added to the soluble protein extract and incubated at 4°C overnight on rotary shaker. The chitin beads were subjected to several washing steps until the protein concentration in flow through reached ~0. In total approximately 50 ml of chitin-lysis buffer was used for washing (centrifugation: 300×g, 5 min, 4°C). To cleave the protein from the chitin binding domain, firstly 5 ml of cleavage buffer was passed through the column to change the buffers, and then, 7 ml of the same buffer was incubated with the beads overnight at 4°C on rotary shaker. After first elution, this procedure was further repeated 3 times to gain more protein from the beads. The elution fractions were frozen and stored at -80°C. Protein concentration was measured by Bradford method and purity was verified by SDS-PAGE.

Cleavage buffer 40 mM Tris-HCl, pH 7.5; 100 mM NaCl; 1 mM EDTA; 50 mM DTT

4.15.2 GST affinity chromatography

The principle of this method is based on high affinity of glutathione *S*-transferase (GST) to its substrate, GSH (tripeptide Glu-Cys-Gly). GST-tagged proteins are captured via the interaction with GSH immobilized to agarose beads. The target protein is then dissociated by addition of GSH, the binding competitor.

Thawed cell pellet was resuspended in 7.5 ml of GST-lysis buffer containing protease inhibitor cocktail. Cells were lysed by dounce homogenizator. The soluble protein extract was obtained by centrifugation (47 000×g, 45 min, 4°C) and incubated with 2 ml of 50% GSH agarose for 2 or 4 h at 4°C on rotary shaker. Beads were washeded by >50 ml of GST-lysis buffer (centrifugation: 300×g; 5 min; 4°C). FBH1 protein was then eluted from the beads by GST-elution buffer containing 10-50 mM GSH.

GST-elution buffer 40 mM Tris-HCl, pH 8.1; 50 mM NaCl; 10% glycerol

4.15.3 Heparin affinity chromatography

Heparin purification utilizes the ability of heparin to bind to DNA-binding proteins. Dissociation of these proteins from heparin, coupled to agarose beads, is performed by a high salt buffer. In our experiments, heparin purification was included as a second purification step after GST-purification.

All elution fractions from previous purification step were mixed together and incubated with 0.5 ml 50% heparin beads for 1 hour at 4°C. After binding, beads were washed three times by Hep-buffer A and protein was eluted by Hep-buffer B. The heparin-elution fractions were mixed together and dialysed overnight in 1 l of dialysis buffer at 4°C. Purified protein sample was aliquoted (10µl), frozen by liquid nitrogen and stored at -80°C until used. All fractions from both purification steps were analysed by SDS-PAGE and western blot. Protein concentration was measured by Bradford and BCA methods.

Hep-buffer A 40 mM Tris-HCl, pH 7.5; 0.1 M NaCl; 1 mM EDTA; 10% glycerol; 1 mM β-mercaptoethanol

Hep-buffer B 40 mM Tris-HCl, pH 7.5; 1 M NaCl; 1 mM EDTA; 10% glycerol; 1 mM β-mercaptoethanol

Dialysis buffer 40 mM Tris-HCl, pH 7.5; 50 mM NaCl; 1 mM EDTA; 40% glycerol; 1 mM β-mercaptoethanol

4.16 Antibody production

Antibodies, also known as immunoglobulins (Ig), constitute one of the principal effectors of the adaptive immune system. Due to their ability to bind an antigen with a high degree of affinity and specificity, antibodies constitute a powerful tool in a variety of medical and scientific disciplines. Antibodies are "Y" shaped proteins composed of heavy and light chains linked together by disulfide bonds. Depending on their structure and function, antibodies are classified into isotypes. In mammals, there are five antibody isotypes: IgG, IgM, IgA, IgD and IgE. In avians, there are three classes: IgY, IgM and IgA.

There are several common ways to obtain antibody against protein of our interest. One can purchase a commercial antibody from a biotechnology company, receive it as a gift or produce it in laboratory. Animal species that are used for the production of antibodies include rabbits and mice, less often sheep, goats, chicken, horses, hamsters or guinea pigs. The selection of laboratory animal depends on numerous aspects, such as amount of antibody needed, purpose for which an antibody is needed, animal origin of the antigen, time demand of production procedure, requirements for breeding of the animals, skills and technology equipment requirements, and also costs.

4.16.1 Extraction of total IgY antibodies from egg yolk

Chicken eggs from immunized hen were collected, marked and stored at 4°C. In the isolation approach, first a total immunoglobulin mixture was isolated from individual egg as described (Gassmann et al., 1990) with some modifications.

Briefly, the yolk (15 ml) was carefully separated from the white and the yolk skin and transferred into a falconi tube. The egg yolk was resuspended in 15 ml of IgY-buffer A and incubated on rotary shaker for 5 min at RT, subsequently mixed with 30 ml of IgY-buffer B and incubated under the same conditions. The precipitate was pelleted by centrifugation (3200×g, 30min, 4°C) and the resulting supernatant was clarified by centrifugation (3200×g, 10 min, 4°C) and filtered. Solid PEG 6000 was added to the filtrate to a final concentration of 12 % (w/v). The mixture was stirred until all PEG was dissolved. The solution was then centrifuged (3200×g, 30min, 4°C), the pellet containing IgY mixture was resuspended in 20 ml of IgY-buffer A and subsequently an equal volume of IgY-buffer C was added for second precipitation step. After incubation for 10 min at RT, the suspension was centrifuged (3200×g, 30min, 4°C); the final pellet was resuspended in 12 ml of IgY-buffer A and dialyzed against large volume of the same buffer overnight at 4°C. Next day, the IgY mixture was clarified by centrifugation as above and filtered through membrane filter (0.2 μm).

IgY-buffer A 0.01 M KH_2PO_4, pH 7.2; 0.1 M NaCl

IgY-buffer B 7% (w/v) PEG 6000 in IgY-buffer A

IgY-buffer C 24% (w/v) PEG 6000 in IgY-buffer A

4.16.2 Affinity purification of the antibody

Isolation of specific IgYs was performed by affinity chromatography using 1 ml NHS-activated agarose column with immobilized antigen. The activated agarose contains N-hydroxysuccinimide (NHS) functional group that reacts with primary amines of a protein to form a stable amide linkage, especially at higher pH. Antigen specific antibodies captured in the column are eluted by low pH buffer.

Preparation of column for affinity purification

Antigen was dialyzed overnight against 1l of coupling buffer at 4°C. To immobilize the protein, the column was firstly activated by 3 × 2 ml of ice cold 1 mM HCl using peristaltic pump with flow rate 1 ml/min. Next, the antigen was loaded into the column by flow rate 0.5 ml/min. Flow through was collected and subjected to second loading into the column with flow rate 0.1 ml/min. All remaining active groups were deactivated and non-specifically bound ligands were washed out by following procedure (flow rate used 0.5 - 1 ml/min):

- injection of 3 × 2 ml of Buffer A
- injection of 3 × 2 ml of Buffer B
- injection of 3 × 2 ml of Buffer A
- incubation of the column for 30 min at RT
- injection of 3 × 2 ml of Buffer B
- injection of 3 × 2 ml of Buffer A
- injection of 3 × 2 ml of Buffer B
- injection of 10 ml of Coupling buffer
- injection of 10 ml of Elution buffer
- injection of 10 ml of Regenerating buffer
- injection of 10 ml of Coupling buffer
- injection of 10 ml of ABB buffer

Affinity purification of anti-FBH1 the antibody

The column with antigen bound to the NHS-activated agarose was employed for affinity purification of specific antibody from total IgY mixture. IgY suspension was loaded to the column and column was subsequently washed by 10 ml of ABB buffer by flow rate 0.25-0.5 ml/min. Bound antibodies were eluted by low pH elution buffer. 1ml elution fractions were collected to tubes containing about 50 µl of 1.5 M Tris-HCl (pH 8.8) to adjust pH to ~8.6. The very low pH can cause protein denaturation. Protein fractions with more than 0.4 mg/ml protein concentration were mixed together as peak fraction and fractions with more than 0.1 mg/ml protein concentration were mixed together as side fraction. Both were dialysed overnight against 1 l of dialysis buffer AB at 4°C. Finally, these antibody containing fractions were clarified by centrifugation (1000×g, 10 min, 4°C), aliquoted (10-50 µl) and stored at -80°C until use.

Coupling buffer	0.2 M $NaHCO_3$, pH 8.3; 0.5 M NaCl
Buffer A	0.5 M ethanolamine, pH 8.3; 0.5 M NaCl
Buffer B	0.1 M sodium acetate, pH 4; 0.5 M NaCl
Elution buffer	0.1 M glycine, pH 2.5; 100 mM NaCl
Regeneration buffer	50 mM KH_2PO_4, pH 11.5; 100 mM NaCl
ABB buffer	20 mM NaH_2PO_4; 100 mM NaCl, pH 7.5
Dialysis buffer AB	40 mM Tris-HCl, pH 7.5; 100 mM NaCl; 10% glycerol

4.17 Determination of protein concentration

Two colorimetric methods were applied to estimate the concentration of protein in a solution, Bradford assay and bicinchoninic acid assay. In both methods, the amount of protein is quantified by measuring the absorbation and concentration of the sample protein is determined from a calibration curve derived from BSA standards of known protein concentration.

4.17.1 Bradford protein determination assay

Bradford assay is based on the proportional binding of Coomassie Brilliant Blue G-250 to proteins causing a visible color change (Bradford, 1976). The advantage of this method is quite easy handling where no heating is required. On the other hand, higher concentrations of detergents often present in protein samples may interfere with the assay. Different amounts (ordinarily 5-20 µl) of protein sample or BSA standard solutions (ordinarily 10 µl) were added

to 1 ml of 5x diluted Bradford Assay Reagent solution, mixed and transferred to plastic cuvettes. Absorbance was measured on spectrometer BOECO S-30 at 595 nm.

Bradford Assay Reagent 0.01% Coomassie Blue G250; 0.475% (v/v) ethanol; 0.85% (w/v) H_3PO_4

4.17.2 Bicinchoninic acid protein determination assay

Bicinchoninic acid assay (BCA) is based on reduction of Cu^{2+} to Cu^{1+} by protein in presence of bicinchoninic acid in alkaline environment (pH 11.25). The reaction produces purple-colored complexes (Smith et al., 1985).

The working reagent was prepared by mixing of 49 parts of BCA solution with 1 part of 4% (w/v) $CuSO_4 \cdot 5H_2O$ solution. 200 µl of the working reagent was mixed with 10 µl of protein sample or BSA standard solution in 96well plate, which was then incubated at 37°C for 30 min. The absorbance was measured at 560 nm using Multiscan EX spectrophotometer.

BCA solution 2% (w/v) $Na_2CO_3 \cdot H_2O$; 0.95% (w/v) $NaHCO_3$; 0.16% (w/v) sodium tartarate; 0.4% (w/v) NaOH; 1% BCA sodium salt, pH 11.25

4.18 Sodium dodecyl sulphate polyacrylamide gel electrophoresis

Sodium dodecyl sulphate-polyacrylamide gel electrophoresis (SDS-PAGE) is a method used for separation of proteins according to their size. SDS is an anionic detergent that binds to proteins in constant weight ratio. Proteins heated in presence of SDS denature into their primary polypeptides and gain an overall identical negative charge density. These polypeptides, migrating in an electric field towards the positive anode, can be then separated in a polyacrylamide gel according to their size (Laemmli, 1970).

Resolving gel was applied between two glass plates with spacer and overlaid with distilled water and kept in the stand at RT until polymerized. Then the water was removed, stacking gel was applied and the well-former was inserted. The gel was kept in the stand at RT until polymerized, placed into the tank and filled with 1×SDS-PAGE running buffer. The well-former was removed. Protein samples were diluted in Laemmli buffer, boiled at 95°C for 5 min and loaded into the wells formed in the stacking gel. Electrophoresis was run at 80 V for 20 min and then at 120 V for 1.5 - 2.5 hours. Gels were prepared according to following recepie:

Table 1 Composition of SDS-PAGE stacking and resolving gels

	Stacking gel (2.5 ml)	Resolving gel (7.5 ml)				
	4%	7%	8%	9%	10%	12%
H_2O [ml]	1.5	4.2	4.0	3.9	3.7	3.3
1.5 M Tris-HCl,pH 8.8; 0.4% (w/v) SDS [ml]	-	1.875	1.875	1.875	1.875	1.875
0.5 M Tris-HCl,pH 6.8; 0.4% (w/v) SDS [ml]	0.63	-	-	-	-	-
40% acrylamide/bis solution [ml]	0.25	1.3	1.5	1.7	1.88	2.25
10% (w/v) SDS [µl]	25	75	75	75	75	75
10% Ammonium persulphate [µl]	10	20	22.5	26	30	37.5
TEMED [µl]	10	10	10	10	10	10

Laemmli buffer (4×) 500 mM Tris-HCl, pH 6.8; 4% (w/v) SDS; 40% glycerol; 40 mM DTT; 0.05% bromphenol blue

SDS-PAGE running buffer (1×) 25 mM Tris-HCl, pH 8.3; 192 mM glycine; 0.1% (w/v) SDS

4.18.1 Staining of gels

Coomassie staining

Gels were stained in Coomassie solution at RT for 1 hour with agitation and destained afterwards in destaining solution at RT.

Coomassie solution 0.1% (w/v) Coomassie Brilliant Blue R250; 10% acetic acid; 40% methanol

Destaining solution 7.5% acetic acid; 10% isopropanol

Silver staining

Silver staining is a highly sensitive method with a detection level ~50 times lower than Coomassie staining, i.e. 0.3-10 ng of a protein. Detection depends on the binding of silver ions to the amino acid, followed by reduction to free metallic silver. The protein bands are visualized as spots on the gel where the reduction occurs (Kerényi and Gallyas, 1973).

Gels were incubated in fixation solution for 20-60 min, then in 50% methanol for 10-30 min and washed 3×10 min in H_2O. Followed by incubation with 0.02% (w/v) sodium thiosulphate for 10 min and washing 2×5 min in H_2O. Gels were stained by 0.1% (w/v) silver

nitrate for 20 min and rinsed 2×1 min in H_2O. Proteins were visualized in developer solution and fixed in 5% acetic acid for 5-10 min. Stained gels were stored in H_2O.

Fixation solution 50% methanol; 5% acetic acid
Developer solution 2% (w/v) Na_2CO_3; 0.04% (w/v) formaldehyde

4.19 Western blot analysis

Western blot is a method used for the identification and quantification of specific proteins. Proteins are usually first separated using SDS-PAGE and then transferred to a membrane by electric field. For immunodetection of proteins, the membrane is probed with primary and secondary antibodies against target protein and primary antibody, respectively.

Separated proteins on polyacrylamide gel were first transferred to Amersham Hybond-P PVDF membrane using semi-dry transfer. Whatman filter papers and PVDF membrane (activated by incubation in methanol for 2 min) were soaked in transfer buffer and placed on anode in following order: 3 pieces of filter paper, PVDF membrane, gel, 3 pieces of filter paper, and covered by cathode. The transfer ran at 150 mA/gel for 1.5 h at RT. To check the transfer efficiency, the PVDF membrane was stained by Ponceau solution for ~10 min at RT. The membrane was blocked in 5% (w/v) non-fat dry milk or 3% (w/v) BSA in TBST for 1 hour and incubated with primary antibody overnight at 4°C in ~2% (w/v) non-fat dry milk or 1% (w/v) BSA in TBST. Next day, the membrane was washed three times with TBST for 15 min at RT, incubated with corresponding horseradish peroxidase (HRP) conjugated secondary antibody for 1 hour at RT in ~2% (w/v) non-fat dry milk or 1% (w/v) BSA in TBST and washed three times with TBST for 15 min at RT. Then the PVDF membrane was soaked in enhanced chemiluminescence (ECL) reagent, covered with saran foil, exposed to X-ray film in dark room and developed in X-ray film processor Optimax 2010.

Transfer buffer 0.1 M Tris-HCl, pH 7.5; 0.192 M glycine; 5% methanol
Ponceau solution 0.1% (w/v) Ponceau S; 5% acetic acid
TBST 30 mM Tris-HCl, pH 7.5; 150 mM NaCl; 0.05% (v/v) Tween-20

4.19.1 Dot-blot analysis

Dot-blot is a quick technique used to examine if an antibody recognizes target protein. The principle of this method is similar to common western blot analysis. Protein is directly applied

on the membrane and visualized by primary and secondary antibodies. Dot-blot may be also used to determine appropriate starting concentration of primary antibody for western blot.

Antigen and BSA as a control were diluted into following series: 0.5, 1, 5, 25, 50, 125 ng/µl, and gradually dropped (à 1 µl) onto activated Amersham Hybond-P PVDF membranes. Dried and blocked in 5% (w/v) non-fat dry milk in TBST (0.5-1 hour, RT) membranes were incubated with different dilutions of primary antibody in 0.5% (w/v) non-fat dry milk in TBST for 1.5 hour at RT and developed after incubation with secondary antibody as described in chapter 4.11.

4.20 Protein-protein interaction study techniques

4.20.1 Protein complex-immunoprecipitation

Protein complex-immunoprecipitation (co-IP) is used to capture and determine a protein interacting with protein of interest.

Mammalian cells grown to about 80% confluency in a 10-cm or 15-cm Petri dishes were washed by PBS and scraped into 0.5 or 1.0 ml of lysis buffer. Samples were vortexed and sonicated using Bioruptor 7-10×30s cycles. The cell lysates were clarified by centrifugation (16 000×g; 45 min; 4°C).

For co-IP, 1 mg of the soluble protein extract was incubated with 200 ng of purified GST-FBH1-His6x, 3 µg of rabbit anti-RAD51 antibody or control rabbit IgG in a final volume of 0.5 ml of IP buffer for 4 h at 4°C on rotator. Then, 15 µl of Protein A/G PLUS-Agarose slurry was added followed by incubation for further 1 h under the same conditions. Beads were collected by centrifugation (300×g; 3 min; 4°C), washed 4 times by 1 ml of IP buffer and boiled with 12 µl of 2×Laemmli buffer at 95°C for 5 min. Samples were subjected to SDS-PAGE on 9% gel and WB analysis.

Lysis buffer 50 mM Tris-HCl, pH 7.5; 120 mM NaCl; 1 mM EDTA;
0.5% (v/v) Nonidet P-40; 20 mM NaF; 0.5 mM sodium orthovanadate;
15 mM sodium pyrophosphate; protease inhibitor cocktail

IP buffer 50 mM Tris-HCl, pH 7.5; 120 mM NaCl; 20 mM NaF;
15 mM sodium pyrophosphate; protease inhibitor cocktail

4.20.2 GST pull-down assay

Pull-down assay is *in vitro* method used for determination of bait-prey protein interaction where the bait protein is immobilized on beads through its affinity tag.

100 ng of RAD51^{K133R} was incubated with 200 ng of purified GST-FBH1-His6x or 200 ng of control (40 ng of GST + 160 ng of BSA) in a final-volume of 0.4 ml of NET-N150 buffer or NET-N150 buffer containing 1mM DTT for 4 h at 4°C on a rotator. Then, 15 µl of GSH agarose beads slurry were added to the reaction samples and incubated for another 1 h at 4°C on rotator. Beads were collected by centrifugation (300×g; 3 min; 4°C), washed 4 times by 1 ml of NET-N150 buffer and boiled with 12 µl of 2×Laemmli buffer at 95°C for 5 min. Samples were subjected to SDS-PAGE on 9% gel and WB analysis. GST-FBH1-His6x and GST as a control were used in equimolar ratio.

NET-N150 buffer 10 mM Tris-HCl, pH 8.0; 150 mM NaCl; 1 mM EDTA; 0.2% (v/v) Triton X-100

4.20.3 Far-western blot analysis

Far-western blot is another *in vitro* technique to study protein-protein interaction. The procedure is similar to standard western blot analysis. Separated prey protein by SDS-PAGE is transferred on a membrane and probed with bait protein solution. The bait-prey interaction is visualized using anti-bait antibody.

Far-western blot analysis was performed as described in (Selak et al., 2008). Purified recombinant proteins, 900 ng of RPA, 300 ng of RAD51^{K133R}, and 750 ng of BSA were separated by SDS-PAGE on 12% gel and transferred to Amersham Hybond-P PVDF membrane. The membrane was blocked by 10% (w/v) non-fat dry milk in far-TBST for 1 hour and briefly washed by far-TBST. Membrane was then incubated in protein solution, 0.42 µg/ml of GST-FBH1-His6x or 0.14 µg/ml GST in 3 ml of hybridization solution, or in 10% (w/v) non-fat dry milk in far-TBST for 2 h at RT with agitation. Membranes were washed 3×15 min by far-TBST, incubated with rabbit anti-GST antibody overnight at 4°C and developed after incubation with secondary antibody as described in chapter 4.11.

Far-TBST 30 mM Tris-HCl, pH 7.5; 150 mM NaCl; 0.3% (v/v) Tween-20

Hybridization solution 0.25% (w/v) non-fat dry milk and 1 mM DTT in far-TBST

4.21 Enzymatic assays

4.21.1 Malachite green ATPase assay

Malachite Green ATPase assay provides an elegant and rapid way to observe ATPase activity of particular enzyme. This colorimetric assay is based on spectrophotometric quantification of inorganic phosphate (P_i) released after ATP hydrolysis (Figure 15). In presence of ammonium molybdate and malachite green the P_i forms a phosphomolybdenate-malachite green complex causing a visible color change.

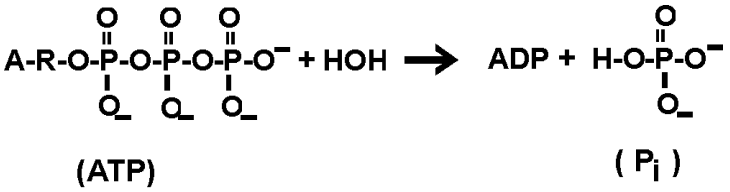

Figure 15 Scheme of ATP hydrolysis.

Reaction mixtures (typically 20 µl) contained varying concentration (20-80nM) of ATPase enzyme (FBH1, FBH1^{D698N}, or RECQ5β) in presence of different DNA structures. DNA structures used were single-stranded phagemid M13mp8.32, plasmid dsDNA in concentration of 25µg/ml and oligonucleotides, 25- and 37-mer , 53- and 93-mer in 1µM concentration. To check for residual phosphate in protein sample that could interfere with measurement, FBH1 was inactivated by incubation at 55°C for 20 min. Reactions were usually initiated by addition of ATP to a final concentration of 2-16 mM and terminated after 30 min incubation at 37°C by addition of one reaction volume of 0.1M EDTA (pH 8.0). 20 µl of reaction mixture was then two times diluted by H_2O in a 96-well microplate. To that mixture, 100 µl of ammonium molybdate solution and 50 µl of malachite green solution were added and incubated for few minutes before absorbance at 620 nm was measured in a microplate reader Multiscan EX spectrophotometer. The concentration of inorganic phosphate was determined from a calibration curve derived from solutions of known P_i concentration (KH_2PO_4). Reactions were done in duplicates in two or more independent experiments.

ATPase buffer	50 mM Tris-HCl, pH 7.5; 50 mM NaCl; 2 mM $MgCl_2$; 1 mM DTT; 50 µg/ml BSA
Ammonium molybdate solution	[2.32% (w/v) of $(NH_4)_6Mo_7O_{24}$ in 6 M HCl] diluted in H_2O (ration 1:3)
Malachite green solution	[5.72% (w/v) of malachite green in H_2O] diluted in H_2O (ratio 1:100)

4.21.2 Topoisomerase I-linked DNA topology modification assay

Topoisomerase I-linked DNA Topology Modification Assay is an approach to examine the ability of a helicase to disrupt RAD51 from ssDNA region. In a brief description of the procedure (Figure 16): Relaxed plasmid DNA trap RAD51 molecules displaced from ssDNA by a DNA helicase. RAD51 also forms a helical nucleoprotein filament on dsDNA and thus forces it to adopt an extended conformation (Sung and Robberson, 1995). RPA has high affinity for ssDNA and can cope with RAD51 for binding to ssDNA. Binding of RAD51 to topologically relaxed covalently closed circular dsDNA induces lengthening of the DNA and formation of positive supercoils that can be observed as change in the DNA linking number after treatment with eukaryotic topoisomerase I. Positive supercoils in the plasmid DNA subsequently results in negative supercoiling after proteinase K treatment. The different DNA species present in the reaction: ssDNA, dsDNA in relaxed and supercoiled form, are separated by electrophoresis in agarose gel and visualized by ethidium bromide straining.

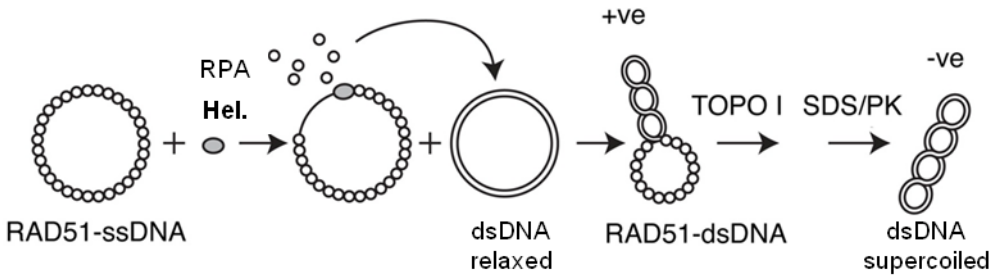

Figure 16 Reaction scheme of Topoisomerase I-linked DNA topology modification assay. Single-stranded DNA, ssDNA; double-stranded DNA, dsDNA; Hel., helicase; TopoI, topoisometase I; PK, proteinase K; possitive supercoiling, +ve; negative supercoiling, -ve. (Hu et al., 2007)

Reactions were carried out at 37°C in an final-volume of 25 µl of Buffer R supplemented with an ATP-regenerating system consisting of 10 U/ml creatine phosphokinase, 12 mM creatine phosphate and 2 mM ATP. 2 µM RAD51^{K133R} was preincubated with circular M13mp8.32 ssDNA (9 µM nucleotides) for 6 min, followed by addition of 150 nM RPA and a DNA helicase. Helicases used were: RECQ5β (80 and 160 nM), FBH1 (50, 160, 210, and 320 nM) and FBH1^{D698N} (320 nM). After a 6-min incubation, topologically relaxed pGEM-7Zf(+) DNA (7 µM base pairs) and 3 U of topoisomerase I were added to complete the reaction, which was then incubated for further 8 min. Reactions were terminated by addition of 5 µl of STOP buffer followed by 25-min incubation at 37°C. During this process, proteinase K present in the STOP buffer caused degradation of all proteins. DNA was thus released from the protein coat and could be evenly separated in the following step. Stopped reactions were mixed with

3.3 µl of 10×DNA loading buffer, resolved by 1% agarose gel electrophoresis in 0.5×TBE buffer at 100V for 1 h 45 min, stained in ethidium bromid solution (0.5 µg/ml) and visualized using a UV transilluminator.

Signal of the particular bands was quantified using ImageJ software and the quantity of supercoiled DNA products was first expressed as a percentage of total dsDNA and then calculated as a percentage of the amount of product generated in the reaction carried out in the absence of helicase and RPA (Figure 34, line 3; - control, 0% of supercoiled DNA) and in the absence of ssDNA, helicase, and RPA (Figure 34, line 4; + control, 100% of supercoiled DNA).

To generate topologically relaxed dsDNA, 4 µl of supercoiled pGEM-7Zf(+) DNA was incubated with 1.6 µg of *E. coli* topoisomerase I at 37°C for 30 min in 40 µl of Buffer R supplemented by 100 µg/ml BSA. This enzyme was then heat inactivated at 65°C for 10 min.

Buffer R	25 mM Tris-HCl, pH 7.5; 50 mM KCl; 1 mM DTT; 1 mM $MgCl_2$; 100µg/ml BSA
STOP buffer	6% (w/v) SDS; 0.1 M EDTA; 5 mg/ml proteinase K
DNA loading buffer (10×)	0.25% (w/v) Bromophenol Blue; 50 mM Tris-HCl, pH 7.6; 60% glycerol
TBE buffer (5×)	0.5 M Tris, pH 8.0; 0.45 M boric acid; 10 mM EDTA

5 Results

5.1 Anti-FBH1 antibody production

5.1.1 Antigen production

To produce the antigen for yield anti-FBH1 antibody, N-terminal part (1.27 kbp; 1-484 aa) of the full-length human *FBH1* (1-969 aa) gene encoding the isoform 4 was subcloned into the pTYB12 vector by PCR using the following set of primers: **F** 5´-catg **gct agc** atg gcc aaa agc aat tct gtt g -3´; **R** 5´- gca **ctc gag** ttc ggc ctg ctt tgc gat -3´, and following set of RE: *Nhe I/Xho I*. The antigen was expressed in bacteria as a fusion with N-terminal self-cleavable affinity tag containing a chitin binding domain (CBD) [CBD-FBH1(1-484 aa)] (Figure 17).

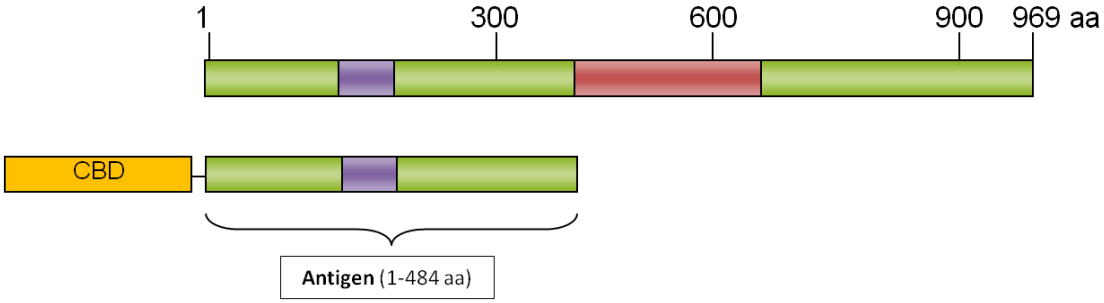

Figure 17 A schematic outline of FBH1 and of the antigen used for anti-FBH1 antibody production. N-terminal fragment of full-length FBH1 containing F-box motif was expressed as a fusion protein with chitin binding domain (CBD) and used for antigen production. Violet box = F-bow motif; red box = DNA helicase domain; bp, base pair.

Antigen used for chicken immunization was prepared by Igor Chevelev, Ph.D. Immunization was performed in cooperation with Jiří Plachý, Ph.D., in an animal farm in Koleč. To purify antigen for affinity purification of the antibody, optimal conditions for antigen expression in soluble form were found by series of pilot expression experiments (Figure 18). Total and soluble cell extract of the lysed treated cells, alternatively total fraction of non-induced cells, were separated by SDS-PAGE. Antigen expression was first checked in XA90 bacterial cells. Protein expression was induced by addition of 1 mM IPTG followed by incubation at 37°C for 2 hours. The antigen was expressed under these conditions but was not present in soluble cytosolic fraction. Next we tried to decrease temperature and IPTG concentration and prolong time of expression to obtain soluble protein. We also compared antigen expression in two different bacterial strains, XA90 and BL 21. The expression level of the antigen increased under conditions of 0.5 mM IPTG at 37°C for 2 hours in both cell strains.

However the antigen was not in soluble form. Under the conditions of 0.2 mM IPTG at 16°C for 20 hours, the antigen was present in soluble fraction in both strains, but not in a sufficient amount.

In the next experiments, we thus further decreased the temperature and IPTG concentration and prolonged the time of protein induction to 36 hours. Finally, expression under the conditions of 0.1 mM IPTG at 14°C for 36 hours, and 0.2 mM IPTG at 14°C for 36 hours, gave satisfying results in XA90 cells. Under these conditions, the antigen was present is soluble fraction at the same level as in total cell fraction. Expression level in BL21 cells was comparable with non-induced control.

Large-scale expression of antigen was performed in XA90 cells using 0.2 mM IPTG and induction for 43 hours at 12°C. Antigen was purified by chitin affinity chromatography and five elution fractions of FBH1 antigen were collected (Table 2) and analyzed by SDS-PAGE (Figure 19). Finally, all antigen elution fractions were put together (5.26 mg in 36 ml) and used for anti-FBH1 antibody purification.

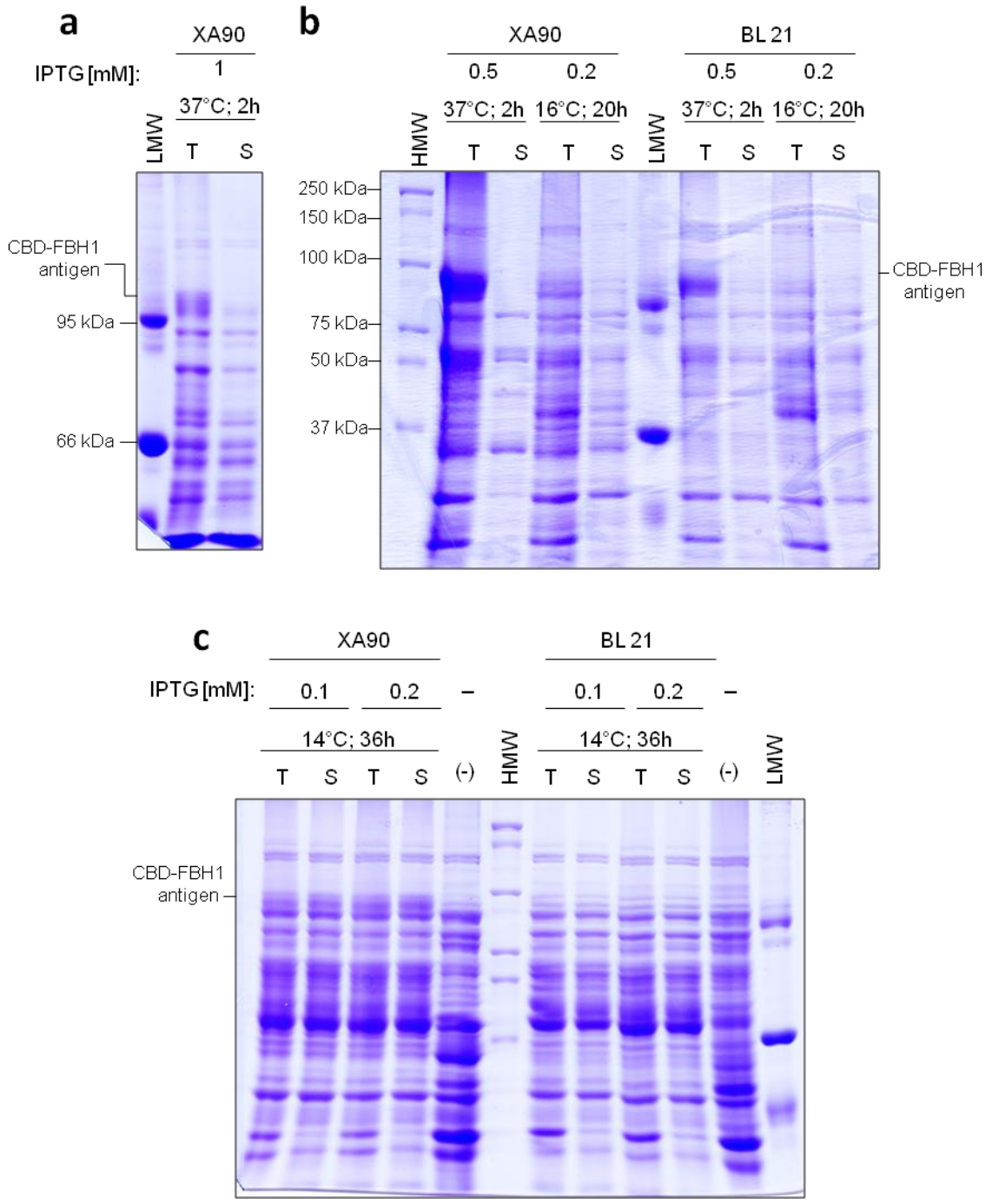

Figure 18 Optimization of FBH1 antigen expression.
Cell fractions analysed by SDS-PAGE. Expression in XA90 and BL21 bacterial strains was induced by **(a)** 1 mM IPTG at 37°C for 2 hours; **(b)** 0.5 mM IPTG at 37°C for 2 hours, and 0.2 mM IPTG at 16°C for 20 hours; and **(c)** 0.1 mM IPTG at 14°C for 36 hours and 0.2 mM IPTG at 14°C for 36 hours. Total cell extract, T; soluble protein extract, S; non-induced cells, (-); HMW-SDS Marker, HMW; LMW-SDS Marker, LMW. Expected positions of FBH1 antigen are denoted.

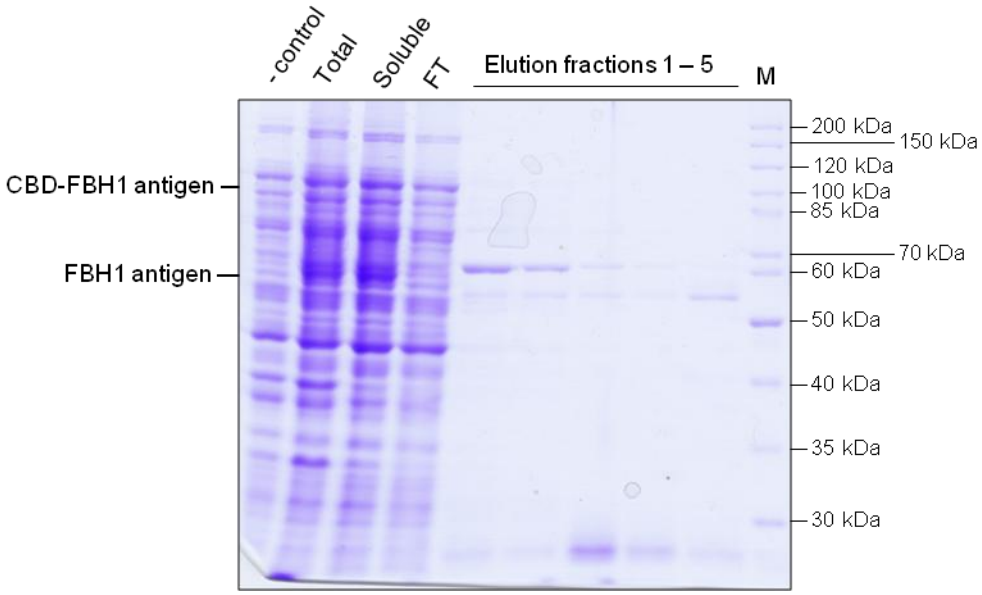

Figure 19 Large-scale expression and purification of FBH1 antigen.
Total cell extract before, -control, and after induction of expression, Total; soluble protein extract, Soluble; flow through from chitin beads, FT; and five elution fractions are shown. PageRuler™ Unstained Protein Ladder, M.

Table 2 Purification of FBH1 antigen by chitin affinity chromatography.
Five elution fractions obtained after affinity purification of the antigen in large-scale.

Elution fraction	Volume of elution fraction (ml)	Protein concentration (mg/ml)	Protein weight (mg)
1.	11.5	0.204	2.35
2.	5.0	0.128	0.64
3.	7.0	0.148	1.04
4.	7.0	0.104	0.73
5.	5.5	0.092	0.51
Pooled fractions	36.0	0.146	5.26

5.1.2 Isolation and characterization of anti-FBH1 antibody

Eggs from the immunized hen were collected and utilized for extraction of the antibody. First, a total immunoglobulin extract containing a mixture of various IgYs was isolated from ten egg yolks. In the next step, specific anti-FBH1 IgYs were purified by affinity chromatography utilizing purified FBH1 antigen immobilized on an NHS-activated agarose column (Table 3).

Table 3 Anti-FBH1 antibody purification.

10 eggs	Volume (ml)	Protein concentration (mg/ml)	Protein weight (mg)
Total IgY fraction	140.0	1.97	275.8
Pure anti-FBH1 antibody	4.2	1.3	5.5

Purified anti-FBH1 antibody was subjected to dot-blot analysis (Figure 20) using different amounts of the antigen (0.5 - 125 ng) and four different antibody dilutions (1:5 000-1:100 000) to find optimal conditions. From these results we see, that the antibody recognizes antigen in a concentration dependent manner. We next wanted to examine the ability of the antibody to detect recombinant and endogenous FBH1 in extract from human cells (HeLa, U2OS, and HEK293). The expected position of endogenous FBH1 is approximately 110-140 kDa. At this position, there is more than one band apparent on western blot of human cell lysates (Figure 21). Moreover, we observed that the antibody was bound non-specifically to other proteins in cell lysate. From this test, we chose the 1:50 000 antibody dilution as the working dilution, which was used in all following experiments.

To distinguish which band represents endogenous FBH1 we employed a specific small-interfering RNA (siRNA) to deplete endogenous FBH1 (Figure 22). We also included siLuciferase as a control and over-expressed exogenous FBH1 (GFP-FBH1). Samples were run twice on separate membranes and incubated with two different anti-FBH1 antibodies (newly purified and commercial mouse monoclonal anti-FBH1). To reduce the background caused by nonspecific binding, we tried to block the membrane using 3% (w/v) BSA solution instead of 5% (w/v) dry milk in TBST, and additionally, 1% (w/v) BSA was added to both, primary and secondary antibody solution. We found that none of the bands on western blot disappeared upon siFBH1 treatment. Recombinant and over-expressed FBH1 were recognized by both antibodies.

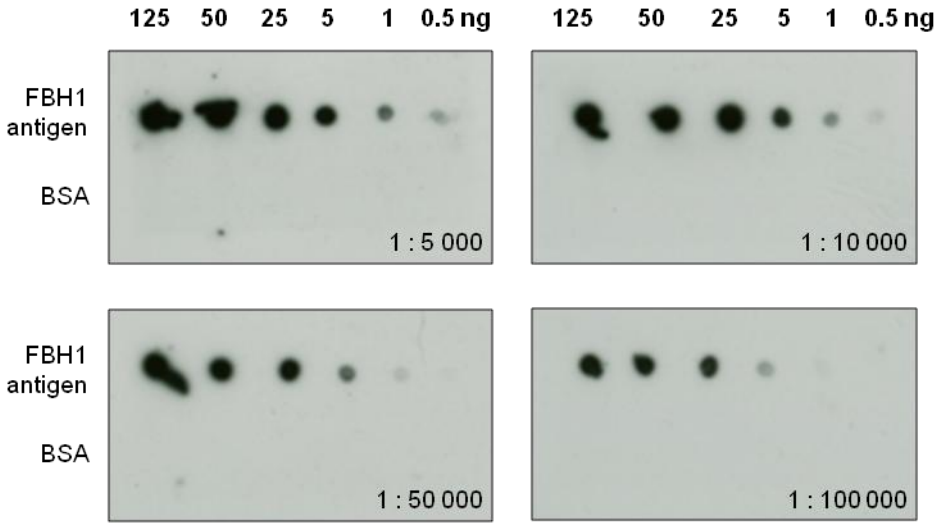

Figure 20 Sensitivity test of purified anti-FBH1 antibody.
Test of functionality and sensitivity of purified anti-FBH1 antibody. The FBH1 antigen and BSA as a negative control were dropped on PVDF membranes in decreasing amount as shown and incubated with different dilutions of anti-FBH1 antibody as denoted on bottom right edge of the membranes.

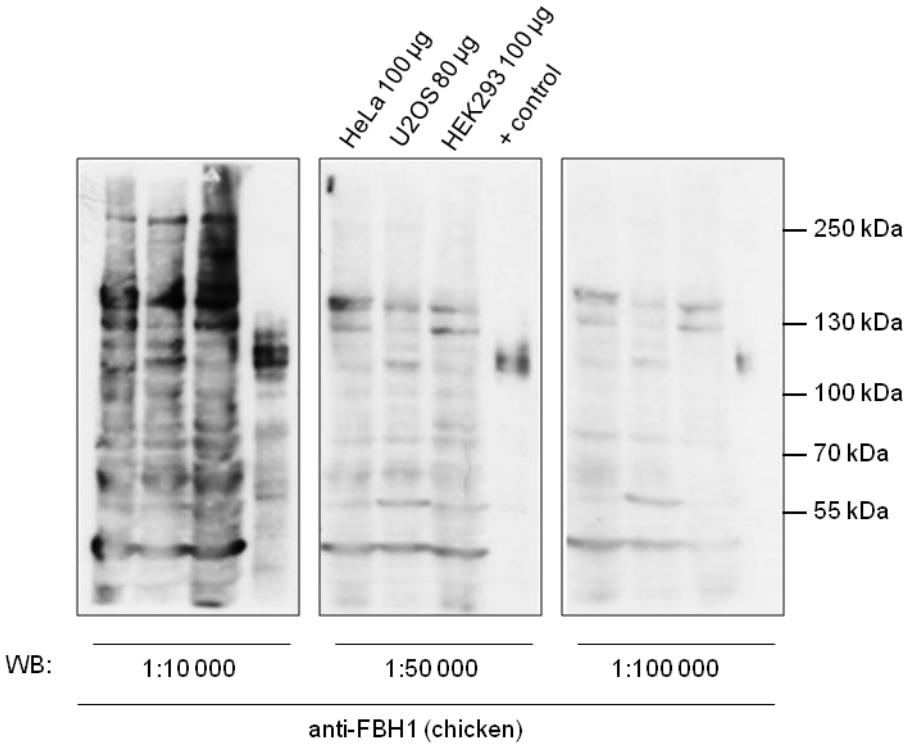

Figure 21 Western blot analysis of human cell extracts using anti-FBH1 antibody.
Lysates of human cell lines, HeLa; U2OS; and HEK293 were separated by SDS-PAGE and analyzed western blot using three dilutions (1:10 000; 1:50 000; and 1:100 000) of chicken anti-FBH1 antibody. Positive control, + control, is expressed streptavidin-FBH1-His6× in Sf9 cell lysate. Expected position of endogenous FBH1 is ~110 - 140 kDa.

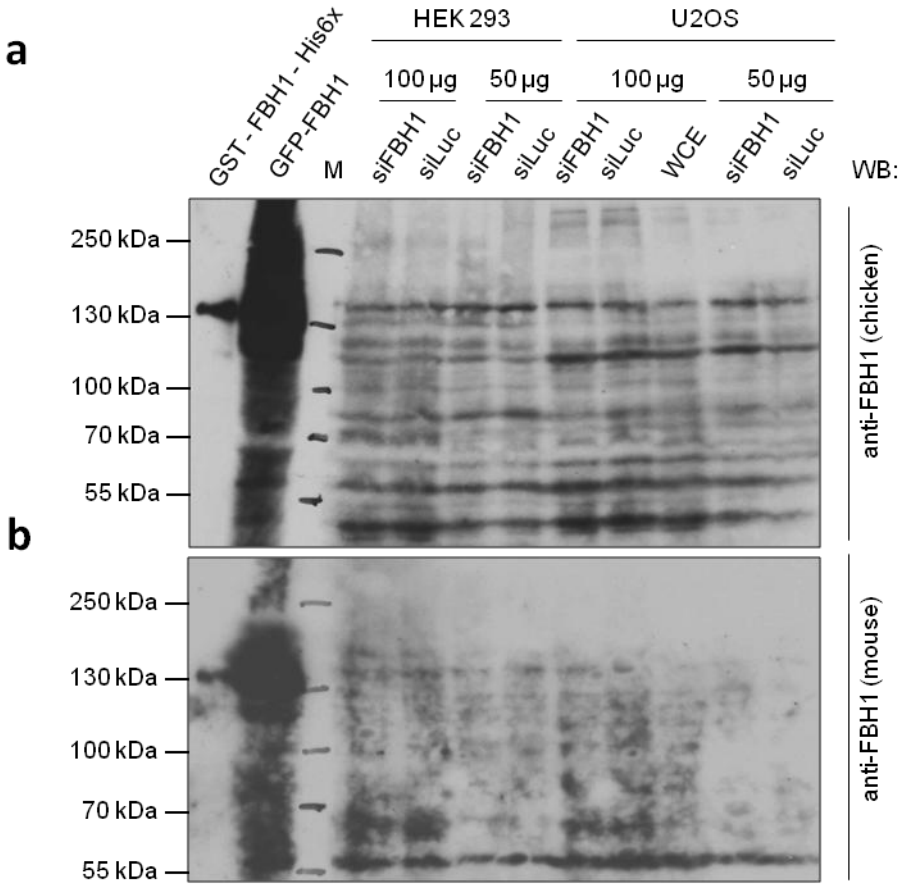

Figure 22 Ability of anti-FBH1 antibody to recognize FBH1.
Western blot (WB) analysis of purified recombinant GST-FBH1-His6x (100 ng); HEK293 cell lysate with over-expressed GFP-FBH1 (30 µg); and HEK293 and U2OS cell non-transfected (whole cell lysate, WCE) or transfected with siFBH1 and siLuciferase, siLuc. Membranes were incubated with **(a)** chicken anti-FBH1 antibody or **(b)** commercial mouse anti-FBH1antibody. Analysed fractions were loaded in amounts as denoted in upper part (50 or 100 µg). Expected positions of FBH1 signal are: 135 kDa of GST-FBH1-His6x and GFP-FBH1; ~110 - 140 kDa of endogenous FBH1. PageRuler™ Plus Prestained Protein Ladder, M.

5.2 Production of full-length FBH1 and FBH1^{D698N} proteins in insect cells

The construct for expression of the full-length *FBH1* gene, the shortest isoform (969 aa), was derieved from *pFastBac-streptavidin-FBH1(2.9kbp)-His6x*. The *streptavidin tag* was replaced with a *GST tag* using *NheI* and *NdeI* restriction enzymes. The created construct was used for transformation of DH10Bac *E. coli* cells containing bacmid DNA. Here, the subcloned DNA fragment was transposed into the bacmid downstream of polyhedrin promoter. Sf9 cells were transfected by the purified bacmid DNA to produce virus.

Beside FBH1 we also produced the ATPase-dead variant of FBH1 protein (FBH1^{D698N}). Numbering of the amino acid substitution is adopted from the longest isoform of FBH1 (1094 aa) used by Fugger et al. (2009) and does not correspond to numbering in the shortest isoform. In the shortest isoform, it is D573N (see supplement). For better order we kept the original numbering. Site directed mutagenesis was performed by Igor Chevelev, Ph.D.

Both proteins were expressed as fusions with a GST tag at the N-terminus and a histidine (His6x) tag on the C-terminus. The resulting proteins were: GST-FBH1-His6x (here FBH1) and GST-FBH1^{D698N}-His6x (here FBH1^{D698N}) (Figure 23).

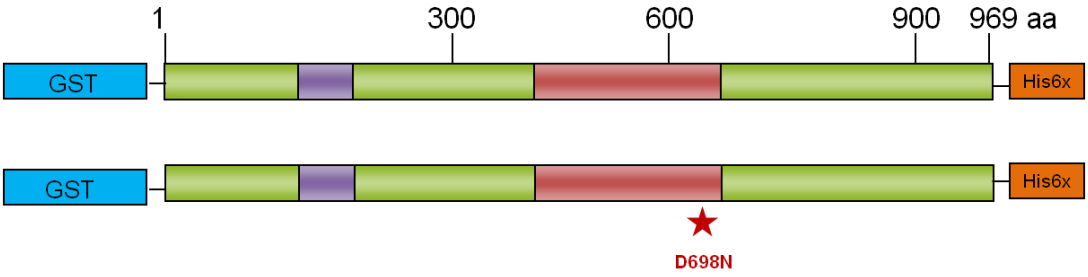

Figure 23 Schematic depiction of FBH1 proteins.
Both, FBH1 (upper sequence) and ATPase defective mutant FBH1^{D698N} (bottom sequence), were expressed with glutathion S-transferase (GST, blue box) and histidine (His6x, orange box) affinity tags. F-box motif is displayed as violet box and DNA helicase domain as red box. Red asterisk denotes approximate position of amino acids (aa) substitution on the FBH1^{D698N} primary sequence.

Transfection, virus stock amplification and large-scale protein expression (3-days) of FBH1 was performed by RNDr. Kamila Burdová. Protein was purified in two steps. Firstly, FBH1 was captured via GST tag to GSH agarose beads during 4h-incubation and subsequently eluted by increasing concentration of GSH, the binding competitor. Due to an extensive

contamination in the elution fractions caused by GST from insect cells (Figure 24, Table) we were forced to integrate second purification step by heparin affinity chromatography. Sufficiently pure FBH1 was obtained. Amount of protein was monitored by protein concentration determination in all fractions in both purification steps (Table 4).

The FBH1 protein was tested for ATPase activity by malachit green assay and was found to be active (for details see chapter 5.3). Next we prepared new virus for expression of FBH1 and FBH1^{D698N}. Expression efficiency of both proteins was compared by 2- and 3-days expressions in small-scale. Additionally, we examined minimal time necessary for sufficient binding of both proteins to GSH agarose by incubation for 2 and 4 hours (Figure 25). We found that both proteins are sufficiently expressed in 2 days in a soluble form, whereas after 3-days expression cells were already lysed and protein released into the medium. Expression of soluble FBH1^{D698N} was at least 2 times lower than that of FBH1. Both proteins were efficiently bound to the GSH agarose within 2 hours.

Next, the FBH1^{D698N} was produced in large-scale under the same conditions used for FBH1 production (Figure 26). The only exceptions were those conditions found as more profitable in the small-scale expression described above, e.g. 2-days expression and 2 hours of binding to GSH agarose. The total amount of purified FBH1^{D698N} protein (~7.5 μg from 2.5×10^8 insect cells) was considerably reduced in comparison to the FBH1 (~147 μg from 1.5×10^8 insect cells) as summarized in Table 4.

To compare purity of FBH1 and FBH1^{D698N}, we analyzed 200 ng of each protein, by SDS-PAGE followed by silver staining (Figure 26). However FBH1^{D698N} seems to be more contaminated, the amount of purified FBH1 and FBH1^{D698N} in these fractions was comparable, even slightly higher in case of FBH1^{D698N}. Nevertheless, for further enzymatic experiments we kept this ratio and adjusted the concentration of FBH1^{D698N} to 0.05 mg/ml.

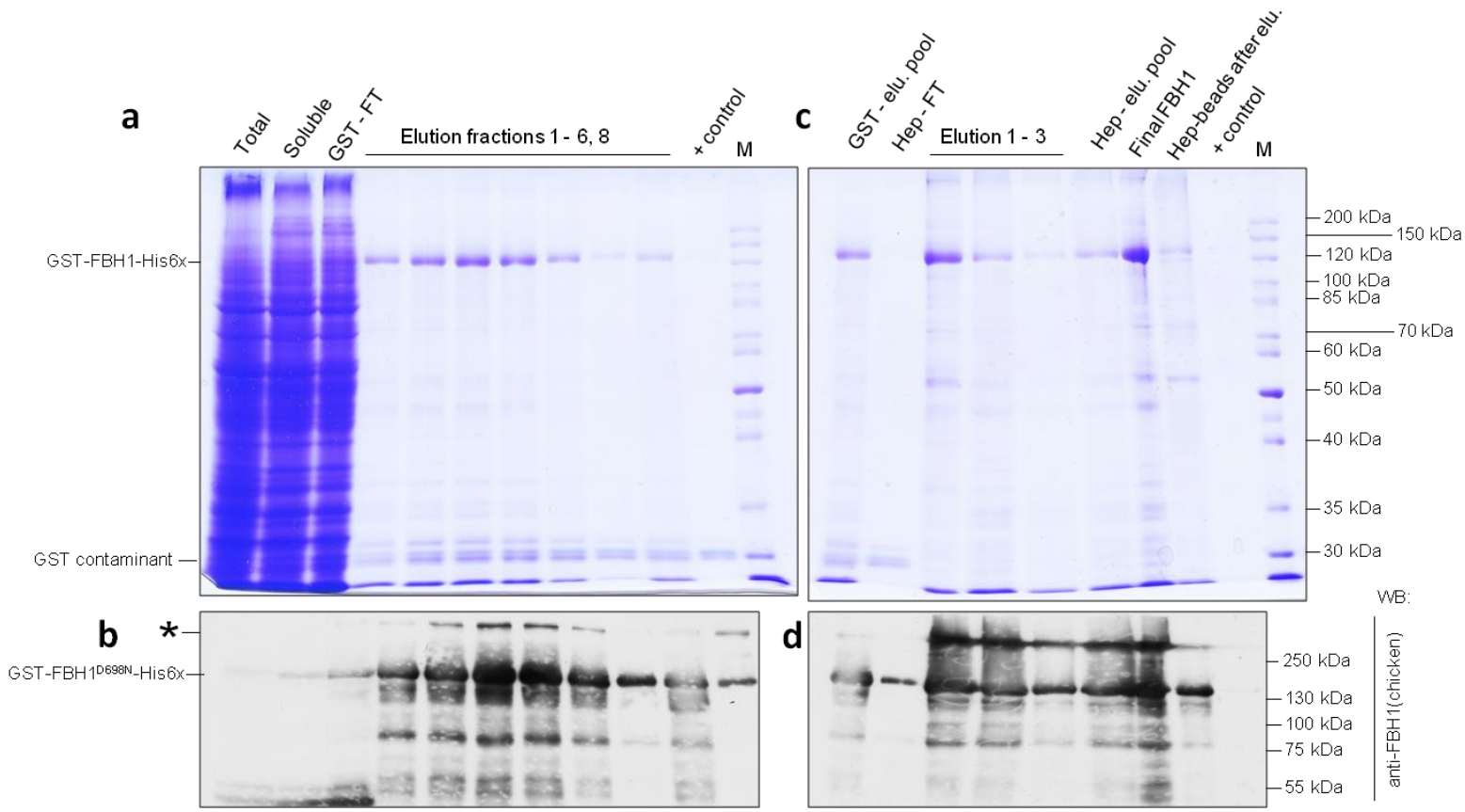

Figure 24 Large-scale expression and purification of FBH1.
FBH1was isolated using GST **(a, b)** and heparin **(c, d)** affinity chromatography purification steps. Protein fractions were separated by SDS-PAGE **(a, c)** and analysed by western blotting (WB) using chicken anti-FBH1 antibody **(b, d)**. Total cell extract, Total; soluble protein extract, soluble; flow through from GSH and heparin agarose, GST-FT and Hep-FT, respectively; particular elution fractions; former isolated FBH1 as a positive control, +control; mixed elution fractions from GSH agarose, GST-elu. pool; mixed elution fractions from heparin beads before dialysis, Hep-elu. pool; final FBH1 protein sample after dialysis, Final FBH; and heparin beads after elution, Hep-beads after elu., are shown. PageRuler™ Unstained Protein Ladder, M. Asterisk denotes oligomerization of FBH1. GST contaminant is shown at position of 26 kDa.

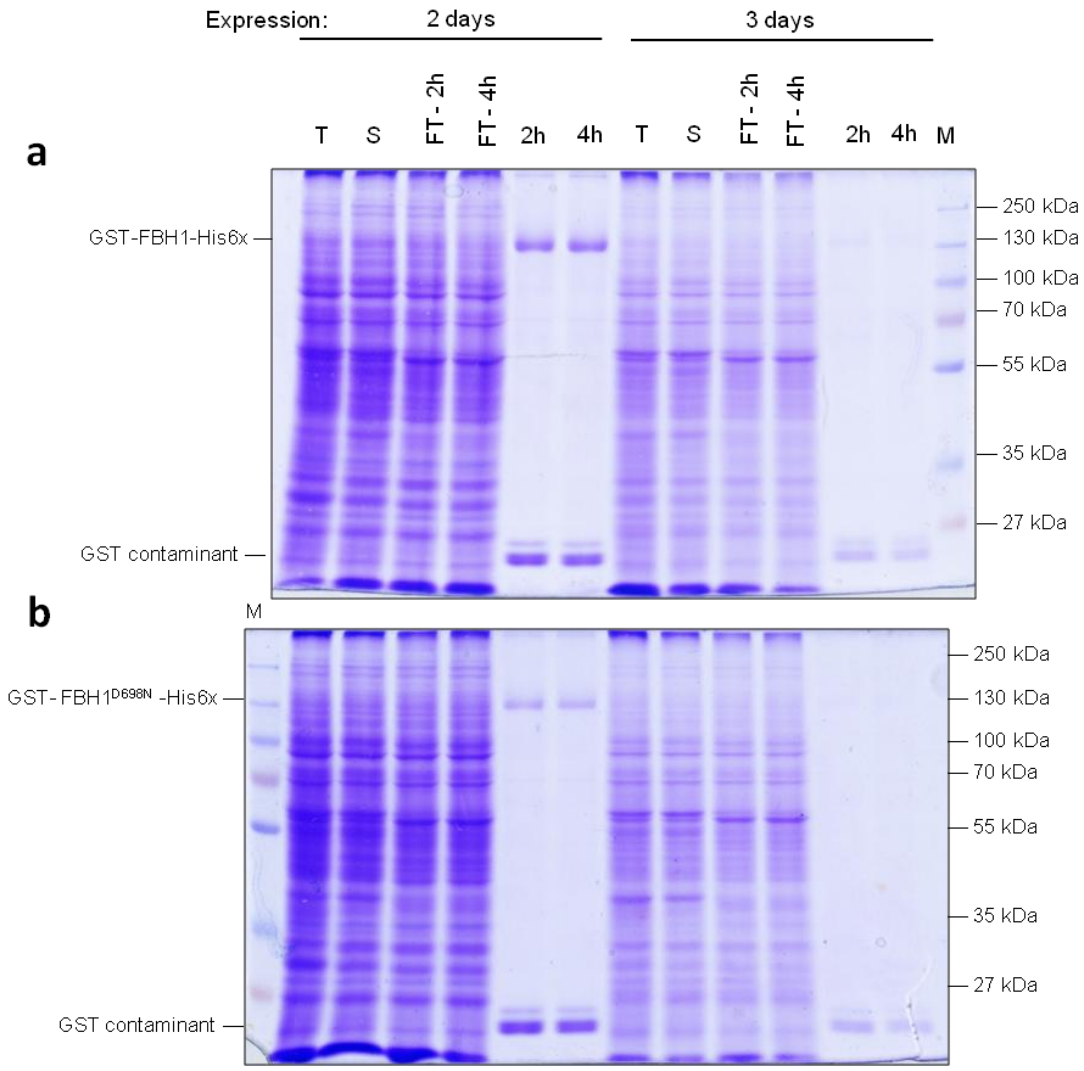

Figure 25 Production of FBH1 and FBH1^{D698N} proteins in small-scale.
FBH1 **(a)** and FBH1^{D698N} **(b)** were expressed for 2 or 3 days. Soluble protein extract was incubated with GSH agarose for 2 hours (2h) and 4 hours (4h). Protein fractions were separated by SDS-PAGE. 135kDa bands represent FBH1wt or FBH1^{D698N} protein. Total cell extract, T; soluble protein extract, S; flow through from GSH agarose upon 2 and 4 hours of incubation, FT-2h and FT-4h, respectively; PageRuler™ Plus Prestained Protein Ladder, M. GST contaminant is shown at position of 26 kDa.

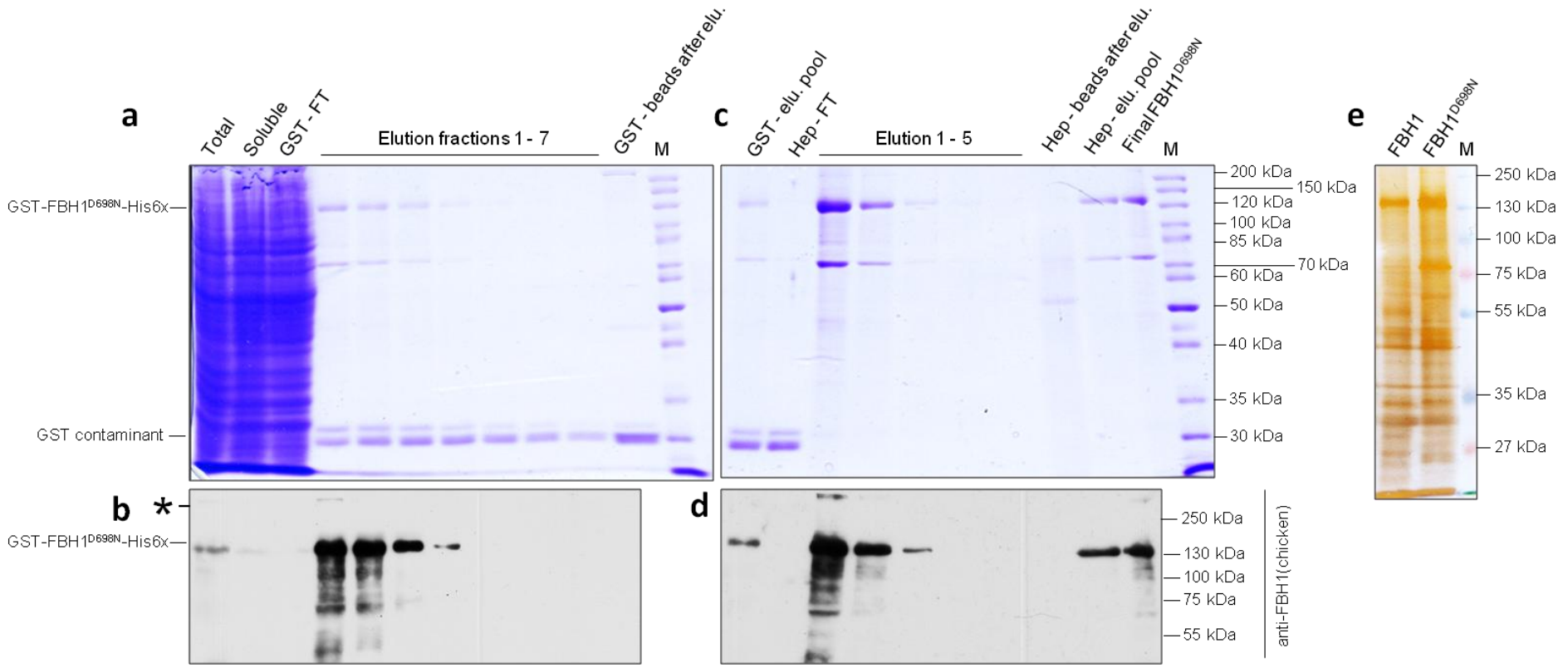

Figure 26 Large-scale expression and purification of FBH1^{D698N}.
FBH1^{D698N} was isolated by two-step purification using GST **(a, b)** and heparin **(c, d)** affinity chromatography. Protein fractions were separated by SDS-PAGE **(a, c)** and analysed by western blotting (WB) using chicken anti-FBH1 antibody **(b, d)**. Total cell extract, Total; soluble protein extract, soluble; flow through from GSH and heparin agarose, GST-FT and Hep-FT, respectively; particular elution fractions; GSH and heparin agarose after elution, GST- and Hep-beads after elu., respectively; mixed elution fractions from GSH agarose, GST-elu. pool; mixed elution fractions from heparin beads before dialysis, Hep-elu. pool; final FBH1^{D698N} sample after dialysis, final FBH1^{D698N}; and PageRuler™ Unstained Protein Ladder, M,. Asterisk denotes oligomerization of FBH1^{D698N}. GST contaminant is shown at position of 26 kDa. **e)** Comparison of 200 ng of purified FBH1 and FBH1^{D698N}. Proteins were separated by SDS-PAGE followed by silver staining. PageRuler™ Plus Prestained Protein Ladder, M.

Table 4 Protein fractions of two-step purification of FBH1 and FBH1^{D698N} in large-scale.

GST-purification step						
	FBH1			FBH1^{D698N}		
Number of cells	1.5×10^8			2.5×10^8		
Fraction	Volume (ml)	c (mg/ml)	∑ protein (mg)	Volume (ml)	c (mg/ml)	∑ protein (mg)
Soluble protein extract	8.5	6.100	52.000	15.0	4.000	60.000
Elution 1	0.5	0.231	0.116	0.5	0.170	0.085
2	0.6	0.335	0.201	0.5	0.170	0.085
3	0.5	0.369	0.185	0.5	0.150	0.075
4	0.4	0.310	0.139	0.5	0.090	0.045
5	0.4	0.268	0.107	0.5	0.050	0.025
6	0.5	0.219	0.110	0.5	0.024	0.012
7	0.5	0.167	0.084	0.5	0.001	0.005
8	0.4	0.136	0.054	-	-	-
9	0.5	0.140	0.070	-	-	-
10	0.5	0.121	0.061	-	-	-
11	0.5	0.094	0.047	-	-	-
12	0.5	0.112	0.056	-	-	-
Elution pool	5.0	0.120	0.6	3.5	0.093	0.325
Heparin-purification step						
Elution 1	0.25	0.213	0.053	0.10	0.220	0.022
2	0.50	0.209	0.105	0.10	0.058	0.006
3	0.50	0.049	0.025	0.10	0.001	0.000
4	-	-	-	0.10	0.000	0.000
5	-	-	-	0.10	0.000	0.000
Total elution pool	1.25	0.14	0.175	0.45	0.056	0.025
Final protein	0.4	0.368	0.147	0.15	~0.050	~0.007

5.3 Characterization of ATPase activity of FBH1

To check whether purified FBH1 is enzymatically active, we measured its DNA-dependent ATPase activity, which is a hallmark activity of any DNA helicase. The ability of FBH1 to hydrolyse ATP was investigated by malachite green assay.

We compared the enzymatic activities of FBH1 and RECQ5β (Figure 27). Inactivated FBH1 was included in these measurements to exclude that the detected activity is due to presence of phosphate in FBH1 sample. To rule out the possibility of contaminating enzymatic activity, $FBH1^{D698N}$ was examined as well.

These experiments demonstrated that in the presence of ssDNA, purified FBH1 catalysed ATP hydrolysis in a dose dependent manner. In comparison to RECQ5β, FBH1 exerted 2-3 times lower activity. $FBH1^{D698N}$ did not show any ATPase activity. This observation ensured us that the observed ATP hydrolysis was derived exclusively from FBH1 and not from other co-purified contaminants.

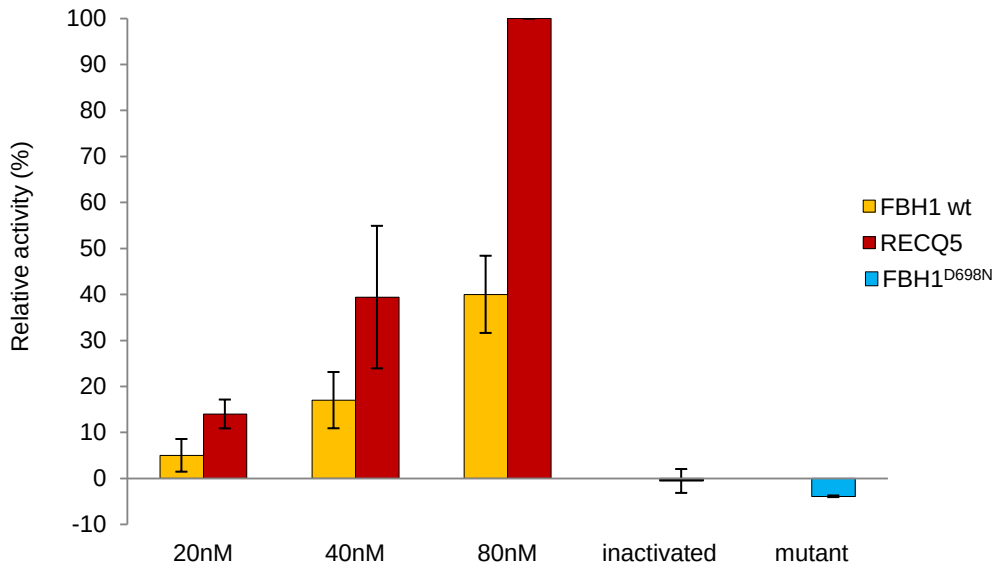

Figure 27 Examination of ATPase activity of FBH1.
ATPase activity measured by malachite green ATPase assay. Increasing concentrations (20-80 nM) of FBH1 and RECQ5β were used in the reactions. Both controls, inactivated FBH1 and $FBH1^{D698N}$, were present at 80 nM concentration. The plot bars display average of values from two or more independent experiments. Error bars indicate standard deviation about the mean.

The DNA-dependent ATPase activity of FBH1 was further characterized under different reaction conditions (Figure 28-30). In these experiments, the typical reaction conditions were: 40 nM FBH1, 25 μg/ml of ssDNA and 2 mM ATP, if not specified otherwise. First, we measured the ATPase of FBH1 at different ATP concentrations (0-16 mM) as shown in Figure 28. We observed that FBH1 displayed the maximal activity at 8 mM.

To determine the DNA substrate preference, ssDNA, dsDNA (25 μg/ml) and four oligonucleotides of different length, 25-, 37-, 53-, and 93-nucleotides (1μM) were examined for their ability to support ATPase activity of FBH1 (Figure 29). The results confirmed that FBH1 preferentially acts on ssDNA. dsDNA and other oligonucleotides supported the ATPase activity of FBH1 less efficiently. We also examined the ability of FBH1 to utilize other NTPs and dNTPs, as energy source (Figure 30). We found that dATP could also serve as substrate for FBH1 with 77% efficiency compared to ATP. Other nucleotides were hydrolyzed poorly by FBH1 with 45-15% efficiency as compared to ATP.

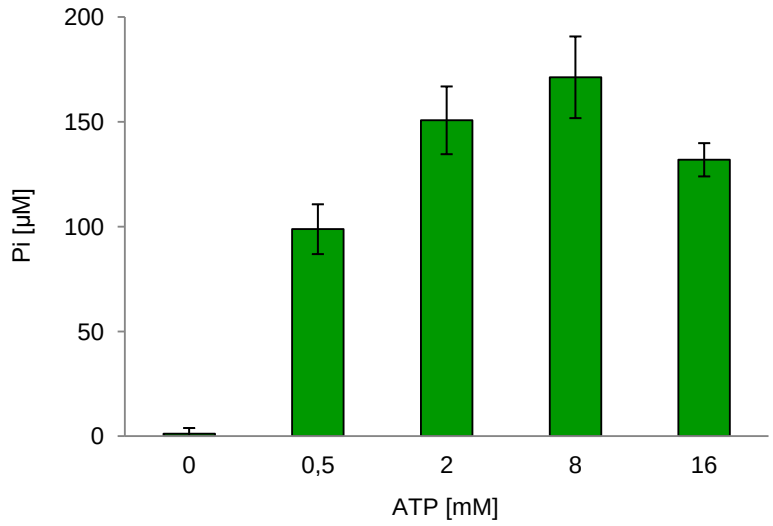

Figure 28 ATPase activity of FBH1 at different ATP concentrations.
ATP was present at concentrations (0; 0.5; 2; 8; and 16mM) in the reactions. The plot bars indicate average of values from three independent experiments. Error bars represent the standard deviation about the mean.

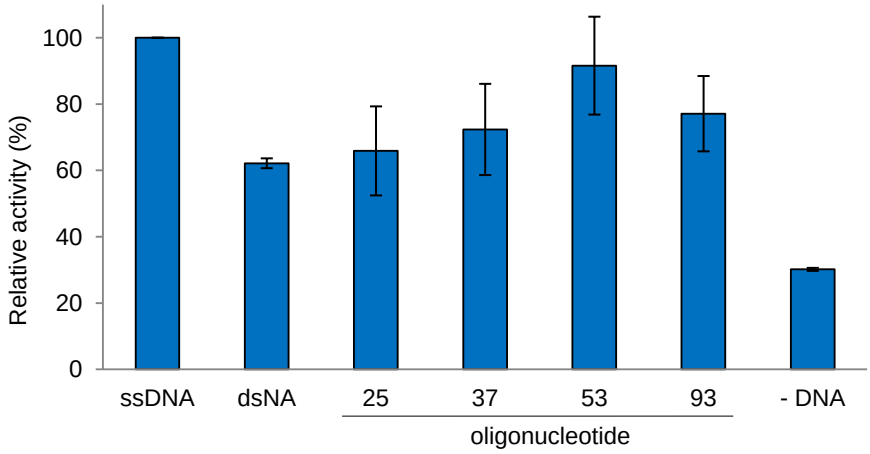

Figure 29 ATPase activity of FBH1 in the presence of different DNA substrates.
Single-stranded DNA (ssDNA) and double-stranded DNA (dsDNA) plasmid DNA in 25 µg/ml concentration, oligonucleotides in length of 25-, 37-, 53-, and 93-nucleotides in 1 µM concentration were used as DNA substrates. 40nM FBH1 helicase was used in all reactions. The values in this experiment are related to concentration of released P_i upon hydrolysis of ATP in presence of ssDNA. The data presented are the average of three independent experiments. Error bars represent the standard deviation about the mean.

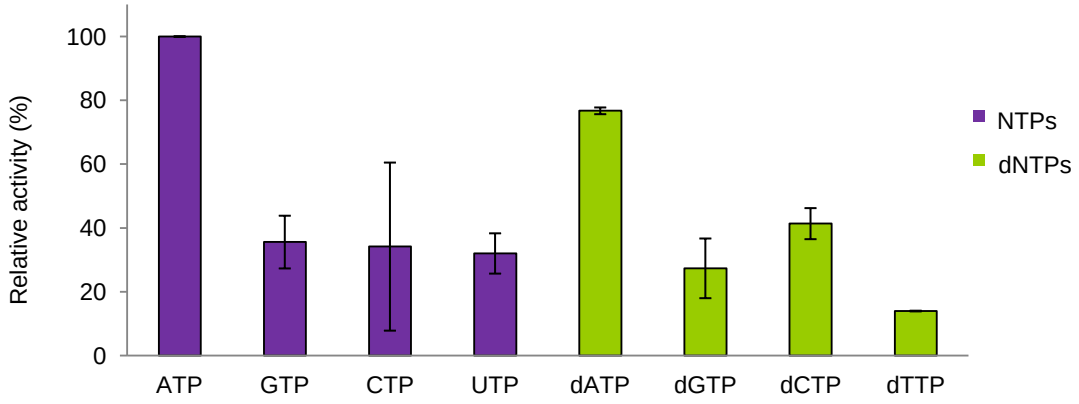

Figure 30 Ability of FBH1 to utilize NTPs or dNTPs as an energy source.
Different nucleotide cofactors, NTPs (ATP, GTP, CTP and UTP) or dNTPs (dATP, dGTP, dCTP and dTTP) were present at 4 mM concentration in reactions. The values in this experiment are related to concentration of released P_i upon hydrolysis of ATP. The plot bars display average of values from two or more independent experiments. Error bars represent the standard deviation about the mean.

5.4 Protein interactions study

In an attempt to identify novel interaction partners of FBH1 helicase, we first decided to investigate its interaction with RAD51. Due to the fact that we were not able to detect endogenous FBH1 by western blotting, we were forced to rely on experiments with recombinant FBH1. For this purpose, we used a protein complex-immunoprecipitation (co-IP) assay using the GST-FBH1-His6x protein, which was added to cell extracts. In this approach, FBH1 protein was captured via endogenous RAD51 protein from HEK293 or U2OS human cells by anti-RAD51 antibody. Control IgG were used as a control of nonspecific binding of RAD51 and FBH1 to the beads. Proteins bound to beads were examined by western blotting (Figure 31). These results indicate that FBH1 interacts with RAD51, however the interaction seems to be very weak.

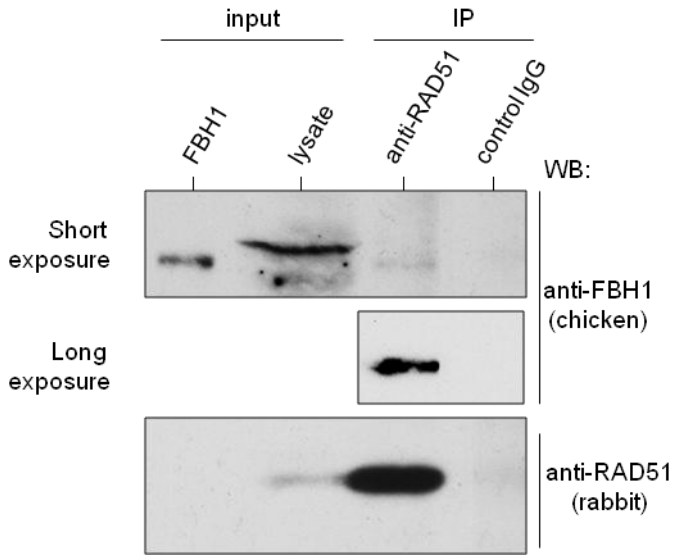

Figure 31 Co-immunoprecipitation of FBH1 with RAD51 from human cells extracts.
GST-FBH1-His6x (FBH1) protein was incubated with HEK293 cell lysate containing anti-RAD51 antibody or IgG as a control. Immunoprecipitated proteins bound to beads were eluted and analyzed by western blotting (WB) using chicken anti-FBH1and rabbit anti-RAD51antibodies. FBH1 (20%) and HEK293 cell lysate (5%) were loaded as input.

Next, we wanted to examine whether the observed interaction is direct or mediated by another protein. To prove this, we decided to perform pull-down assay using recombinant proteins, the GST-FBH1-His6x and human RAD51^{K133R}. The RAD51^{K133R} is ATPase-defective mutant of RAD51 and is more suitable for experiments with nucleoprotein filament described in chapter 5.5. We employed this protein because recombinant wild type RAD51 was not

available in our laboratory. In the interaction studies, the mutant is believed to behave the same as RAD51wt because ATPase motifs are not involved in protein-protein interactions.

The principal aim of the pull-down approach in this experiment is to pull-down RAD51^{K133R} protein via its interaction with FBH1, which is captured to beads through the GST tag. GST protein in equimolar concentration was used as a control. As demonstrated in Figure 32, we confirmed that FBH1 physically interacts with recombinant RAD51^{K133R} protein, however this interaction is weak. Additionally, reducing conditions increased the binding efficiency to GSH agarose.

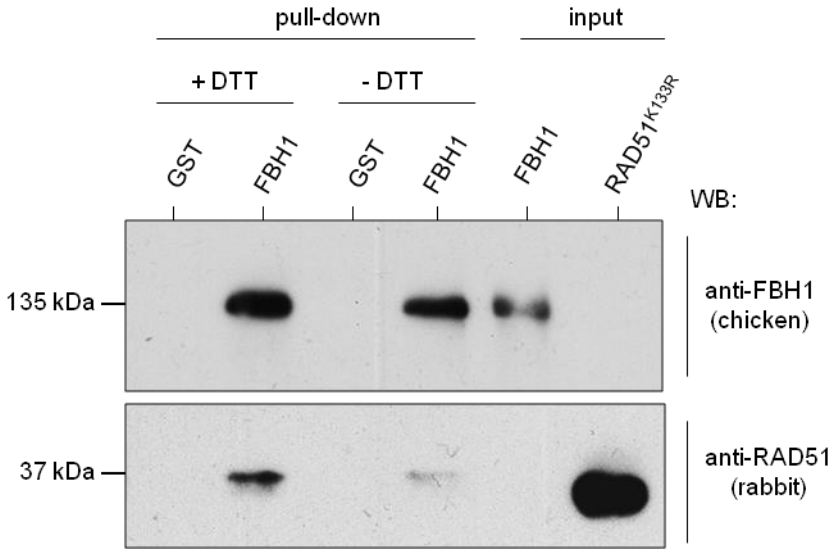

Figure 32 Direct physical interaction between FBH1 and RAD51.
Pull-down experiment with recombinant proteins. RAD51^{K133R} was incubated with GST-FBH1-His6x (FBH1) protein or GST as a control and GSH agarose beads in buffer with or without DTT, +DTT and -DTT, respectively. Elutions from the GSH agarose were separated by SDS-PAGE and analysed by western blotting (WB) using chicken anti-FBH1 and rabbit anti-RAD51 antibodies. FBH1 (40%) and RAD51 (5%) were loaded as input.

Next, we decided to examine interaction between FBH1 and RPA. As mentioned in chapter 2.2.2, RPA is heterotrimeric complex composed of three subunits (RPA70; RPA30; and RPA14). To see which of these subunits interacts with FBH1, we decided to use another *in vitro* approach to analyze direct protein-protein interactions, far western blotting technique. Beside RPA, we also included the RAD51^{K133R} protein and BSA. Prey proteins (RPA, RAD51^{K133R} and BSA) were separated by SDS-PAGE and transferred to membrane. The membrane was incubated in solution of GST or GST-FBH1-His6x, the bait protein. The interaction was then visualized using rabbit anti-GST antibody. Our results indicate that FBH1

interacts with the largest subunit of RPA complex, RPA70 (Figure 33). Weak interaction between FBH1 and RAD51 is apparent as well.

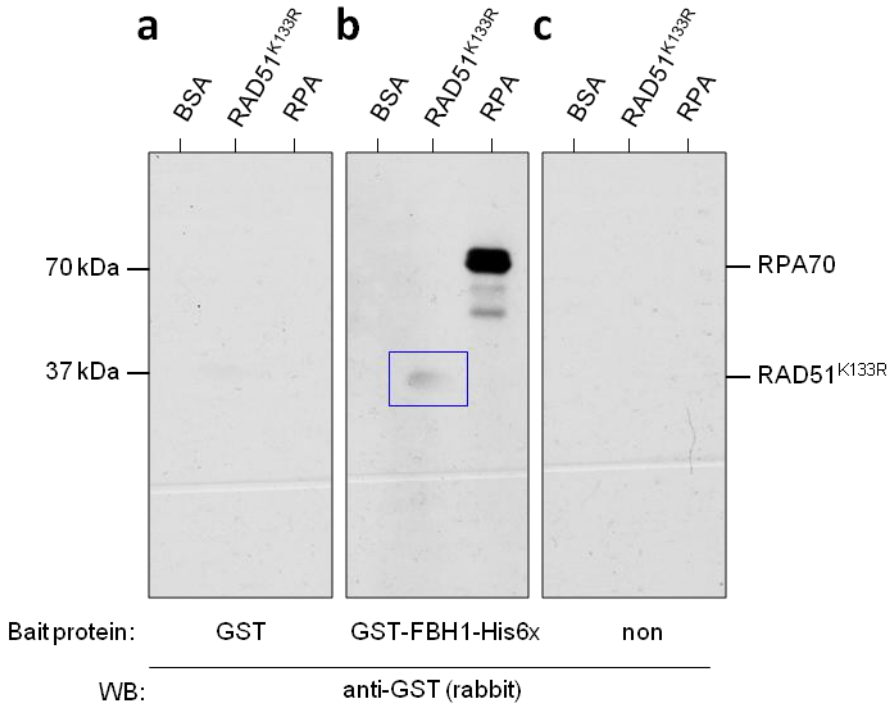

Figure 33 Far-western blot analysis of interaction between FBH1 with RAD51 and RPA. $RAD51^{K133R}$, RPA and BSA recombinant proteins were separated by SDS-PAGE and transferred to membrane. Membrane pieces were incubated with solution of bait protein: **a)** GST; **b)** GST-FBH1-His6x; and **c)** solution containing no bait protein. All membranes were incubated with rabbit anti-GST antibody. Position of $RAD51^{K133R}$ is denoted by blue box.

5.5 Analysis of FBH1 action on RAD51 nucleoprotein filament

The main aim of this project was to determine the function of FBH1 helicase on RAD51 nucleoprotein filament. To examine this task, we employed Topoisomerase I-linked DNA topology modification assay that allows detection of free RAD51 molecules in solutions. In our experiments, we used the $RAD51^{K133R}$, which has been shown to form stable nucleoprotein filaments in an ATP-bound state (Chi et al., 2006). We tested RAD51 disruption activity with increasing concentrations (50, 160, 210, and 320 nM) of FBH1 (GST-FBH1-His6x). Observed activity was compared to RECQ5β helicase, which is known to exert anti-recombinase activity (Schwendener et al., 2010). The purified $FBH1^{D698N}$ mutant, which lacks the capability to hydrolyse ATP and thus function to act as a helicase (Figure 27) was employed as negative control.

In presence of FBH1, as well as of RECQ5β, we can see concentration-dependent formation of supercoiled dsDNA products (Figure 34). This is not true in presence of $FBH1^{D698N}$, which has no effect on supercoiled DNA generation. Compared to RECQ5β, FBH1 exerts 3 times lower $RAD51^{K133R}$ filament disruption activity. Our results thus provide evidence that FBH1 mediates displacement of RAD51 from nucleoprotein filament.

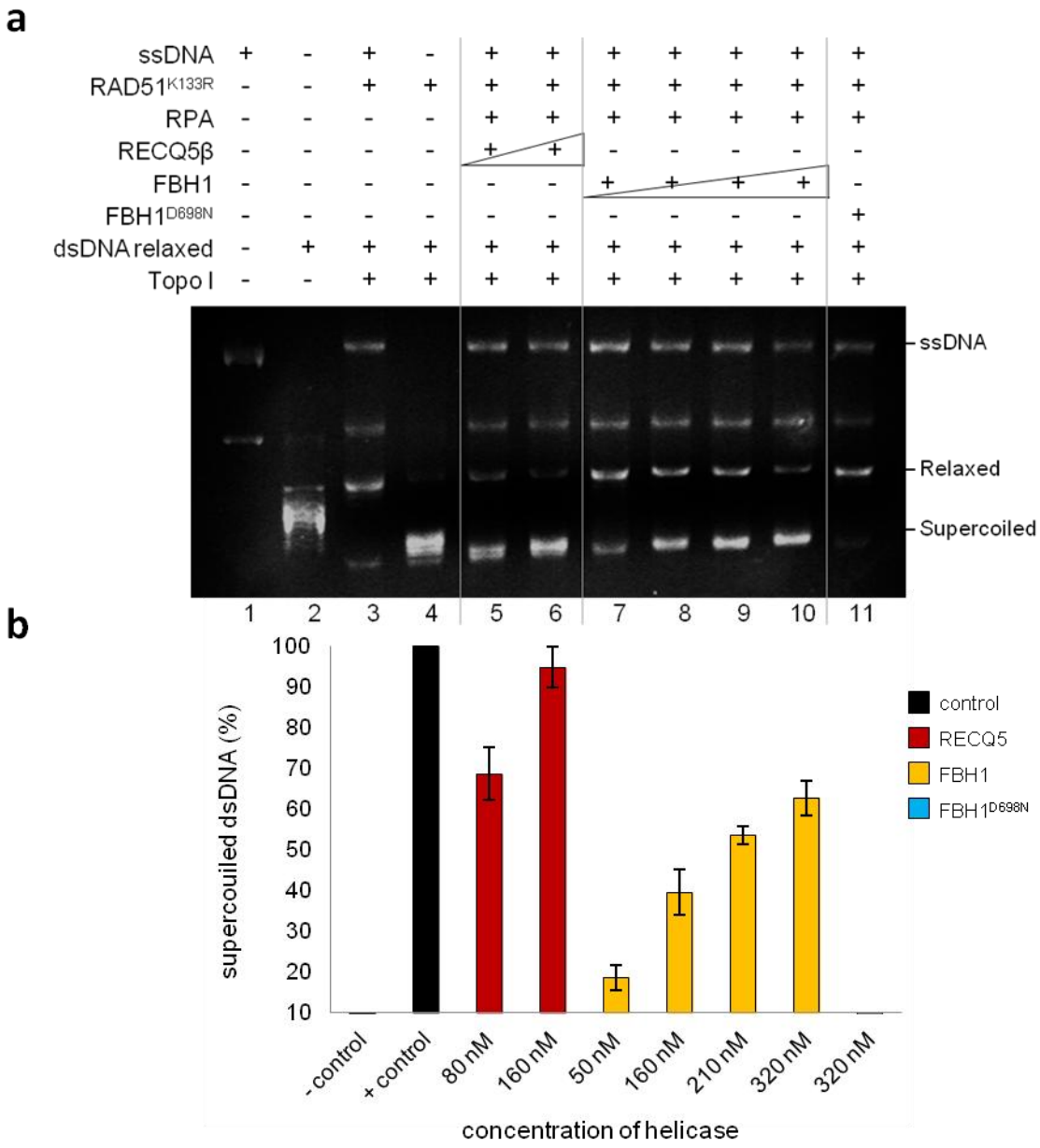

Figure 34 RAD51^{K133R} nucleoprotein filament disruption activity of FBH1.
a) Representative image of the effect of RECQ5β, FBH1 and FBH1^{D698N} on the stability of RAD51^{K133R} nucleoprotein filament in agarose gel. **b)** Quantification of the intensity of the supercoiled DNA. Single-stranded DNA, ssDNA; double-stranded DNA, dsDNA; TopoI, topoisometase I. The chart under the gel displays the average values from three independent experiments. Error bars represent the standard deviation about the mean.

6 Discussion

In the process of regulation of HR, FBH1 is known to inhibit accumulation of RAD51 at sites of DNA damage and thus suppresses recombination events (Fugger et al., 2009, Morishita et al., 2005). However, the molecular mechanism of how FBH1 acts as an antirecombinase is still unresolved issue. In this thesis, we have brought a new insight into the mechanism of FBH1 function.

We have produced the full-length human FBH1 protein in insect cells and characterized its enzymatic activities. To detect FBH1, we have raised chicken polyclonal antibody against an N-terminal fragment of human FBH1. We have investigated physical interactions of FBH1 with RAD51 and RPA. Moreover, we have examined whether FBH1 possesses the ability to disrupt RAD51 nucleoprotein filament.

Due to low quality of commercially available anti-FBH1 antibody, we decided to produce it on our own. Chicken species was chosen because they offer a number of advantages, among them are the possibility to quite easily harvest a large amount of antibodies, phylogenetic divergence from humans and low costs of hens breeding. We examined expression of various parts of FBH1 in *E.coli* but almost all gave either no expression or were produced into inclusion bodies (data not shown). The best results were obtained with N-terminal fragment (1-484 aa) of FBH1, so we decided to use this fragment as an antigen for antibody production, although the choice to produce antigen containing a highly conserved the F-box protein motif was quite risky. This protein was highly insoluble when expressed in bacteria at 37°C but a series of pilot expressions revealed appropriate conditions to yield the antigen in soluble form (Figure 18).

When used for western blotting, affinity-purified anti-FBH1 antibody could clearly detect purified recombinant full-length FBH1 protein (80 ng) and FBH1 ectopically expressed in human cells (Figure 22). However, in accordance with previous studies, we were not able to detect endogenous FBH1 (Figure 21, 22) (Kim et al., 2002, Fugger et al., 2009). This is probably due to a very low cellular concentration of FBH1. Fugger et al. (2009) observed that over-expressed FBH1 appears to be toxic to cells (Fugger et al., 2009). Thus it seems that FBH1 levels are tightly regulated in the cells to prevent deleterious effect of FBH1 on DNA metabolism.

We set up a protocol for large-scale production of full-length FBH1 (1-969 aa), the isoform 4, in insect cells using baculovirus expression system. Isoform 4 was the only isoform, which was available at the date of cloning (Internet source 3). Both FBH1 and FBH1^{D698N}

proteins were expressed as fusions with GST (N-terminus) and His6× (C-terminus) tags (Figure 23) and purified from the soluble cell extract. Cells were not sonicated to avoid binding of DNA from Sf9 cells to purified FBH1 protein. Large-scale expression of FBH1 was performed for three days, and we obtained high quantity of purified protein (Figure 24). After that we examined the expression efficiencies of both protein variants in small-scale (Figure 25). We compared expression levels and solubility of protein 2-3 days after infection and found that the cells were already lysed by the third day. So, cells from large-scale expression of FBH1^{D698N} were harvested 2 days after infection (Figure 26). Strikingly, there was an enormous difference in the protein yield between the two FBH1 variants.

Purification of FBH1 and FBH1^{D698N} was performed under the same conditions. The only exception was the time range for binding to GSH agarose. In small-scale production we found out that both proteins are fully bound within 2 hours (Figure 25). The less time a protein spends in surrounding of cell lysate rich for numerous proteases, the better. Due to high level of contamination by GST after GST-affinity purification, we were forced to integrate an additional purification step. The His6x tag on the C-terminus was originally supposed to be utilized for purification. However, because of poor binding of the recombinant FBH1 proteins to nickel agarose (data not shown), we decided to use heparin affinity chromatography for purification. Heparin has the ability to bind proteins that interact with DNA. That is what FBH1 does whereas GST does not. This allowed us to obtain sufficient quantities of pure proteins for biochemical analyses. However, the protein yield of FBH1^{D698N} was substantially lower, about 5% of FBH1 yield, even though the cell number was about 60% higher (Table 4). There are several possible explanations of this expression variability. Most probably, it was caused by different virus stock titer that was used for infection because we did not exactly determine the concentration of infectious virus in our stocks. So, in our approach, the virus titer was either too weak to give sufficient expression level, or vice versa, it was too concentrated that the cells were already lysed by the day of harvesting and protein was released to medium. Secondly, we should not omit the possibility that even a single amino acid mutation in a protein can cause improper folding of the protein. This is consistent with our observation that the purified FBH1^{D698N} variant was slightly degraded (Figure 26).

By means of malachite green ATPase assay, we proved that purified FBH1 is an active enzyme (Figure 27). The ATPase defective form of FBH1, FBH1^{D698N}, was created to demonstrate that this activity is not caused by any co-purified enzymatic contamination. We showed that in comparison to RECQ5β, a well-characterized antirecombinase. FBH1 exerts 2-3 times lower ATPase activity than RECQ5β under the same conditions. This may be a consequence of different production conditions or it is simply the characteristic of the enzyme.

In agreement with previous studies (Kim et al., 2004), we found that FBH1 ATPase activity was stimulated by ssDNA, but not by dsDNA (Figure 29). Relatively high ATPase activity observed with FBH1 in the presence of supercoiled plasmid DNA can be explained by the presence of ssDNA regions in DNA substrate. To prove this hypothesis, we linearized plasmid by restriction enzymes and this activity was lost (observation by RNDr. Kamila Burdová). Partial activity in absence of any additional DNA may be caused by co-purified ssDNA in the FBH1 sample. Our results also confirmed that ATP/dATP is the most utilized energy source of FBH1 as in case of majority of DNA helicase. Other NTPs or dNTPs were hydrolyzed poorly by FBH1 (Figure 30).

In an effort to find novel interaction partners of FBH1, we first sought to investigate the interaction between FBH1 and RAD51, a key player in homologous recombination. Since we were not able to detect endogenous FBH1 in cell lysate by western blotting, we settled for interaction studies *in vitro* using purified recombinant FBH1. Using co-IP and pull-down assays, we revealed that FBH1 physically interacts with RAD51. We were able to immunoprecipitate recombinant FBH1 via endogenous RAD51 from human cell lysate (Figure 31). By means of the pull-down assay, the recombinant $RAD51^{K133R}$ was pulled down via recombinant FBH1 (Figure 32). Since the functional mutation in the $RAD51^{K133R}$ does not affect its protein binding properties, we can conclude that FBH1 directly interacts with RAD51 as well. However, it should be noted that the observed interaction is very weak. It is possible that the proper recognition and interaction between FBH1 and RAD51 is triggered upon occurrence of DNA damage and requires a posttranslational modification that is missing in our *in vitro* system. Below, we provide another explanation for this observation. Interestingly, in the pull-down experiments, we observed that DTT enhances binding of FBH1 to GSH agarose via the GST-tag. DTT maintains a reducing environment and thus prevents formation of disulfide bonds that may affect binding properties of GSH agarose.

By immunofluorescence, it was shown that FBH1 colocalizes with RPA in nuclei of human cells (Fugger et al., 2009). This observation together with a note in the study by of (Kim et al., 2004) that FBH1 interacts with RPA in yeast two-hybrid system led us to examine FBH1-RPA interaction using purified recombinant proteins. By far-western blotting, we found that FBH1 was bound specifically to the largest subunit of RPA, RPA70 (Figure 33).

Formation of RAD51 nucleoprotein filament on ssDNA is a key step in homologous recombination that is essential for pairing and strand exchange of homologous DNA molecules (Sung and Robberson, 1995). FBH1 has been implicated in the control of the RAD51 action (Chiolo et al., 2007, Fugger et al., 2009). Since FBH1, as an F-box protein, forms a functional SCF ubiquitin ligase, it is tempting to speculate that FBH1 could disrupt the nucleoprotein

filament by a unique mechanism based on RAD51 ubiquitination targeting the protein for degradation. The identity of the physiological substrate of the SCF^{FBH1} complex is still unresolved question. However, the finding that the level of endogenous RAD51 was unaffected in upon FBH1 over-expression argues against this kind of mechanism (Fugger et al., 2009).

It has been suggested, although not yet experimentally proven, that FBH1 utilizes its translocase activity to inhibit the nucleoprotein filament formation. The core objective of this thesis work was to investigate the ability of FBH1 to displace RAD51 from the ssDNA. Using Topoisomerase I-linked DNA topology modification assay, we demonstrated that FBH1 is indeed able to dislodge RAD51 from nucleoprotein filament *in vitro* (Figure 34). Evidence that active translocation of FBH1 on ssDNA is required for this function comes from our finding that ATPase-dead mutant of FBH1, $FBH1^{D698N}$, lacks this activity. Nevertheless, the filament disruptions activity of FBH1 was found to be ~3 times lower than that of RECQ5β helicase. This may be explained by the fact that RECQ5β as a member of SF2 family of helicases utilizes another, probably more efficient, mechanism to translocate along the DNA.

In our experiments, we observed an additional band, which migrated at the position between ssDNA and relaxed dsDNA on the agarose gel. Our explanation of this unexpected band is that the ssDNA was probably contaminated by double-stranded form of this DNA.

To summarize our finding from protein interaction and enzymatic studies of FBH1, we compiled a potential model suggesting a mechanism of how FBH1 controls the nucleoprotein filament function (Figure 35). According to this model, FBH1 is recruited to the ssDNA regions covered by RAD51 recombinase. FBH1 then translocates along the ssDNA and functions as an "ice-breaker" catalyzing the cleaning of RAD51 polymers from the DNA. For this action, FBH1 utilizes the free energy from ATP hydrolysis, which is required for its DNA helicase/translocase activity. Displacement of RAD51 molecules from ssDNA might by stimulated by the FBH1-RAD51 interaction. In the next step, RPA is recruited to the uncovered ssDNA regions to prevent re-loading of free RAD51. The binding of RPA to ssDNA might be also promoted via the FBH1-RPA70 interaction. It is worth to mention that a strong interaction between FBH1 and RAD51 is not welcome in this case. It is rather a dynamic relationship than tight binding because the particular RAD51 molecules need to be removed.

Whether FBH1 acts according to our model remains to be further investigated. It is possible that FBH1 inhibits the nucleoprotein filament formation to suppress excessive HR events and hence prevent production of unwanted crossovers and interference of the HR machinery with other DNA repair pathway. It is also possible that the antirecombinase

function of FBH1 is required at sites of stalled replication forks where ssDNA gaps or DSBs are generated and can thus lead to loading of RAD51 recombinase and promote unscheduled recombination reactions (Barbour and Xiao, 2003). This idea is supported by the experimental data obtained from studies with Fbh1 in *S. pombe*. It was shown that Fbh1 suppresses spontaneous nucleoprotein filament formation, which can lead to accumulation of recombination intermediates (Morishita et al., 2005).

Another DNA helicase, which is known to disrupt RAD51 from ssDNA, is the *S. cerevisiae* Srs2 (Krejci et al., 2003, Veaute et al., 2003). Srs2 shares several similarities with FBH1 and belongs to the same family as FBH1. All three antirecombinases, FBH1, RECQ5β and Srs2 have been shown to physically interact with RAD51 recombinase (Antony et al., 2009, Schwendener et al., 2010). According to current presumption for Srs2, the protein-protein interaction allosterically triggers the ATP hydrolysis within the RAD51 nucleoprotein filament resulting in the RAD51 dissociation (Antony et al., 2009). It is possible that similar mechanism accounts for FBH1. Since there is no apparent human homolog of Srs2, it is therefore tempting to speculate that FBH1 might be the functional and mechanistic homolog of Srs2 in humans.

It should be emphasized that in all our experiments, only the shortest isoform of FBH1, isoform 4, was used. Thus, it is possible that the other isoforms may exert different phenotype. The longest isoform, isoform 1, containing a 125-aa extension at the N-terminus should be examined in future experiments. The ability of FBH1 to dislodge RAD51 from ssDNA should be further tested by visualization of nucleoprotein filament using electron microscopy. Another approach to check for the antirecombinase activity *in vitro* is a pull-down assay with ssDNA fragment linked to agarose beads. To elucidate the FBH1 mechanism in more detail, it is necessary to investigate which domain of FBH1 is responsible for the interaction with RAD51. It would be interesting to test if the direct interaction between FBH1 and RAD51 stimulates the nucleoprotein filament disruption activity of FBH1. More knowledge is needed to understand the role of FBH1 as an antireconbinase. For instance, it is not clear how does FBH1 distinguish between appropriate and inappropriate RAD51 nucleoprotein filaments. Why does the cell require several anrirecombinases and what is the interplay between each other? Or, where in the cell and under which circumstances does FBH1 operates? As a component of SCF complex, FBH1 is endowed by a great ability to target proteins for degradation. It is therefore highly interesting to speculate about the identity of the physiological substrates of SCF^{FBH1} complex and its possible contribution to regulation of HR.

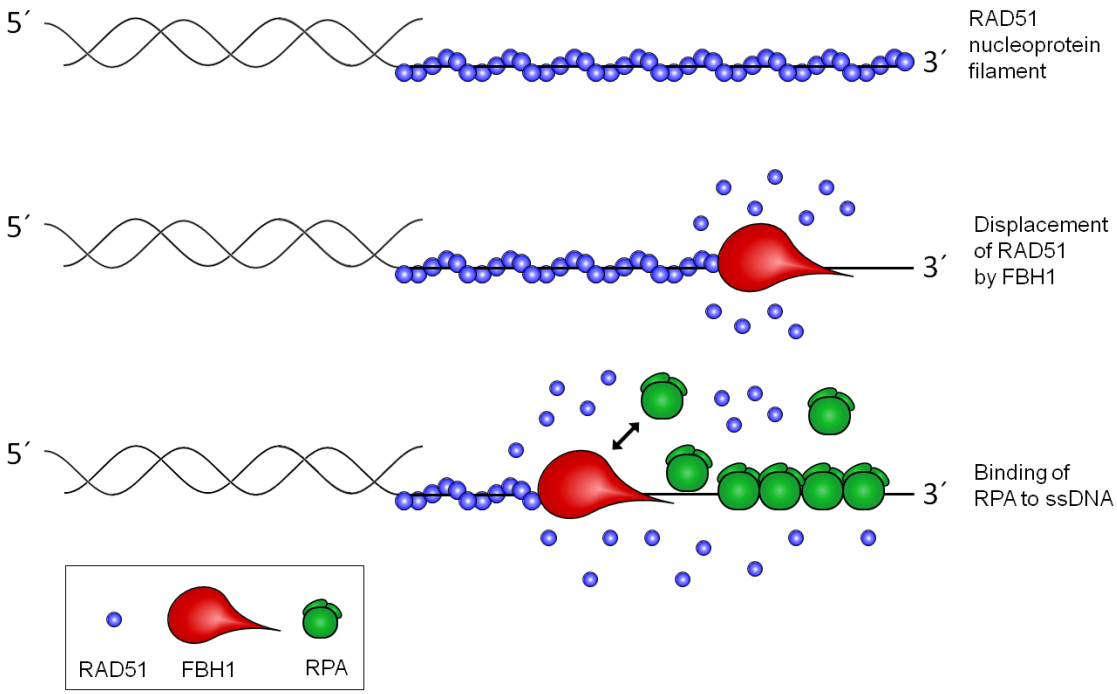

Figure 35 A potential model representing the mechanism of the FBH1 action on RAD51 nucleoprotein filament. FBH1 catalyzes disruption of RA51 nucleoprotein filament via translocating along the single-stranded (ssDNA). The reaction is supported by a dynamic interaction between FBH1 and RAD51. The freed ssDNA regions are captured by the ssDNA-binding protein, RPA, to prevent re-loading of RAD51. The recruitment of RPA is stimulated by the interaction of FBH1 with the largest subunit of RPA.

7 Conclusions

- N-terminal fragment of human FBH1 spanning amino acids 1-484 was expressed, purified and utilized to raise chicken polyclonal anti-FBH1 antibody. Purified antibody specifically recognizes recombinant FBH1. However, we failed to detect endogenous FBH1.

- Wild type and ATPase dead forms of FBH1 were expressed and purified from baculovirus-infected Sf9 insect cells. We confirmed that FBH1 is a ssDNA-stimulated ATPase.

- We found that FBH1 physically interacts with RAD51 and the largest subunit of RPA (RPA70) *in vitro*. The interaction with RAD51 is very weak.

- We experimentally showed that FBH1 has the ability to disrupt RAD51 nucleoprotein filament. This capability is dependent on its ssDNA-translocase activity.

References

Antony, E., E. J. Tomko, Q. Xiao, L. Krejci, T. M. Lohman and T. Ellenberger (2009), "Srs2 disassembles Rad51 filaments by a protein-protein interaction triggering ATP turnover and dissociation of Rad51 from DNA.", *Mol Cell,* Vol. 35, No. 1, Jul.

Assenmacher, N. and K. P. Hopfner (2004), "MRE11/RAD50/NBS1: complex activities.", *Chromosoma,* Vol. 113, No. 4, Oct.

Bai, C., P. Sen, K. Hofmann, L. Ma, M. Goebl, J. Harper and S. Elledge (1996), "SKP1 connects cell cycle regulators to the ubiquitin proteolysis machinery through a novel motif, the F-box.", *Cell,* Vol. 86, No. 2, Jul.

Barber, L., J. Youds, J. Ward, M. Mcilwraith, N. O'neil, M. Petalcorin, J. Martin, S. Collis, S. Cantor, M. Auclair, H. Tissenbaum, S. West, A. Rose and S. Boulton (2008), "RTEL1 maintains genomic stability by suppressing homologous recombination.", *Cell,* Vol. 135, No. 2, Oct.

Barbour, L. and W. Xiao (2003), "Regulation of alternative replication bypass pathways at stalled replication forks and its effects on genome stability: a yeast model.", *Mutat Res,* Vol. 532, No. 1-2, Nov.

Birnboim, H. C. and J. Doly (1979), "A rapid alkaline extraction procedure for screening recombinant plasmid DNA.", *Nucleic Acids Res,* Vol. 7, No. 6, Nov.

Bochkareva, E., S. Korolev, S. P. Lees-Miller and A. Bochkarev (2002), "Structure of the RPA trimerization core and its role in the multistep DNA-binding mechanism of RPA.", *EMBO J,* Vol. 21, No. 7, Apr.

Bradford, M. M. (1976), "A rapid and sensitive method for the quantitation of microgram quantities of protein utilizing the principle of protein-dye binding.", *Anal Biochem,* Vol. 72, May.

Bransteitter, R., J. L. Sneeden, S. Allen, P. Pham and M. F. Goodman (2006), "First AID (activation-induced cytidine deaminase) is needed to produce high affinity isotype-switched antibodies.", *J Biol Chem,* Vol. 281, No. 25, Jun.

Brush, G. S., C. W. Anderson and T. J. Kelly (1994), "The DNA-activated protein kinase is required for the phosphorylation of replication protein A during simian virus 40 DNA replication.", *Proc Natl Acad Sci U S A,* Vol. 91, No. 26, Dec.

Bugreev, D., X. Yu, E. Egelman and A. Mazin (2007), "Novel pro- and anti-recombination activities of the Bloom's syndrome helicase.", *Genes Dev,* Vol. 21, No. 23, Dec.

Cardozo, T. and M. Pagano (2004), "The SCF ubiquitin ligase: insights into a molecular machine.", *Nat Rev Mol Cell Biol,* Vol. 5, No. 9, Sep.

Champion, M. D. and R. S. Hawley (2002), "Playing for half the deck: the molecular biology of meiosis.", *Nat Cell Biol,* Vol. 4 Suppl, Oct.

Chanet, R., M. Heude, A. Adjiri, L. Maloisel and F. Fabre (1996), "Semidominant mutations in the yeast Rad51 protein and their relationships with the Srs2 helicase.", *Mol Cell Biol,* Vol. 16, No. 9, Sep.

Chi, P., S. Van Komen, M. G. Sehorn, S. Sigurdsson and P. Sung (2006), "Roles of ATP binding and ATP hydrolysis in human Rad51 recombinase function.", *DNA Repair (Amst),* Vol. 5, No. 3, Mar.

Chiolo, I., M. Saponaro, A. Baryshnikova, J. Kim, Y. Seo and G. Liberi (2007), "The human F-Box DNA helicase FBH1 faces Saccharomyces cerevisiae Srs2 and postreplication repair pathway roles.", *Mol Cell Biol,* Vol. 27, No. 21, Nov.

Chu, W. K. and I. D. Hickson (2009), "RecQ helicases: multifunctional genome caretakers.", *Nat Rev Cancer,* Vol. 9, No. 9, Sep.

Colavito, S., M. Macris-Kiss, C. Seong, O. Gleeson, E. C. Greene, H. L. Klein, L. Krejci and P. Sung (2009), "Functional significance of the Rad51-Srs2 complex in Rad51 presynaptic filament disruption.", *Nucleic Acids Res,* Vol. 37, No. 20, Nov.

Colavito, S., R. Prakash and P. Sung (2010), "Promotion and regulation of homologous recombination by DNA helicases.", *Methods,* Vol. 51, No. 3, Jul.

Cui, M., W. Li, W. Liu, K. Yang, Y. Pang and L. Haoran (2007), "Production of recombinant orange-spotted grouper (Epinephelus coioides) luteinizing hormone in insect cells by the baculovirus expression system and its biological effect.", *Biol Reprod,* Vol. 76, No. 1, Jan.

Delacôte, F. and B. S. Lopez (2008), "Importance of the cell cycle phase for the choice of the appropriate DSB repair pathway, for genome stability maintenance: the trans-S double-strand break repair model.", *Cell Cycle,* Vol. 7, No. 1, Jan.

Ding, H., M. Schertzer, X. Wu, M. Gertsenstein, S. Selig, M. Kammori, R. Pourvali, S. Poon, I. Vulto, E. Chavez, P. Tam, A. Nagy and P. Lansdorp (2004), "Regulation of murine telomere length by Rtel: an essential gene encoding a helicase-like protein.", *Cell,* Vol. 117, No. 7, Jun.

Dupaigne, P., C. Le Breton, F. Fabre, S. Gangloff, E. Le Cam and X. Veaute (2008), "The Srs2 helicase activity is stimulated by Rad51 filaments on dsDNA: implications for crossover incidence during mitotic recombination.", *Mol Cell,* Vol. 29, No. 2, Feb.

Eggler, A. L., R. B. Inman and M. M. Cox (2002), "The Rad51-dependent pairing of long DNA substrates is stabilized by replication protein A.", *J Biol Chem,* Vol. 277, No. 42, Oct.

Fanning, E., V. Klimovich and A. R. Nager (2006), "A dynamic model for replication protein A (RPA) function in DNA processing pathways.", *Nucleic Acids Res,* Vol. 34, No. 15.

Fugger, K., M. Mistrik, J. Danielsen, C. Dinant, J. Falck, J. Bartek, J. Lukas and N. Mailand (2009), "Human Fbh1 helicase contributes to genome maintenance via pro- and anti-recombinase activities.", *J Cell Biol,* Vol. 186, No. 5, Sep.

Gagne, J. M., B. P. Downes, S. H. Shiu, A. M. Durski and R. D. Vierstra (2002), "The F-box subunit of the SCF E3 complex is encoded by a diverse superfamily of genes in Arabidopsis.", *Proc Natl Acad Sci U S A,* Vol. 99, No. 17, Aug.

Garcia, P. L., Y. Liu, J. Jiricny, S. C. West and P. Janscak (2004), "Human RECQ5beta, a protein with DNA helicase and strand-annealing activities in a single polypeptide.", *EMBO J,* Vol. 23, No. 14, Jul.

Gassmann, M., P. Thömmes, T. Weiser and U. Hübscher (1990), "Efficient production of chicken egg yolk antibodies against a conserved mammalian protein.", *FASEB J,* Vol. 4, No. 8, May.

Goodsell, D. S. (2005), "The molecular perspective: RAD51 and BRCA2.", *Stem Cells,* Vol. 23, No. 9, Oct.

Guirouilh-Barbat, J., S. Huck, P. Bertrand, L. Pirzio, C. Desmaze, L. Sabatier and B. S. Lopez (2004), "Impact of the KU80 pathway on NHEJ-induced genome rearrangements in mammalian cells.", *Mol Cell,* Vol. 14, No. 5, Jun.

Hanada, K. and I. D. Hickson (2007), "Molecular genetics of RecQ helicase disorders.", *Cell Mol Life Sci,* Vol. 64, No. 17, Sep.

Heyer, W. D., K. T. Ehmsen and J. Liu (2010), "Regulation of homologous recombination in eukaryotes.", *Annu Rev Genet,* Vol. 44.

Heyer, W. D., X. Li, M. Rolfsmeier and X. P. Zhang (2006), "Rad54: the Swiss Army knife of homologous recombination?", *Nucleic Acids Res,* Vol. 34, No. 15.

Hickson, I. D. (2003), "RecQ helicases: caretakers of the genome.", *Nat Rev Cancer,* Vol. 3, No. 3, Mar.

Hiom, K. (2010), "Coping with DNA double strand breaks.", *DNA Repair (Amst),* Vol. 9, No. 12, Dec.

Hoeijmakers, J. H. (2001), "Genome maintenance mechanisms for preventing cancer.", *Nature,* Vol. 411, No. 6835, May.

Hoeijmakers, J. H. (2009), "DNA damage, aging, and cancer.", *N Engl J Med,* Vol. 361, No. 15, Oct.

Holthausen, J. T., C. Wyman and R. Kanaar (2010), "Regulation of DNA strand exchange in homologous recombination.", *DNA Repair (Amst),* Vol. 9, No. 12, Dec.

Hu, Y., S. Raynard, M. Sehorn, X. Lu, W. Bussen, L. Zheng, J. Stark, E. Barnes, P. Chi, P. Janscak, M. Jasin, H. Vogel, P. Sung and G. Luo (2007), "RECQL5/Recql5 helicase regulates homologous recombination and suppresses tumor formation via disruption of Rad51 presynaptic filaments.", *Genes Dev,* Vol. 21, No. 23, Dec.

Jin, J., T. Cardozo, R. C. Lovering, S. J. Elledge, M. Pagano and J. W. Harper (2004), "Systematic analysis and nomenclature of mammalian F-box proteins.", *Genes Dev,* Vol. 18, No. 21, Nov.

Jiricny, J. (2006), "The multifaceted mismatch-repair system.", *Nat Rev Mol Cell Biol,* Vol. 7, No. 5, May.

Kerényi, L. and F. Gallyas (1973), "[Errors in quantitative estimations on agar electrophoresis using silver stain].", *Clin Chim Acta,* Vol. 47, No. 3, Sep.

Kim, J., J. Kim, D. Kim, G. Ryu, S. Bae and Y. Seo (2004), "SCFhFBH1 can act as helicase and E3 ubiquitin ligase.", *Nucleic Acids Res,* Vol. 32, No. 8.

Kim, J., J. Kim, S. Lee, D. Kim, H. Kang, S. Bae, Z. Pan and Y. Seo (2002), "The novel human DNA helicase hFBH1 is an F-box protein.", *J Biol Chem,* Vol. 277, No. 27, Jul.

Kipreos, E. and M. Pagano (2000), "The F-box protein family.", *Genome Biol,* Vol. 1, No. 5.

Kohzaki, M., A. Hatanaka, E. Sonoda, M. Yamazoe, K. Kikuchi, N. Vu Trung, D. Szüts, J. Sale, H. Shinagawa, M. Watanabe and S. Takeda (2007), "Cooperative roles of vertebrate Fbh1 and Blm DNA helicases in avoidance of crossovers during recombination initiated by replication fork collapse.", *Mol Cell Biol,* Vol. 27, No. 8, Apr.

Krejci, L., S. Van Komen, Y. Li, J. Villemain, M. Reddy, H. Klein, T. Ellenberger and P. Sung (2003), "DNA helicase Srs2 disrupts the Rad51 presynaptic filament.", *Nature,* Vol. 423, No. 6937, May.

Kunkel, T. A. (2004), "DNA replication fidelity.", *J Biol Chem,* Vol. 279, No. 17, Apr.

Laemmli, U. K. (1970), "Cleavage of structural proteins during the assembly of the head of bacteriophage T4.", *Nature,* Vol. 227, No. 5259, Aug.

Lamarche, B. J., N. I. Orazio and M. D. Weitzman (2010), "The MRN complex in double-strand break repair and telomere maintenance.", *FEBS Lett,* Vol. 584, No. 17, Sep.

Laulier, C., A. Cheng, N. Huang and J. M. Stark (2010), "Mammalian Fbh1 is important to restore normal mitotic progression following decatenation stress.", *DNA Repair (Amst),* Vol. 9, No. 6, Jun.

Lawrence, C., N. Jones and C. Wilkinson (2009), "Stress-induced phosphorylation of S. pombe Atf1 abrogates its interaction with F box protein Fbh1.", *Curr Biol,* Vol. 19, No. 22, Dec.

Lawrence, C., H. Maekawa, J. Worthington, W. Reiter, C. Wilkinson and N. Jones (2007), "Regulation of Schizosaccharomyces pombe Atf1 protein levels by Sty1-mediated phosphorylation and heterodimerization with Pcr1.", *J Biol Chem,* Vol. 282, No. 8, Feb.

Lim, D. S. and P. Hasty (1996), "A mutation in mouse rad51 results in an early embryonic lethal that is suppressed by a mutation in p53.", *Mol Cell Biol,* Vol. 16, No. 12, Dec.

Liu, V. F. and D. T. Weaver (1993), "The ionizing radiation-induced replication protein A phosphorylation response differs between ataxia telangiectasia and normal human cells.", *Mol Cell Biol,* Vol. 13, No. 12, Dec.

Lohman, T. M., E. J. Tomko and C. G. Wu (2008), "Non-hexameric DNA helicases and translocases: mechanisms and regulation.", *Nat Rev Mol Cell Biol,* Vol. 9, No. 5, May.

Lorenz, A., F. Osman, V. Folkyte, S. Sofueva and M. Whitby (2009), "Fbh1 limits Rad51-dependent recombination at blocked replication forks.", *Mol Cell Biol,* Vol. 29, No. 17, Sep.

Matson, S. W. and J. W. George (1987), "DNA helicase II of Escherichia coli. Characterization of the single-stranded DNA-dependent NTPase and helicase activities.", *J Biol Chem,* Vol. 262, No. 5, Feb.

Mazin, A. V., E. Zaitseva, P. Sung and S. C. Kowalczykowski (2000), "Tailed duplex DNA is the preferred substrate for Rad51 protein-mediated homologous pairing.", *EMBO J,* Vol. 19, No. 5, Mar.

Mcilwraith, M. J., M. J. Mcllwraith, A. Vaisman, Y. Liu, E. Fanning, R. Woodgate and S. C. West (2005), "Human DNA polymerase eta promotes DNA synthesis from strand invasion intermediates of homologous recombination.", *Mol Cell,* Vol. 20, No. 5, Dec.

Mimori, T. and J. A. Hardin (1986), "Mechanism of interaction between Ku protein and DNA.", *J Biol Chem,* Vol. 261, No. 22, Aug.

Moldovan, G. L. and A. D. D'andrea (2009), "How the fanconi anemia pathway guards the genome.", *Annu Rev Genet,* Vol. 43.

Morishita, T., F. Furukawa, C. Sakaguchi, T. Toda, A. Carr, H. Iwasaki and H. Shinagawa (2005), "Role of the Schizosaccharomyces pombe F-Box DNA helicase in processing recombination intermediates.", *Mol Cell Biol,* Vol. 25, No. 18, Sep.

Neale, M. J. and S. Keeney (2006), "Clarifying the mechanics of DNA strand exchange in meiotic recombination.", *Nature,* Vol. 442, No. 7099, Jul.

Noll, D. M., T. M. Mason and P. S. Miller (2006), "Formation and repair of interstrand cross-links in DNA.", *Chem Rev,* Vol. 106, No. 2, Feb.

Ogawa, T., X. Yu, A. Shinohara and E. H. Egelman (1993), "Similarity of the yeast RAD51 filament to the bacterial RecA filament.", *Science,* Vol. 259, No. 5103, Mar.

Okamoto, S. Y., M. Sato, T. Toda and M. Yamamoto (2012), "SCF Ensures Meiotic Chromosome Segregation Through a Resolution of Meiotic Recombination Intermediates.", *PLoS One,* Vol. 7, No. 1.

Osman, F., J. Dixon, A. Barr and M. Whitby (2005), "The F-Box DNA helicase Fbh1 prevents Rhp51-dependent recombination without mediator proteins.", *Mol Cell Biol,* Vol. 25, No. 18, Sep.

Ou, C. Y., H. Pi and C. T. Chien (2003), "Control of protein degradation by E3 ubiquitin ligases in Drosophila eye development.", *Trends Genet,* Vol. 19, No. 7, Jul.

Park, J., E. Choi, S. Lee, C. Lee and Y. Seo (1997), "A DNA helicase from Schizosaccharomyces pombe stimulated by single-stranded DNA-binding protein at low ATP concentration.", *J Biol Chem,* Vol. 272, No. 30, Jul.

Pfeiffer, P. and W. Vielmetter (1988), "Joining of nonhomologous DNA double strand breaks in vitro.", *Nucleic Acids Res,* Vol. 16, No. 3, Feb.

Pâques, F. and J. E. Haber (1999), "Multiple pathways of recombination induced by double-strand breaks in Saccharomyces cerevisiae.", *Microbiol Mol Biol Rev,* Vol. 63, No. 2, Jun.

Ristic, D., M. Modesti, T. Van Der Heijden, J. Van Noort, C. Dekker, R. Kanaar and C. Wyman (2005), "Human Rad51 filaments on double- and single-stranded DNA: correlating regular and irregular forms with recombination function.", *Nucleic Acids Res,* Vol. 33, No. 10.

Sakaguchi, C., T. Morishita, H. Shinagawa and T. Hishida (2008), "Essential and distinct roles of the F-box and helicase domains of Fbh1 in DNA damage repair.", *BMC Mol Biol,* Vol. 9.

San Filippo, J., P. Sung and H. Klein (2008), "Mechanism of eukaryotic homologous recombination.", *Annu Rev Biochem,* Vol. 77.

Sartori, A. A., C. Lukas, J. Coates, M. Mistrik, S. Fu, J. Bartek, R. Baer, J. Lukas and S. P. Jackson (2007), "Human CtIP promotes DNA end resection.", *Nature,* Vol. 450, No. 7169, Nov.

Schwendener, S., S. Raynard, S. Paliwal, A. Cheng, R. Kanagaraj, I. Shevelev, J. Stark, P. Sung and P. Janscak (2010), "Physical interaction of RECQ5 helicase with RAD51 facilitates its anti-recombinase activity.", *J Biol Chem,* Mar.

Sekelsky, J. J., M. H. Brodsky, G. M. Rubin and R. S. Hawley (1999), "Drosophila and human RecQ5 exist in different isoforms generated by alternative splicing.", *Nucleic Acids Res,* Vol. 27, No. 18, Sep.

Selak, N., C. Z. Bachrati, I. Shevelev, T. Dietschy, B. Van Loon, A. Jacob, U. Hübscher, J. D. Hoheisel, I. D. Hickson and I. Stagljar (2008), "The Bloom's syndrome helicase (BLM) interacts physically and functionally with p12, the smallest subunit of human DNA polymerase delta.", *Nucleic Acids Res,* Vol. 36, No. 16, Sep.

Shimamoto, A., K. Nishikawa, S. Kitao and Y. Furuichi (2000), "Human RecQ5beta, a large isomer of RecQ5 DNA helicase, localizes in the nucleoplasm and interacts with topoisomerases 3alpha and 3beta.", *Nucleic Acids Res,* Vol. 28, No. 7, Apr.

Shin, D. S., L. Pellegrini, D. S. Daniels, B. Yelent, L. Craig, D. Bates, D. S. Yu, M. K. Shivji, C. Hitomi, A. S. Arvai, N. Volkmann, H. Tsuruta, T. L. Blundell, A. R. Venkitaraman and J. A. Tainer (2003), "Full-length archaeal Rad51 structure and mutants: mechanisms for RAD51 assembly and control by BRCA2.", *EMBO J,* Vol. 22, No. 17, Sep.

Singleton, M. R., M. S. Dillingham and D. B. Wigley (2007), "Structure and mechanism of helicases and nucleic acid translocases.", *Annu Rev Biochem,* Vol. 76.

Sinha, M. and C. L. Peterson (2008), "A Rad51 presynaptic filament is sufficient to capture nucleosomal homology during recombinational repair of a DNA double-strand break.", *Mol Cell,* Vol. 30, No. 6, Jun.

Skaar, J. R., J. K. Pagan and M. Pagano (2009), "SnapShot: F box proteins I.", *Cell,* Vol. 137, No. 6, Jun.

Smith, P. K., R. I. Krohn, G. T. Hermanson, A. K. Mallia, F. H. Gartner, M. D. Provenzano, E. K. Fujimoto, N. M. Goeke, B. J. Olson and D. C. Klenk (1985), "Measurement of protein using bicinchoninic acid.", *Anal Biochem,* Vol. 150, No. 1, Oct.

Soulas-Sprauel, P., P. Rivera-Munoz, L. Malivert, G. Le Guyader, V. Abramowski, P. Revy and J. P. De Villartay (2007), "V(D)J and immunoglobulin class switch recombinations: a paradigm to study the regulation of DNA end-joining.", *Oncogene,* Vol. 26, No. 56, Dec.

Sugiyama, T. and S. C. Kowalczykowski (2002), "Rad52 protein associates with replication protein A (RPA)-single-stranded DNA to accelerate Rad51-mediated displacement of RPA and presynaptic complex formation.", *J Biol Chem,* Vol. 277, No. 35, Aug.

Sun, W., A. Lorenz, F. Osman and M. C. Whitby (2011), "A failure of meiotic chromosome segregation in a fbh1Delta mutant correlates with persistent Rad51-DNA associations.", *Nucleic Acids Res,* Vol. 39, No. 5, Mar.

Sung, P. and H. Klein (2006), "Mechanism of homologous recombination: mediators and helicases take on regulatory functions.", *Nat Rev Mol Cell Biol,* Vol. 7, No. 10, Oct.

Sung, P. and D. L. Robberson (1995), "DNA strand exchange mediated by a RAD51-ssDNA nucleoprotein filament with polarity opposite to that of RecA.", *Cell,* Vol. 82, No. 3, Aug.

Takata, M., M. S. Sasaki, E. Sonoda, C. Morrison, M. Hashimoto, H. Utsumi, Y. Yamaguchi-Iwai, A. Shinohara and S. Takeda (1998), "Homologous recombination and non-homologous end-joining pathways of DNA double-strand break repair have overlapping roles in the maintenance of chromosomal integrity in vertebrate cells.", *EMBO J,* Vol. 17, No. 18, Sep.

Thode, S., A. Schäfer, P. Pfeiffer and W. Vielmetter (1990), "A novel pathway of DNA end-to-end joining.", *Cell,* Vol. 60, No. 6, Mar.

Thomas, J. H. (2006), "Adaptive evolution in two large families of ubiquitin-ligase adapters in nematodes and plants.", *Genome Res,* Vol. 16, No. 8, Aug.

Thorslund, T. and S. C. West (2007), "BRCA2: a universal recombinase regulator.", *Oncogene,* Vol. 26, No. 56, Dec.

Treuner, K., M. Findeisen, U. Strausfeld and R. Knippers (1999), "Phosphorylation of replication protein A middle subunit (RPA32) leads to a disassembly of the RPA heterotrimer.", *J Biol Chem,* Vol. 274, No. 22, May.

Tsuzuki, T., Y. Fujii, K. Sakumi, Y. Tominaga, K. Nakao, M. Sekiguchi, A. Matsushiro, Y. Yoshimura and Moritat (1996), "Targeted disruption of the Rad51 gene leads to lethality in embryonic mice.", *Proc Natl Acad Sci U S A,* Vol. 93, No. 13, Jun.

Tuteja, N. and R. Tuteja (2004), "Unraveling DNA helicases. Motif, structure, mechanism and function.", *Eur J Biochem,* Vol. 271, No. 10, May.

Uringa, E. J., J. L. Youds, K. Lisaingo, P. M. Lansdorp and S. J. Boulton (2011), "RTEL1: an essential helicase for telomere maintenance and the regulation of homologous recombination.", *Nucleic Acids Res,* Vol. 39, No. 5, Mar.

Van Brabant, A. J., T. Ye, M. Sanz, J. L. German Iii, N. A. Ellis and W. K. Holloman (2000), "Binding and melting of D-loops by the Bloom syndrome helicase.", *Biochemistry,* Vol. 39, No. 47, Nov.

Veaute, X., S. Delmas, M. Selva, J. Jeusset, E. Le Cam, I. Matic, F. Fabre and M. A. Petit (2005), "UvrD helicase, unlike Rep helicase, dismantles RecA nucleoprotein filaments in Escherichia coli.", *EMBO J,* Vol. 24, No. 1, Jan.

Veaute, X., J. Jeusset, C. Soustelle, S. Kowalczykowski, E. Le Cam and F. Fabre (2003), "The Srs2 helicase prevents recombination by disrupting Rad51 nucleoprotein filaments.", *Nature,* Vol. 423, No. 6937, May.

Walker, J. E., M. Saraste, M. J. Runswick and N. J. Gay (1982), "Distantly related sequences in the alpha- and beta-subunits of ATP synthase, myosin, kinases and other ATP-requiring enzymes and a common nucleotide binding fold.", *EMBO J,* Vol. 1, No. 8.

Wang, S. W., A. Goodwin, I. D. Hickson and C. J. Norbury (2001), "Involvement of Schizosaccharomyces pombe Srs2 in cellular responses to DNA damage.", *Nucleic Acids Res,* Vol. 29, No. 14, Jul.

Wold, M. S. (1997), "Replication protein A: a heterotrimeric, single-stranded DNA-binding protein required for eukaryotic DNA metabolism.", *Annu Rev Biochem,* Vol. 66.

Wold, M. S. and T. Kelly (1988), "Purification and characterization of replication protein A, a cellular protein required for in vitro replication of simian virus 40 DNA.", *Proc Natl Acad Sci U S A,* Vol. 85, No. 8, Apr.

Wu, L. and I. Hickson (2006), "DNA helicases required for homologous recombination and repair of damaged replication forks.", *Annu Rev Genet,* Vol. 40.

Wu, L. and I. D. Hickson (2003), "The Bloom's syndrome helicase suppresses crossing over during homologous recombination.", *Nature,* Vol. 426, No. 6968, Dec.

You, Z. and J. M. Bailis (2010), "DNA damage and decisions: CtIP coordinates DNA repair and cell cycle checkpoints.", *Trends Cell Biol,* Vol. 20, No. 7, Jul.

Yun, M. H. and K. Hiom (2009), "CtIP-BRCA1 modulates the choice of DNA double-strand-break repair pathway throughout the cell cycle.", *Nature,* Vol. 459, No. 7245, May.

Zou, Y., Y. Liu, X. Wu and S. M. Shell (2006), "Functions of human replication protein A (RPA): from DNA replication to DNA damage and stress responses.", *J Cell Physiol,* Vol. 208, No. 2, Aug.

Instruction Manual, Bac-to-Bac® Baculovirus Expression Systems, Invitrogen, 2002.

Internet source 1: http://www.ncbi.nlm.nih.gov/gene/84893 (accessed 4.5.2012)

Internet source 2: http://www.genenames.org/genefamilies/FBX (accessed 3.4.2012)

Internet source 3: http://www.ncbi.nlm.nih.gov/gene/84893 (accessed 18.5.2010)

Supplement

```
   1 msyevtsgch wtcqvpescd nglhcagplg hlhrrcqrts ahllvfteha emrrfkrkhl
  61 taidcqhlar shlavtqpfg qrwtnrdpnh glypkprtkr gsrgqgsqrc ipefflagkq
 121 pctndmaksn svgqdscqds egdmifpaes scalpqegsa gpgspgsapp srkrswssee
 181 esnqatgtsr wdgvskkapr hhlsvpctrp rearqeaeds tsrlsaesge tdqdagdvgp
 241 dpipdsyygl lgtlpcqeal shicslpsev lrhvfaflpv edlywnlslv chlwreiisd
 301 plfipwkkly hrylmneeqa vskvdgilsn cgiekesdlc vlnlirytat tkcspsvdpe
 361 rvlwslrdhp llpeaeacvr qhlpdlyaaa ggvniwalva avvllsssvn diqrllfclr
 421 rpsstvtmpd vtetlyciav llyamrekgi nisnrihyni fyclylqens ctqatkvkee
 481 psvwpgkkti qltheqqlil nhkmeplqvv kimafagtgk tstlvkyaek wsqsrflyvt
 541 fnksiakqae rvfpsnvick tfhsmayghi grkyqskkkl nlfkltpfmv nsvlaegkgg
 601 firaklvckt lenffasade eltidhvpiw cknsqgqrvm veqseklngv leasrlwdnm
 661 rklgecteea hqmthdgylk lwqlskpsla sfdaifvdea qdctpaimni vlsqpcgkif
 721 vgdphqqiyt frgavnalft vphthvfylt qsfrfgveia yvgatildvc krvrkktlvg
 781 gnhqsgirgd akgqvallsr tnanvfdeav rvtegefpsr ihliggiksf gldriidiwi
 841 llqpeeerrk qnlvikdkfi rrwvhkegfs gfkryvtaae dkeleakiav vekyniripe
 901 lvqriekchi edldfaeyil gtvhkakgle fdtvhvlddf vkvpcarhnl pqlphfrves
 961 fsedewnlly vavtrakkrl imtkslenil tlageyflqa eltsnvlktg vvrccvgqcn
1021 naipvdtvlt mkklpitysn rkenkggylc hscaeqrigp lafltaspeq vramertven
1081 ivlprheall flvf
```

Figure S Amino acid sequence of FBH1.
Amino acid (aa) sequence of FBH1 isoform 1 (1094 aa); FBH1 isoform 4 (NCBI Reference Sequence: NP_001245382.1) with 969 aa is denoted by grey background. Position of the amino acid substitution in FBH1^{D698N} is highlighted in blue (Internet source 1).